FINAL ACTIVITY REPORT

CONTRACT N° : AST4-CT-2005-516183

INSTRUMENT : Specific Targeted Research Project

ACRONYM : SYNCOMECS

TITLE : Synthesis of Compliant Aeronautical Mechanisms

CO-ORDINATOR: SAMTECH s.a. (SAMTECH)

PARTNERS :

1.	Samtech	SAMTECH	Be
2.	University of Cambridge	CAMBRIDGE	UK
3.	University of Clausthal	CLAUSTHAL	G
4.	Intec-Cimec, Univ. Nac. del Litoral	INTEC	Ar
5.	CenAero	CENAERO	Be
6.	CTingenieros	CTING	Sp
7.	ABB Sace	ABB	It
8.	Alenia Aeronautica	ALENIA	It
9.	Snecma	SNECMA	Fr

REPORTING PERIOD : FROM 01/04/2005 TO 30/09/2007

PROJECT START DATE : 01/04/2005 **DURATION :** 30 months

Date of issue of this report : 30/06/2008

Project funded by the European Community within the Sixth Framework Programme (Priority 4 - Aeronautics and Space)

© SYNCOMECS Consortium Members

Table of Contents

1. PUBLISHABLE EXECUTIVE SUMMARY 4

1.1. Project Background 4

1.2. Project Objectives 4

1.3. Description of the work 4

1.4. Expected results 4

1.5. Two representative pictures or graphics 5

1.6. Characterics of the project 5

2. PROJECT EXECUTION PARTNER BY PARTNER 6

2.1. SAMTECH 6
2.1.1 IFEM tool 6
2.1.2 GUI and MDO tool : the SYNCOMECS platform 8

2.2. University of CAMBRIDGE 9

2.3. University of CLAUSTHAL 10
2.3.1. The goal and a brief description of tests 10
2.3.2. Main results 10
2.3.3. The goal and a brief description of tests 18
2.3.4. Main Results 19

2.4. INTEC 25

2.5. CENAERO 44
Introduction 44
The stretch forming benchmark 45
Process description 45
Samcef model 45
Model validation 51
Benchmark objectives 52

Springback: predictions and optimization **52**
Springback measurements 52
Experimental validation 53
Final shape optimization 54

Failure detection 55
Failure criterion 55
Experimental tests 56
Model validation 57

Surface defects: predictions and optimization 58

© 2005 SYNCOMECS Consortium Members

Surface defects criterion 58
PLC constitutive model 60
Surface defects optimization 62

2.6. CT INGENERIOS 65
2.6.1 Project Background 65
2.6.2 Project Objectives 65
2.6.3 Description of the work 65
2.6.4 Expected results 66
2.6.5 Two representative pictures or graphics 66

2.7. ABB Sace 67
2.7.1 Project Objectives 67
2.7.2 Developments 67

2.8. ALENIA Aeronautica 69
2.8.1. Task 1.1: Definition of the design scope 69
2.8.2. Task 1.2: Survey and analysis of the state-of-the-art 70
2.8.3. Task 1.3: Specification of the design system 71
2.8.4. Task 1.4 : System Specification Revision 72
2.8.5. WP2,WP3 and WP7 75

2.9. SNECMA Moteurs 76
2.9.1. Project objectives and main achievements 76

© 2005 SYNCOMECS Consortium Members

1. Publishable executive summary

1.1.Project Background

The activities of the SYNCOMECS project are based on some pre-existing software technologies owned by the partners and on the results of the FP5 project SYNAMEC (focused on synthesis of aeronautical mechanisms, from the rigid kinematical point of view), which guarantees a stable foundation and reduces the risk in R&D activities.

1.2.Project Objectives

The objective of SYNCOMECS is to build an integrated software, using inverse methods, for the design of aeronautical compliant mechanical systems from industrial specifications of functional requirements. The design of these innovative systems poses unique challenges and necessitates the support of advanced prediction software tools since they should have adequate flexibility to undergo desired deformations under the action of applied forces and adequate stiffness to withstand external loading. The focus is to generate the topology and dimensions of a compliant mechanical system starting from input/output force/displacement functional requirements and design constraints. This problem is a non-linear optimisation problem of a non-linear mechanical system that may involve one or several flexible components. In a general case, it involves *Optimisation*, *Multi-Body Simulation* and *Non-linear Finite Element Analysis*. The solution may be non-existent and, if it exists, not necessarily unique. Software to be developed will be applied to aeronautical industrial problems.

1.3.Description of the work

R&D activities are executed in four steps. Firstly, a full specification of the system was made. The result of this step was presented at *Milestone 1*. The second step is the development of separate modules and the simultaneous preparation of benchmarking models. The results, as standalone software tools & associated benchmarks, will has been validated at *Milestone 2*. The third step was about the integration of the separate modules within the SYNCOMECS system. The result has been validated at *Milestone 3*. The fourth step has integrated the outcome from evaluation of the end-users. At this level, *Milestone 4,* the interaction between developers and end-users has led to the final validation of an integrated environment for synthesis and analysis of compliant mechanical systems.

1.4.Expected results

SYNCOMECS has delivered a specialized methodology, which is compliant mechanisms synthesis (concurrent use of optimisation/AI techniques and mechanism/structure modelling techniques). SYNCOMECS has also delivered a new design tool, which supports the compliant mechanical systems design. This specialized methodology and design tool can be exploited in the future by the whole European industry and also by the European education system.

© 2005 SYNCOMECS Consortium Members

1.5. Two representative pictures or graphics

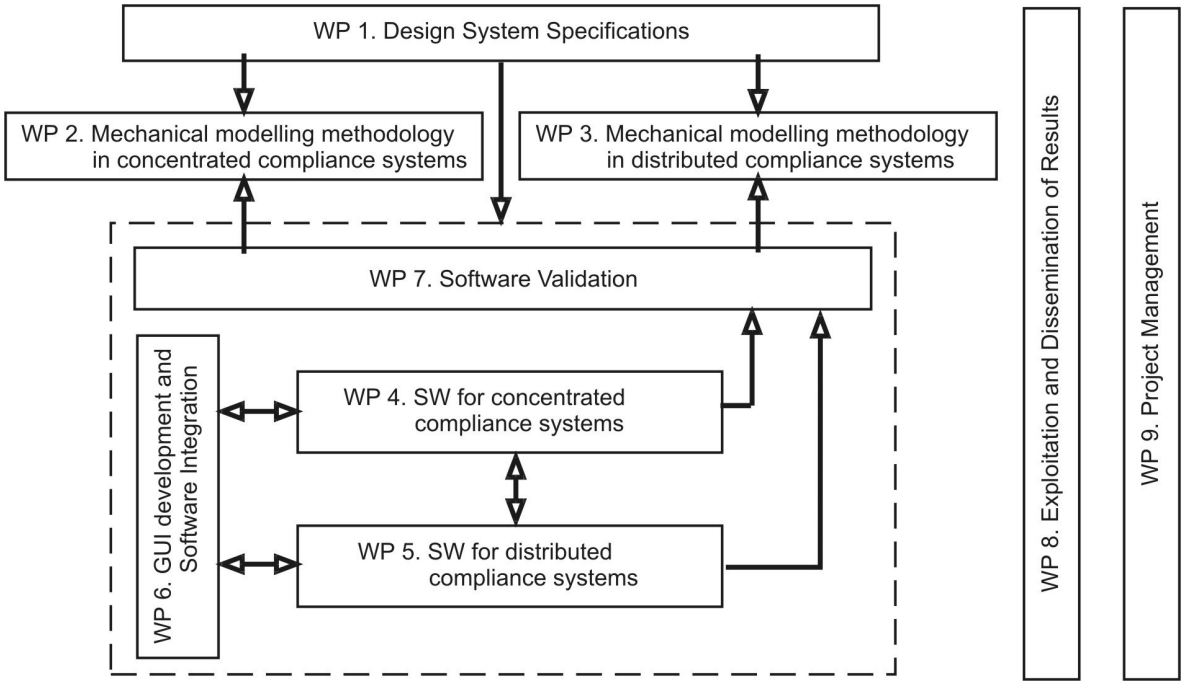

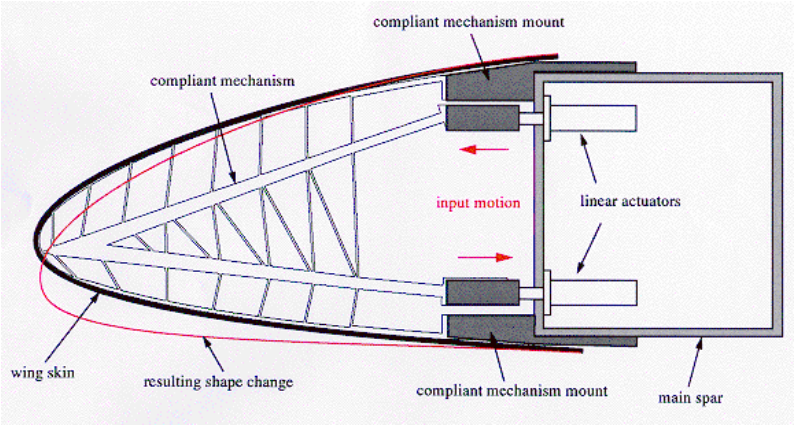

1.6. Characterics of the project

Project Title: Synthesis of Aeronautical Compliant Mechanical Systems

Acronym: SYNCOMECS

Contract Nr.: AST4-CT-2005-516183_SYNCOMECS

Total Cost: 1 836 667 Euros
EU Contribution: 1 099 982 Euros

Starting Date: 01/04/2005

© 2005 SYNCOMECS Consortium Members

Duration: 30 months

Web-site: http://www.syncomecs.org

Coordinator:
Organisation: SAMTECH s.a.
Liège Science Park
Rue des Chasseurs-Ardennais 8
B-4031 Angleur (Liège)

Contact: Mr Philippe Andry
Tel : +32 4 3616969
Fax : +32 4 3616980
Email : philippe.andry@samcef.com

EC Officer: Mr José Martin-Hernandez
Tel: +32 2 2957413
Fax: +32 2 2963307
Email: jose.martin-hernandez@cec.eu.int

Partners:

SAMTECH	BE
University of CAMBRIGDE	UK
University of CLAUSTHAL	DE
INTEC, Universidad Nacional del Litoral	AR
CENAERO	BE
CT INGENIEROS	SP
ABB Sace	IT
ALENIA Aeronautica	IT
SNECMA Moteurs	FR

2. Project execution partner by partner

2.1.SAMTECH

2.1.1 IFEM tool

2.1.1.1 INTRODUCTION

One of the SYNCOMECS objective is to develop a tool for inverse deformation analysis (**IFEM** - **I**nverse deformation **F**inite **E**lement **M**ethod). In contrast with other inverse problems, the inverse deformation problem can be shown to be well-posed. It has been

© 2005 SYNCOMECS Consortium Members

shown that, for finite element calculations, a simple re-examination of the equilibrium equations provides a suitable finite element formulation of inverse motion problems where the deformed configuration and Cauchy traction are given and the un-deformed configuration must be calculated. This formulation was also shown to involve only minor changes to existing elements designed for forward motion calculations in non-linear elasticity. This technique has been studied by Govindjee S., Mihalic P.A., and T. Yamada within others. The formulation has been implemented and extended to cases in which complex loading derived from centrifugal and gyroscopic forces is present, superposed with thermal deformations. The implementation process has been divided in two phases. First SAMTECH and INTEC have written independent prototypes before a joint formulation was adopted and the method integrated in official SAMCEF Mecano release.

2.1.1.2 INTEGRATION

Thanks to this new capability of SAMCEF Mecano, the inverse calculation of deformation of a non-linear mechanical system submitted to complex load patterns can be performed. The direct method integrated in SAMCEF Mecano allows solving inverse problem for both elastic and hyper-elastic behaviours ; material properties can be anisotropic. Different kind of loads can be taken into account : centrifugal effects, pressure, thermal effects, prescribed displacement, acceleration, ... This new Mecano's capability is restricted to volume (2D and 3D) elements, membranes and some kinematical joints.
This new **IFEM Tool** is available from SAMCEF Field. Within this GUI, the user can use results from inverse deformation analysis to perform a SAMCEF Mecano direct analysis allowing to proof results or to use IFEM solution as an initial guess and make final adjustments in an iterative way using direct computation, sensitivities evaluation and correction by using suitable optimisation tools.

2.1.1.3. VALIDATION

In Deliverable 6, several unitary tests have been presented to validate the method when only traction forces are applied, more general loading are considered in this document. Final validation will consist in the appreciation of end-users that will use this technology to solve some industrial applications.

2.1.1.4. SOME EXAMPLES

3D STRUCTURE CONNECTED WITH KINEMATICAL JOINTS
For this example, we consider a 1 m steel (Young modulus of 200000 MPA and 0.3 Poisson coefficient) beam modelled with 3D degree 2 volume elements. Left extremity has fixed displacement and the right is only free to move in the beam direction; rotations are free. The cross section is 0.06 x 0.06 m. The left boundary condition is imposed through some rigid elements connected to a hinge joint fixed to the ground, at structure right extremity rigid elements are connected to a slider; this demonstrates the validity of the simulation when kinematical constraints are present in the model (kinematical joints)

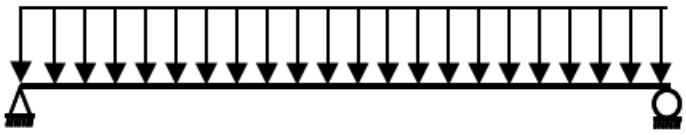

Figure 1 : Model definition

An IFEM simulation is performed to find the initial un-stressed shape that deforms to a straight configuration when a 30 Mpa pressure is applied. The obtained solution (Figure 2) occurs after 5 iterations when a 0.001 relative precision is requested. A second direct simulation is performed starting from the IFEM solution mesh and a perfect prism is obtained; Figure 3 shows that the obtained y-displacement is coherent with the inverse

© 2005 SYNCOMECS Consortium Members

solution.

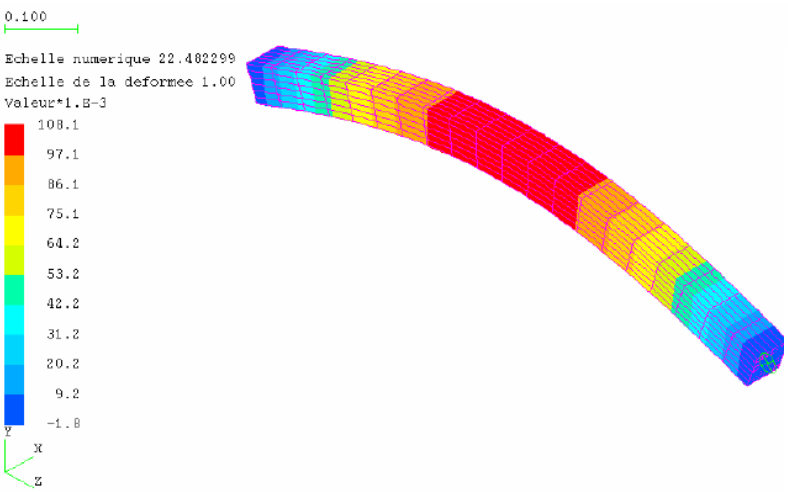

Figure 2 : un-deformed IFEM solution

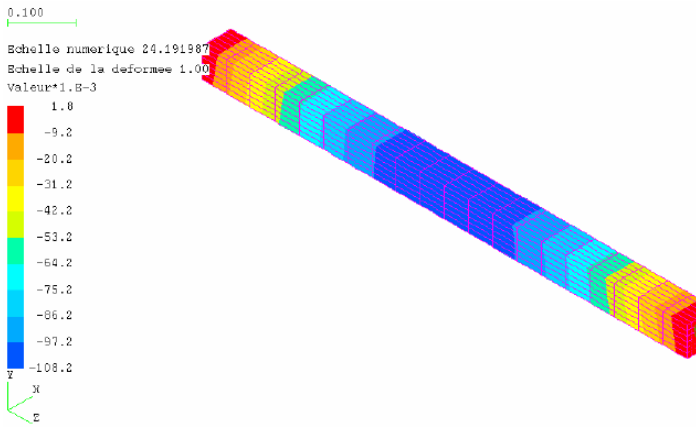

Figure 3 : deformed direct solution

2.1.1.5. Conclusion

An Inverse deformation analysis tool has been successfully integrated in SAMCEF Mecano and SAMCEF Field. It allows solving inverse problem for both elastic and hyper-elastic behaviours ; material properties can be anisotropic. This new Mecano's capability is restricted to volume (2D and 3D) elements, membranes and some kinematical joints. It has been validated in many cases for surface loads (deliverable D6) and general body loads. Additional validation with kinematical joints have also been performed and chaining capabilities between IFEM and direct Mecano simulation allow easy validation of obtained solutions.

2.1.2 GUI and MDO tool : the SYNCOMECS platform

2.1.2.1. IFEM Integration

The unified formulation retained is implemented in SAMCEF Mecano V12. The definition of an inverse model is straightforward. The user has to define the desired deformed geometry under some considered loads given on this deformed configuration. The model creation is exactly the same as for a direct simulation; the activation of the IFEM computation is done by adding the .ALGO INVER 1 command in the BACON data file. As the tangent matrix is non-symmetric,
a non-symmetric solver should be used (INLY parameter of .SUB command).
This capability is thus fully integrated in SAMCEF Mecano. As for any static direct simulation, the resolution method is based on the definition of load increments and Newton-Raphson iterative process to solve equilibrium. The management of the computation (automatic time stepping, convergence criterions, ...) is the same as for a direct simulation, allowing the user to overcome most encountered non-linearities.
IFEM is now available from the SAMCEF Field GUI. In this case the user defines its target geometry and apply directly boundary conditions on it. The management of the computation is similar to the case of usual Mecano's analysis. The interface manages automatically all specific data and restricted list of menus are proposed in order to guaranty calculation validity; main restrictions are :

- Only static analysis
- Materials should be Elastic

© 2005 SYNCOMECS Consortium Members

Available structural elements are limited to volumes and membranes
Only a limited list of kinematical joints (or constraint) is proposed
According to previous limitation, list of boundary conditions is reduced

2.2. University of CAMBRIDGE

Goals
• (WP1) Software requirements for existing problems determined • (WP1) Revisions and modifications made to the specifications subsequent to initial analysis • (WP2) Collaboration formed with Alenia concerning the design of an adaptive compliant wing leading edge • (WP2) Initial implementation of load path topology optimization using Samcef and Boss-quattro • (WP3) Optimization of a compliant bistable snap-through structure carried out with Boss-quattro • (WP3) Adaptive wing leading edge considered as a distributed compliant structure in addition to a concentrated compliant structure • (WP3) Assistance provided to ABB concerning viscoelastic material modelling of the shunt trip device lever • (WP4) Load path topology optimization fully implemented in Samcef and Boss-quattro • (WP4) A network analysis, k-shortest simple path (KSSP) algorithm used to assist with the determination and parameterization of load paths in complex lattice structures, substantially improving the usability of the load path optimization technique • (WP5) In addition to the work carried out in WP4 (which is applicable to WP3) the IFEM tool was investigated for incorporation into a load path topology optimization analysis • (WP7) A complete design process using load path topology optimization was demonstrated, culminating in the fabrication of a life-size fully-functional demonstration model • (WP7) The optimization process was extended to generate mechanisms (which may be implemented as localized compliant structures. This was used to investigate possible solutions for Snecma's compliant variable stator vane (VSV) concept. The approach was initially successful although it is necessary for Boss-quattro to account for non-converged solutions in the future. • (WP7) Load path topology optimization compared with Samtech's implementation of density-based topology optimization – Topol. • (WP8) Public-access project webpage maintained and revised for the duration of the project. • (WP8) Two international conference presentations prepared and presented concerning the compliant adaptive wing case study • (WP8) An article for an international journal concerning the adaptive leading edge was prepared.

© 2005 SYNCOMECS Consortium Members

2.3. University of CLAUSTHAL

The Portevin-Le Chatelier Effect in Alloy 2024 – Part 1

2.3.1. The goal and a brief description of tests

The first stage consisted in doing tests in a large range of strain rates to roughly determine the spread of the PLC domain and general trends for alloy 2024.

We choose the following set of strain rates: $\dot{\varepsilon}_a = 10^{-5}$ s^{-1}, 10^{-4} s^{-1}, 10^{-3} s^{-1}, 10^{-2} s^{-1}, 7x10^{-2} s^{-1}, and 10^{-1} s^{-1}. Here $\dot{\varepsilon}_a$ is the total strain rate imposed by the deformation machine and composed of the plastic strain rate of the sample and the elastic strain rate of the machine-specimen system, i.e. $\dot{\varepsilon}_a = \dot{\varepsilon} + \dot{\varepsilon}_e$.

The same tests were done for each of the three sorts of samples characterized by different tensile specimen axis orientations with regard to the rolling direction (0°, 45°, and 90°).

Since deformation in the unstable (PLC) conditions is strictly heterogeneous, the signal from a standard extensometer collects a local information and may not be representative of the strain undergone by the sample, in particular, when the strain is mostly localized outside the extensometer span. Therefore, engineering stress-strain curves are not suitable for the purpose of comparison between different samples. For this reason, the conventionally defined true strain was calculated, which represents an average ("homogeneous") strain in a sample. Calculation of the true strain usually gives rise to a slight error at small strains (< 0.2%-0.3%) because of the non-linearity of the testing machines. A good coincidence of the initial portions of the measured deformation curves (see Figs. 1-3) proves that this error may be neglected. In what follows, the data are presented in terms of the *engineering stress*, which reflects the actually measured signal.

2.3.2. Main results

Figures 1-3 represent the deformation curves for different strain rates. To make the comparison easier, the same trio of curves, corresponding to three different orientations and recorded at 10^{-5} s^{-1}, are presented on each graph alongside the curves obtained for another strain rate value.

Below we give a summary of the characteristic features of the curves.

- The stress values are close for 90° and 45° samples; 0° samples work-harden faster and are characterized by higher σ values (obviously, this trend is retained if the data are plotted in terms of true stress).

- Fig. 4 represents critical strain and critical stress values for the onset of plastic instability. Starting from low strain rates and up to $\dot{\varepsilon}_a = 10^{-2}$ s^{-1}, the material is in the region of "inverse" dependence of the critical strain on the strain rate, as represented by a descending curve. Note that the upper $\dot{\varepsilon}_a$ value for the transition to the normal dependence (ascend-

© 2005 SYNCOMECS Consortium Members

ing curve) is high in comparison with typical values reported in literature (several units)*10^{-4} s^{-1}.

- The critical strain ε_{cr} increases very fast when ε_a is decreased in the inverse region, so that the deformation curves for 10^{-4} $s^{-1}$are smooth almost throughout. Some jumps occur just before fracture (ε ~ 20%). No jumps were observed at 10^{-5} s^{-1}.

- For strain rates higher than 10^{-2} s^{-1} stress jumps degenerate to undulations on the deformation curve. It should be noted that two factors affect the character of the changes induced by the strain rate increase. One of them is basic, i.e., it stems from the influence of the strain rate on the PLC effect. However, this effect is obscured by an undesirable factor, which can only be neglected at small strain rates: the reloading of the sample during the jump duration that progressively acquires significance with increasing strain rate. This reloading, superimposed on a jump, makes it smoother. The undulations on the deformation curve are undoubtedly associated with the PLC effect as well. Moreover, strain localization, even in the case stress jump degenerate to undulations, can be seen with a naked eye. Usually several bands appear at different sites in the sample and move very fast in different directions. Therefore, the PLC domain covers the entire strain rate region explored, i.e. up to 10^{-1} s^{-1}. Since the undulations appear at strains near or above 10%, the region above 10^{-2} s^{-1} corresponds to the normal behavior. Unfortunately, the waviness of the instability part of the stress-strain curve makes it difficult to determine the point of onset of instability, so that the data points in the right-hand parts of the graphs only show a trend. Error bars obtained from the data scatter for several samples (standard deviation) are shown in Fig. 5 for two strain rates characterized by well developed instability (the same data as in Fig. 4).

- It can be seen from Fig. 4 that 90° samples are characterized by a delayed instability as compared to two other orientations. The 45° and 0° samples differ less. With these orientations, ε_{cr} is somewhat higher for 45°, while σ_{cr} is higher for 0° samples. (Note that the latter are hardnened faster and are characterized by a higher stress value).

- Fig. 6 shows the behavior of the ultimate tensile strength (UTS) and the corresponding strain at maximum load. It is interesting to note that the UTS data obey a logarithmic dependence on the strain rate below 10^{-2} s^{-1}: $UTS = A + B\ln\varepsilon_a$, where B ≅ 10 MPa. Usually no direct relation is observed for these quantities. The UTS shows a tendency to increase at 10^{-1} s^{-1} in the case of 0° and 45° samples and it drops off precipitously for 90° samples. The UTS is slightly higher for 0° samples, which is consistent with the higher flow stress values. However, the strain at maximum load is lowered so that below 10^{-2} s^{-1} the true stress values fall on a curve common for all samples (Fig. 7).

- The strain at maximum load also obeys smooth dependences, monotonous in the region corresponding to the PLC effect and deviating from them for the smallest strain rate (stable flow) and when approaching the highest strain rate (close to the upper boundary of instability). The data scatter is different for different data points and sometimes rather high (one of the points with the maximum error bar is shown), so that the deviation from the curve at the highest strain rate is not established reliably, which calls for additional measurements.

© 2005 SYNCOMECS Consortium Members

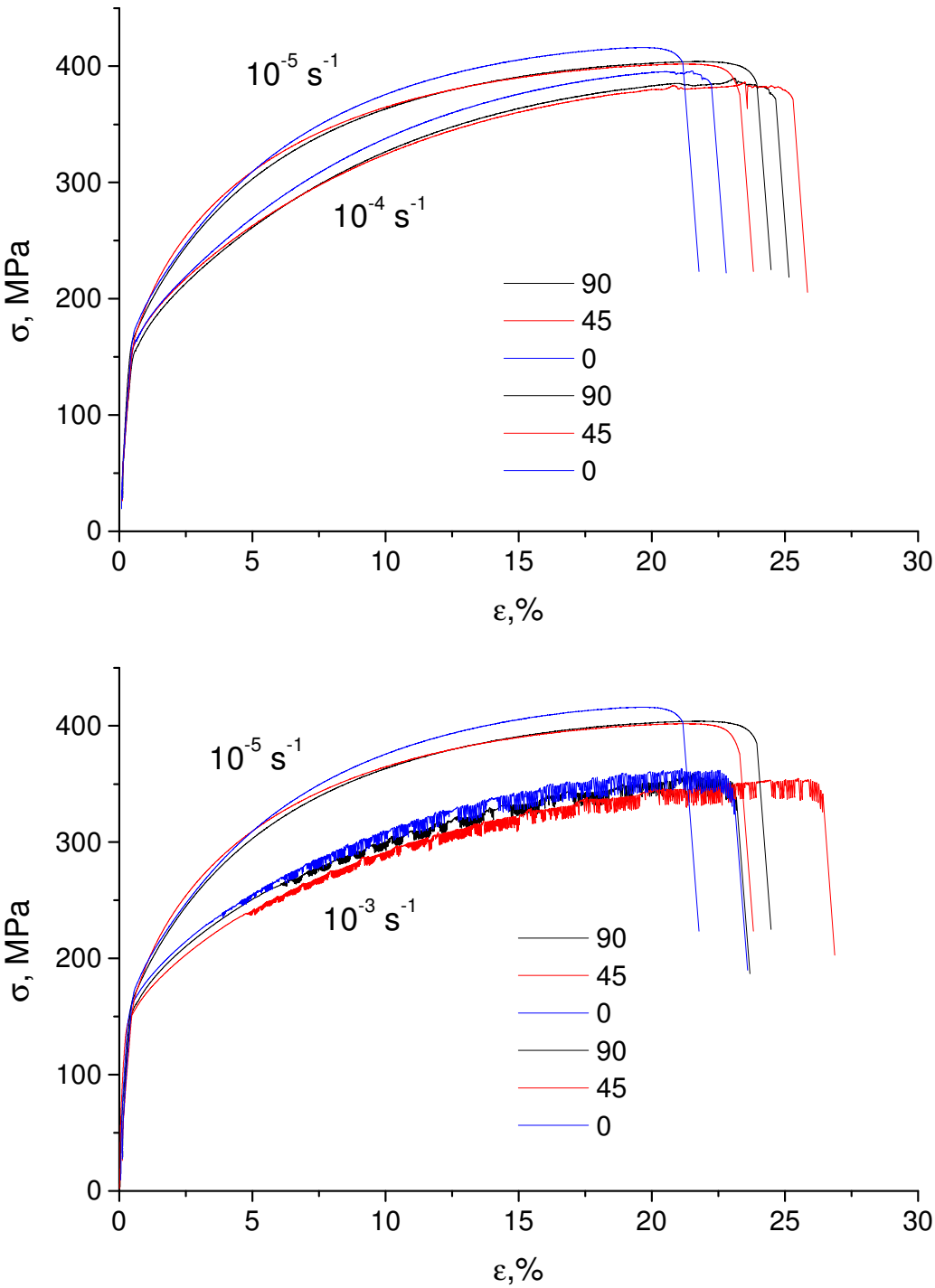

Fig. 1. Deformation curves for different strain rates and different orientations of the tensile axis.

© 2005 SYNCOMECS Consortium Members

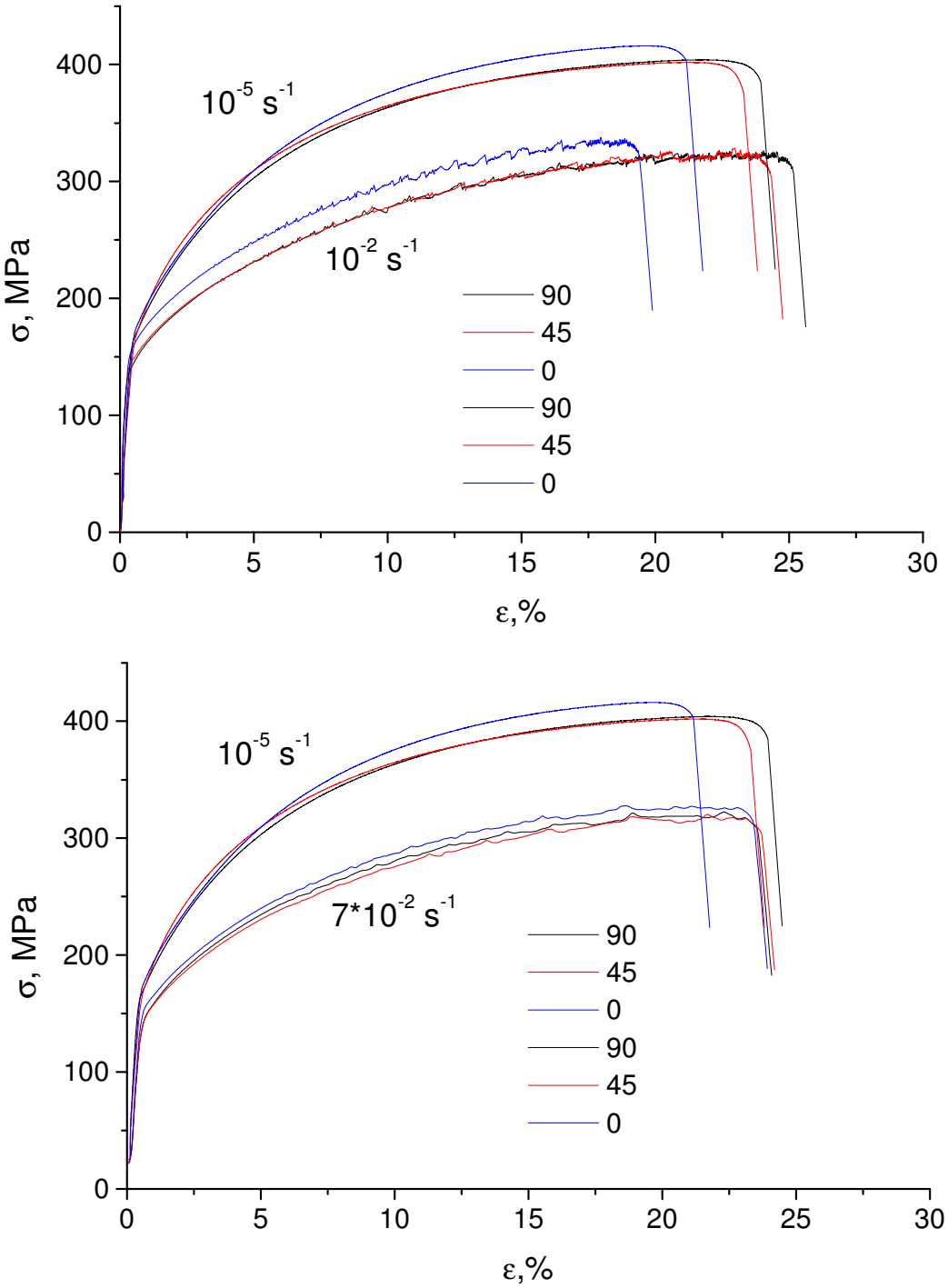

Fig. 2. Deformation curves for different strain rates and different orientations of the tensile axis.

© 2005 SYNCOMECS Consortium Members

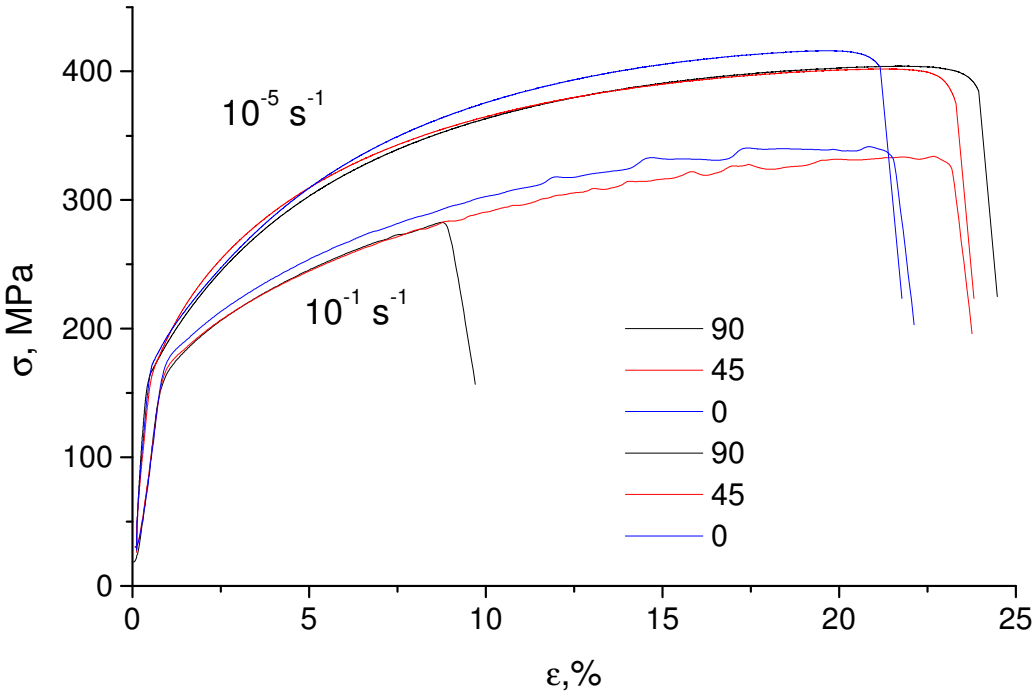

Fig. 3. Deformation curves for different strain rates and different orientations of the tensile axis.

© 2005 SYNCOMECS Consortium Members

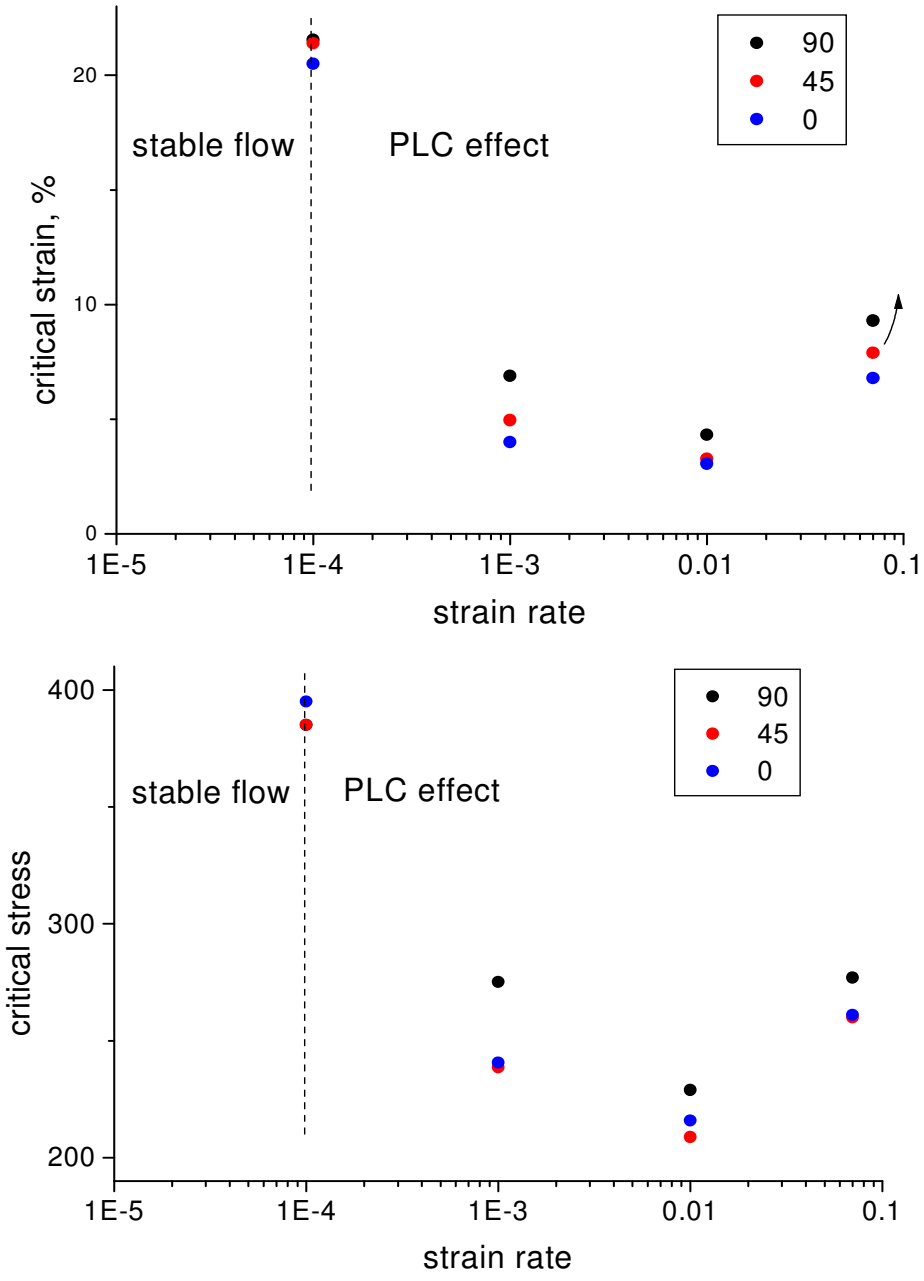

Fig. 4. Critical parameters in dependence on the imposed strain rate. The dashed line roughly indicates the lower boundary of the PLC effect.

© 2005 SYNCOMECS Consortium Members

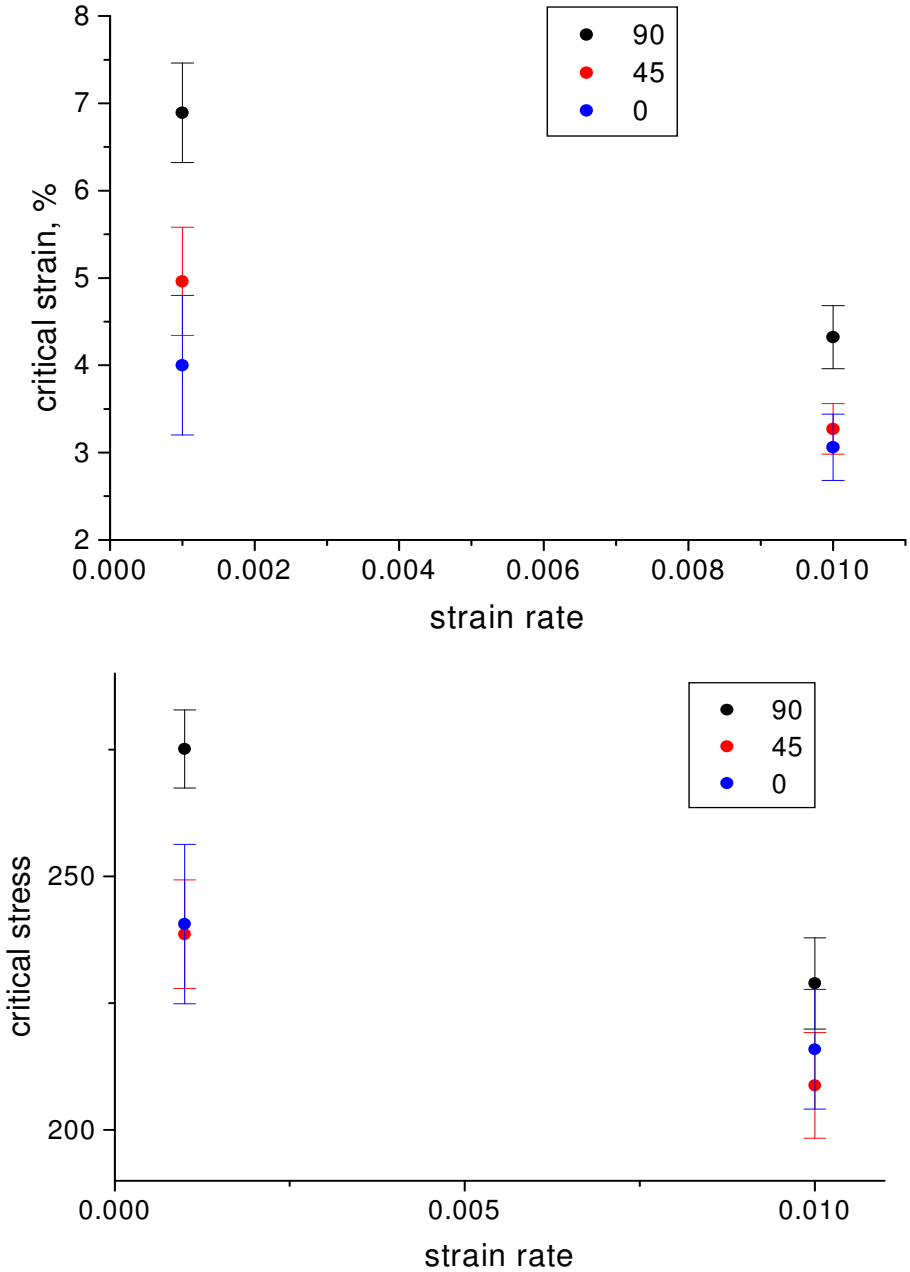

Fig. 5. The same data as in Fig. 4 for two strain rate values. Error bars indicate standard deviation obtained from data for 3 samples of each kind.

© 2005 SYNCOMECS Consortium Members

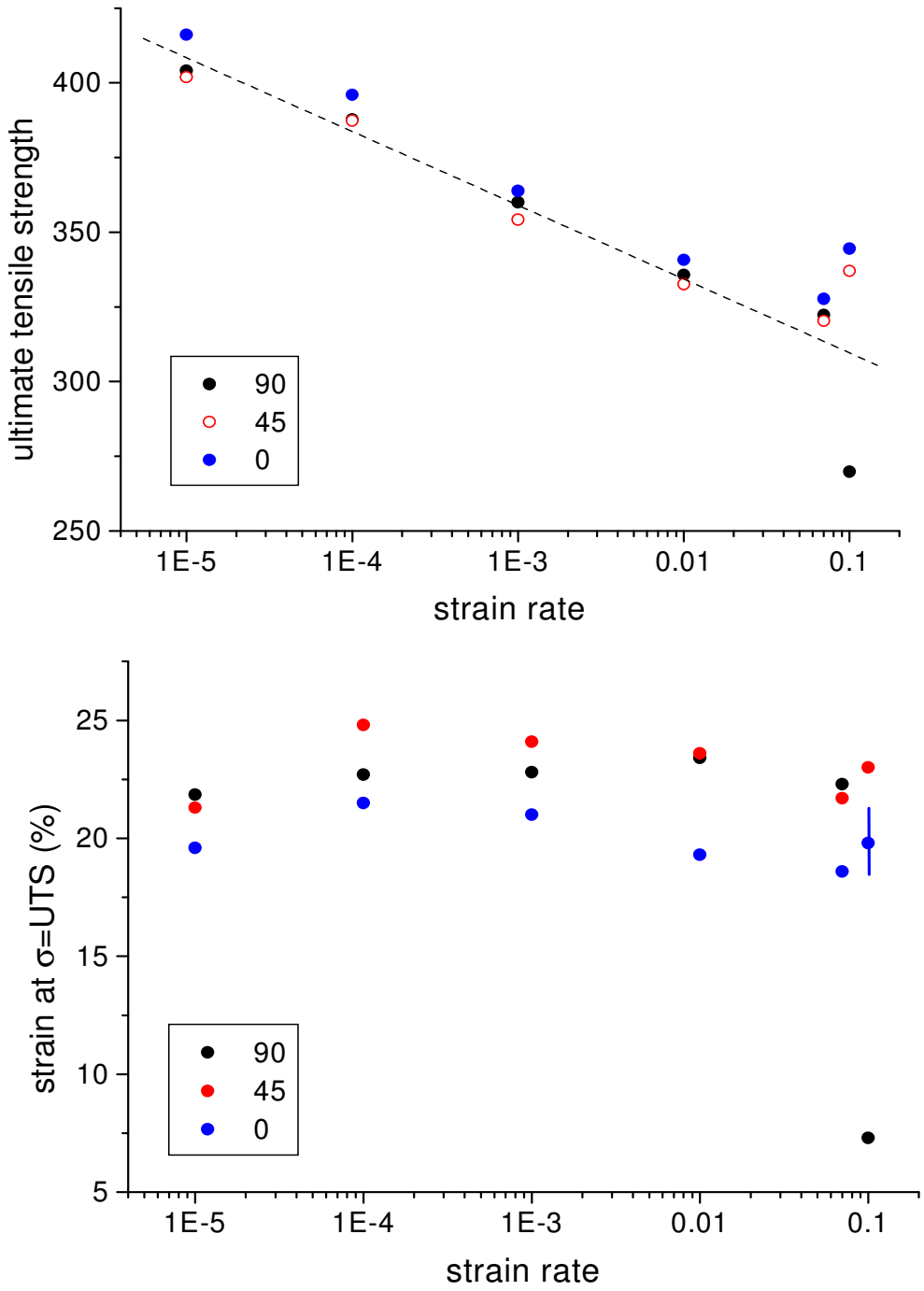

Fig. 6. The UTS and the strain at the maximum load as functions of the strain rate.

© 2005 SYNCOMECS Consortium Members

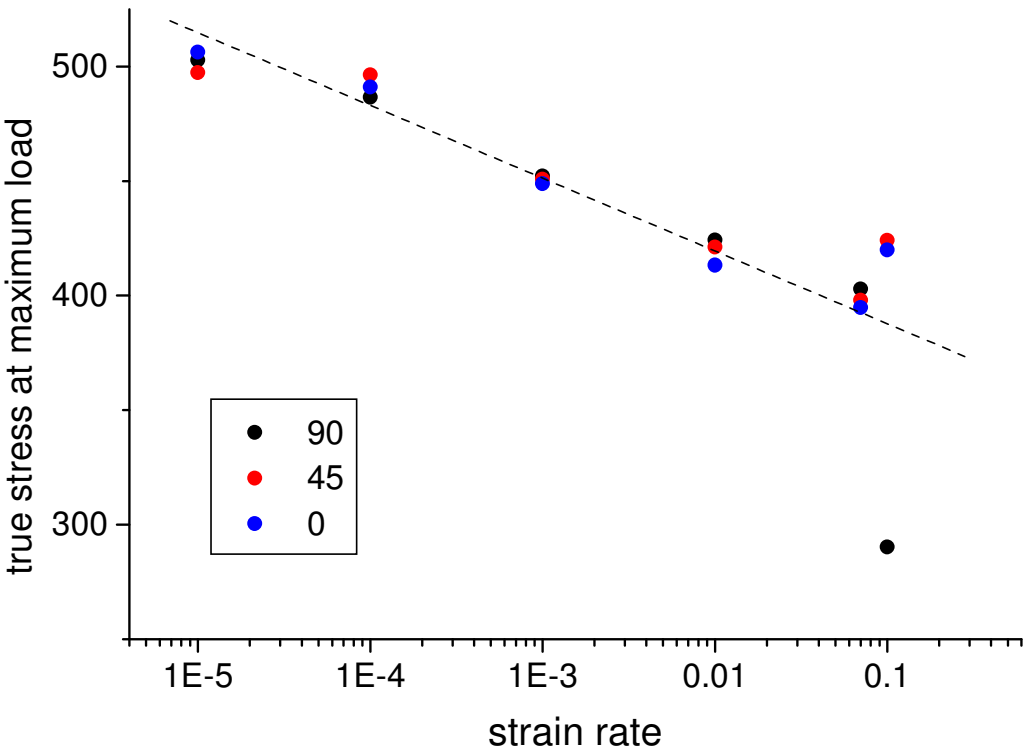

Fig. 7. True stress at the maximum load as a function of strain rate.

The Portevin-Le Chatelier Effect in Alloy 2024 – Part 2 (Further test results)

2.3.3. The goal and a brief description of tests

In Part 1, the strain rate domain of existence of the PLC instability in the alloy under investigation was determined and general trends were found for the strain rate dependencies of macroscopic parameters. The goal of the following tests was to examine these dependencies with shorter strain rate steps in order to check the preliminary conclusions and establish quantitative criteria for numerical models.

The same sets of tests were performed for each of the three batches of samples characterized by different tensile specimen axis orientations with regard to the rolling direction (0°, 45°, and 90°). The following values of the imposed strain rate were chosen: $\dot{\varepsilon}_a = 10^{-5}$ s^{-1}, 2.9x10^{-5} s^{-1}, 10^{-4} s^{-1}, 2.9x10^{-4} s^{-1}, 10^{-3} s^{-1}, 3.1x10^{-3} s^{-1}, 10^{-2} s^{-1}, 3.1x10^{-2} s^{-1}, 7.3x10^{-2}s^{-1}, 10^{-1} s^{-1}, 7.5x10^{-1} s^{-1}. Here, $\dot{\varepsilon}_a$ is the total strain rate imposed by the deformation machine and composed of the

© 2005 SYNCOMECS Consortium Members

plastic strain rate of the sample and the elastic strain rate of the machine-specimen system, i.e. $\varepsilon_a = \varepsilon + \varepsilon_e$ (see the first report). Tests at 10^{-1} s^{-1} and $7.5x10^{-1}$ s^{-1} were performed using both a screw-driven and a servo-hydraulic machines. This made it possible to measure the values of critical parameters for a broad range of strain rates.

In the same way as before, the measured stress vs. time curves were used to calculate the true strain:

$$\varepsilon = \ln \frac{Vt - \sigma / M}{L_0}$$

where V is the grip displacement velocity, t is the time, M is the combined machine-specimen stiffness, L_0 is the initial specimen length. This was done because strain becomes localized in deformation bands when the plastic flow is unstable, so that the signal from a standard extensometer is no longer representative of the average strain associated with the total gauge length. The true stress σ was calculated from the engineering stress σ_{eng} using the true strain values: $\sigma = \sigma_{eng} \exp(\varepsilon)$.

2.3.4. Main Results

Figure 1 schematically shows the domain of existence of the PLC effect for the alloy studied and the corresponding types of the effect in the traditional taxonomy.

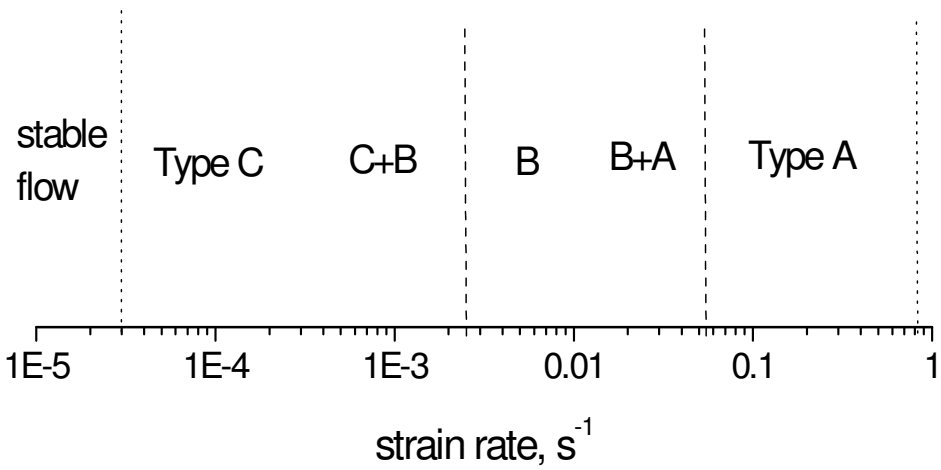

Fig. 1. Schematic map of the PLC effect

2.3.4.1 Critical parameters for occurrence of the PLC effect

Fig. 2 represents critical strain and critical stress values for the onset of plastic instability. To make the figure better readable the error bars representing the scatter of the data are only shown for 0° samples. The error bars only give an estimate of the scatter since most of the data points were obtained using data for as few as 3 specimens. It can be seen from the figure that the data are not noticeably influenced by the specimen orientation, in contrast to the slight trend one could have expected from the preliminary tests.

The inverse behavior is observed in the range of ε_a from 10^{-5} s^{-1} to 10^{-3} s^{-1} and corresponds to the type C or C+B of the PLC effect. The relative scatter is quite high and the behavior is

© 2005 SYNCOMECS Consortium Members

quite irregular in the range of about several times 10^{-4} s^{-1} to several times 10^{-2} s^{-1} corresponding to the plateau with the minimum values of critical parameters. This plateau may be characterized as a progressive transition from the pure C type to the pure A type. This indicates that the nature of spatial correlation of deformation processes is changing progressively when the strain rate is being increased. The transitive character of this region is illustrated in Fig. 3 showing that even the shape of deformation curves (indicative of type of the PLC effect) may vary from sample to sample for the same strain rate.

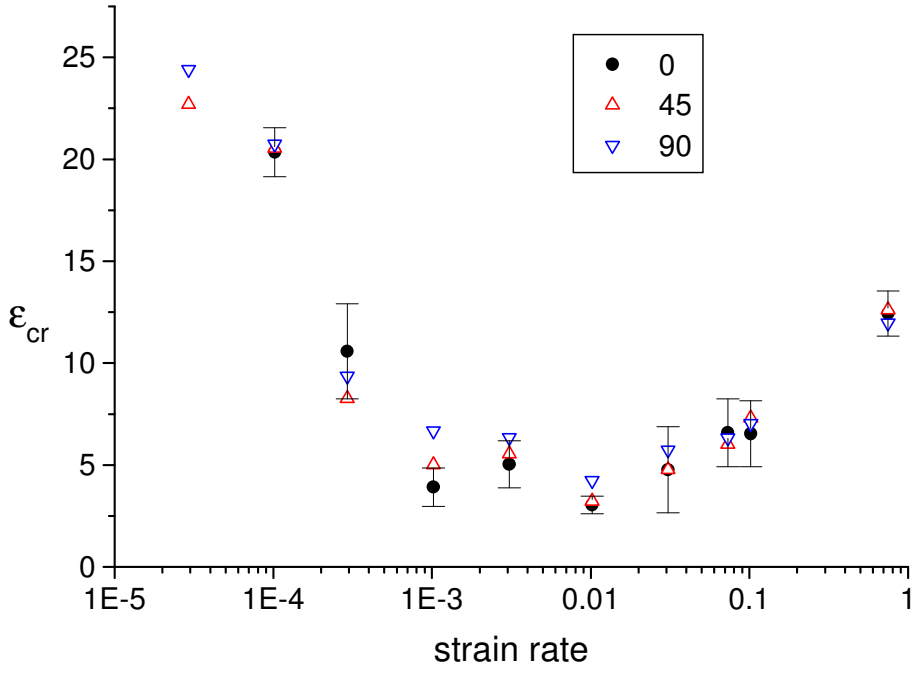

Fig. 2a. Critical strain vs strain rate

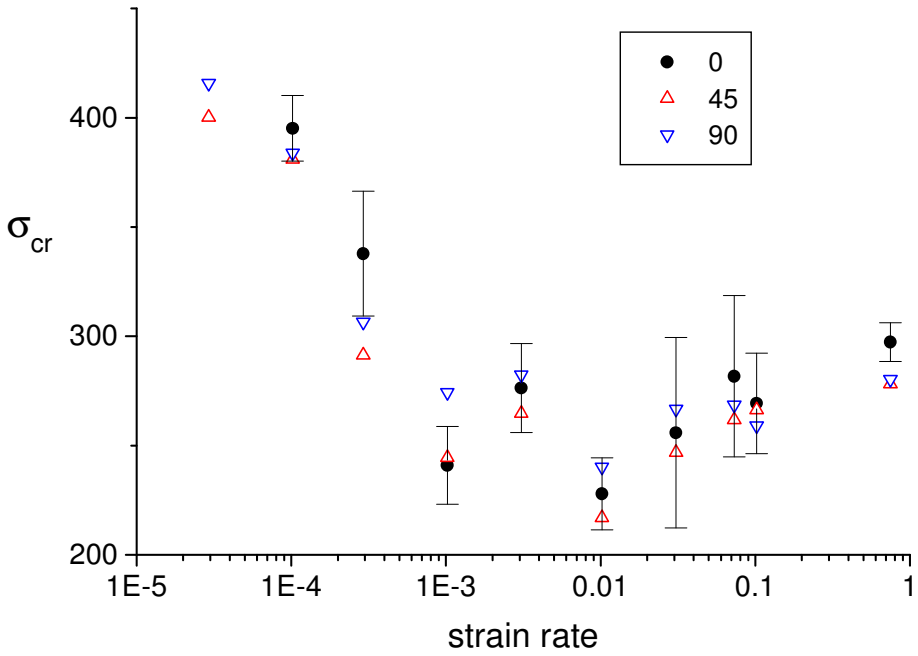

Fig. 2b. Critical stress vs strain rate

© 2005 SYNCOMECS Consortium Members

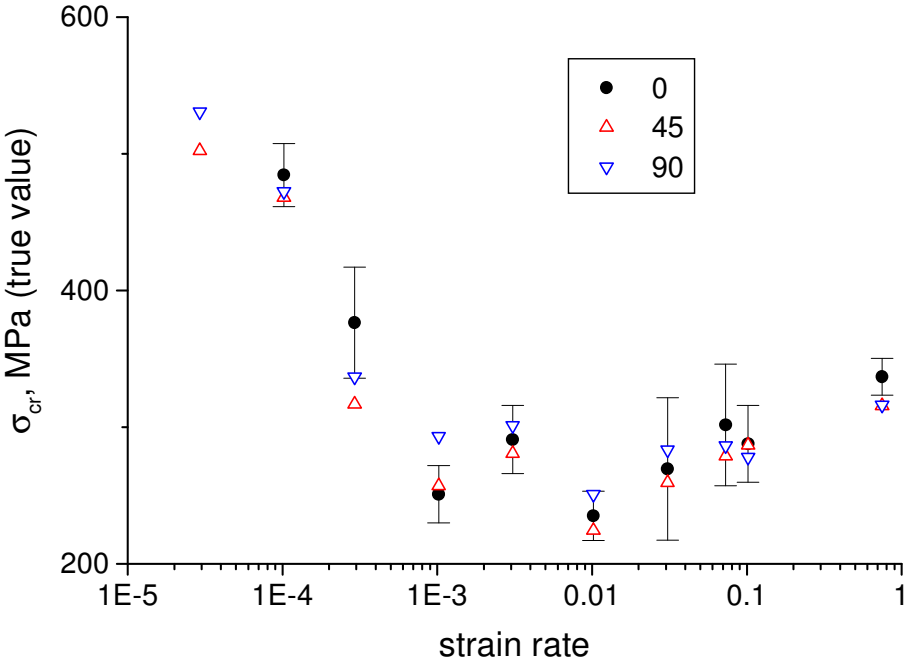

Fig. 2c. True critical stress vs strain rate.

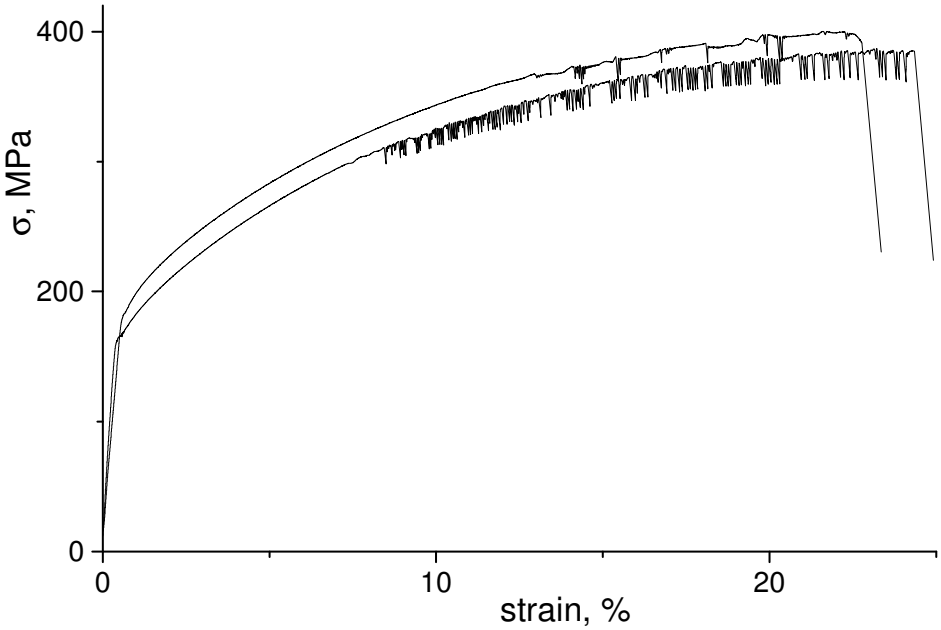

Fig. 3. Examples of deformation curves for the same strain rate of 2.9×10^{-4} s^{-1}.

2.3.4.2 Hardening, Ultimate tensile stress

The variation of the shape and the parameters of deformation curves with the strain rate follows the trends presented in the previous report. Additional tests made for the strain rate of $10^{-1}s^{-1}$ proved that the brittleness of 90° samples tested before was due to their bad quality. It

© 2005 SYNCOMECS Consortium Members

can be recognized from Fig. 4 that the additional set of samples does not show any peculiarities for 90° samples.

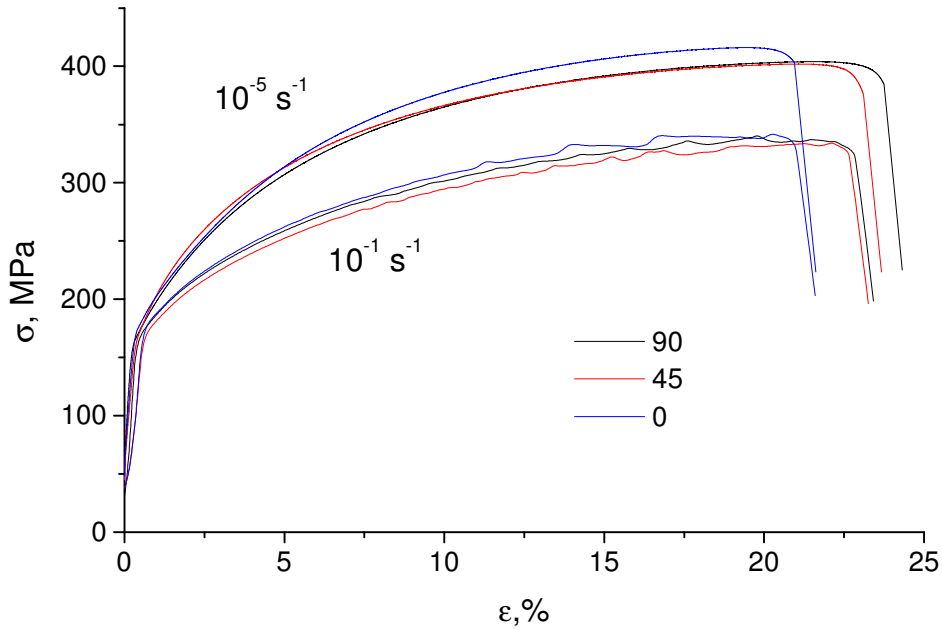

Fig. 4. Deformation curves for a low and a high strain rate for different orientations of the tensile axis.

Figs. 5 and 6 show the behavior of the ultimate tensile strength (UTS) and the corresponding strain at maximum load. Several observations should be stressed.

- The UTS data obey a logarithmic dependence in the whole range of strain rates: $UTS = A + B \ln \dot{\varepsilon}_a$ (B ≅ 20 MPa for nominal UTS; B ≅ 25 MPa for UTS calculated on the basis true stress (UTS_{true})). Usually no direct relation is observed for these quantities. The UTS is slightly higher for 0° samples, which is consistent with the higher flow stress values. However, the strain at maximum load is lowered so that the UTS_{true} values fall on a curve common to all samples (Fig. 6).

- The strain at maximum load depends on the specimen orientation. Moreover, for 0° and 45° samples, the corresponding strain rate dependencies show up slight peculiarities correlating with the strain rate dependencies of critical parameters for the PLC effect (Fig. 2). This indicates a sensitivity of tensile ductility to the PLC instability. At the same time, these peculiarities are not recognizable for 90° samples.

© 2005 SYNCOMECS Consortium Members

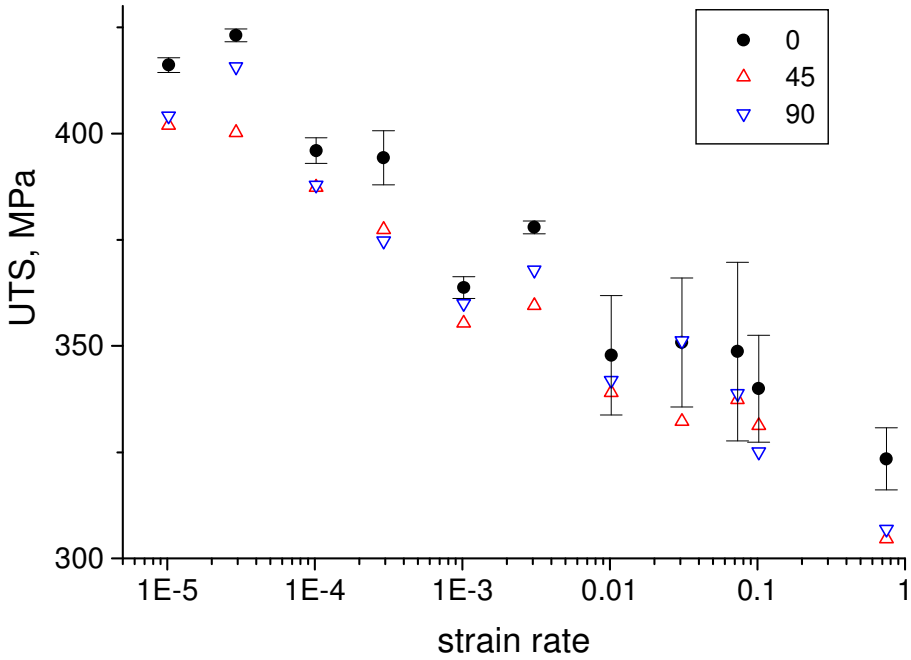

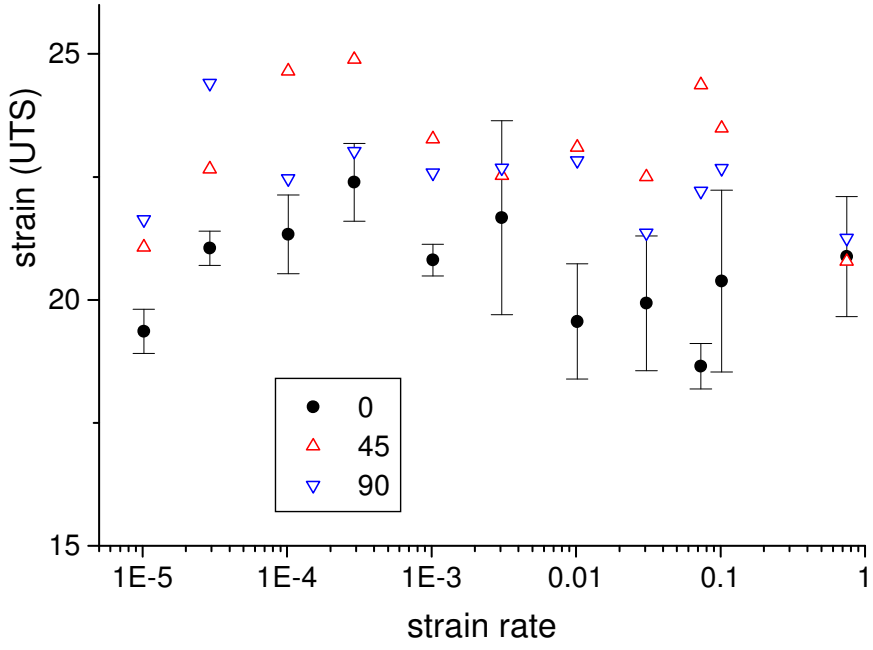

Fig. 5. The UTS and the strain at the maximum load as functions of the strain rate.

© 2005 SYNCOMECS Consortium Members

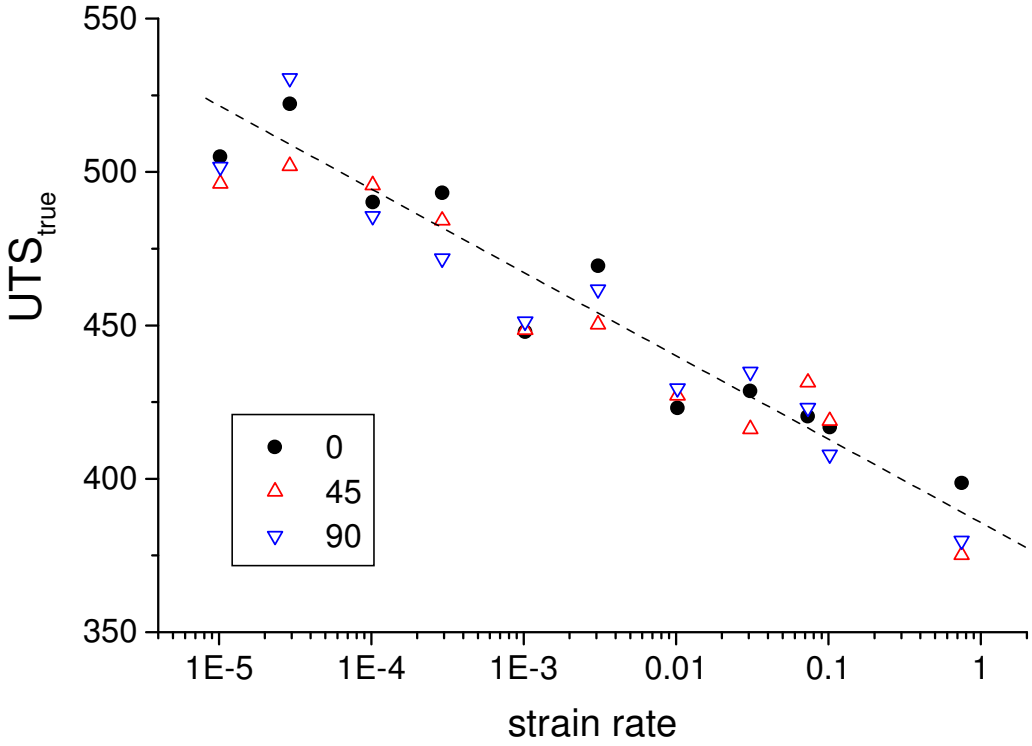

Fig. 6. True stress at the maximum load, UTS_{true} , as a function of strain rate.

© 2005 SYNCOMECS Consortium Members

2.4.INTEC

1 INTRODUCTION

Mechanism synthesis is an inverse problem where the aim is to find the mechanism for a given motion. Specifically, we restrict ourselves to study the synthesis of planar single and multi-loop linkages mechanisms.

Conceptual design of mechanisms has two main stages: (i) Type Synthesis, where the number, type and connectivity of links and joints are determined for the required degree-of-freedoms and structural constraints, and (ii) Dimensional synthesis, where the link lengths and pivot positions at the starting position are computed. In the pursuit of an optimal design, the user must evaluate both, type and dimensional synthesis. For this purpose, we have developed computational tools programming methods for type and dimensional synthesis of mechanisms.

Planar multi-loop linkage mechanisms are used to develop complex and non-linear motions. In classic literature (Sandor and Erdman, 1984; Erdman and Sandor, 1997), three well known customary tasks for kinematics synthesis were deeply studied:

- Path Following (PF), where the purpose of the synthesis is to determine the dimensions
  of a mechanism so that one point of the mechanism moves through a series of preset
  positions.
- Rigid-Body Guidance (RBG), the positions and also the orientations of a point in the mechanisms are prescribed.
- Function Generation (FG), the orientations of two members of the mechanism must follow a prescribed function or law.

In the practice of solving industrial problems, these tasks often appear in a combined way: two or more of these tasks may be required to be performed for different bodies of the same mechanism. The motivation and main objective of the present work is to complete those already developed methods to solve these multiple tasks, trying also to preserve the generality needed in Computer-Aided Synthesis Methods.

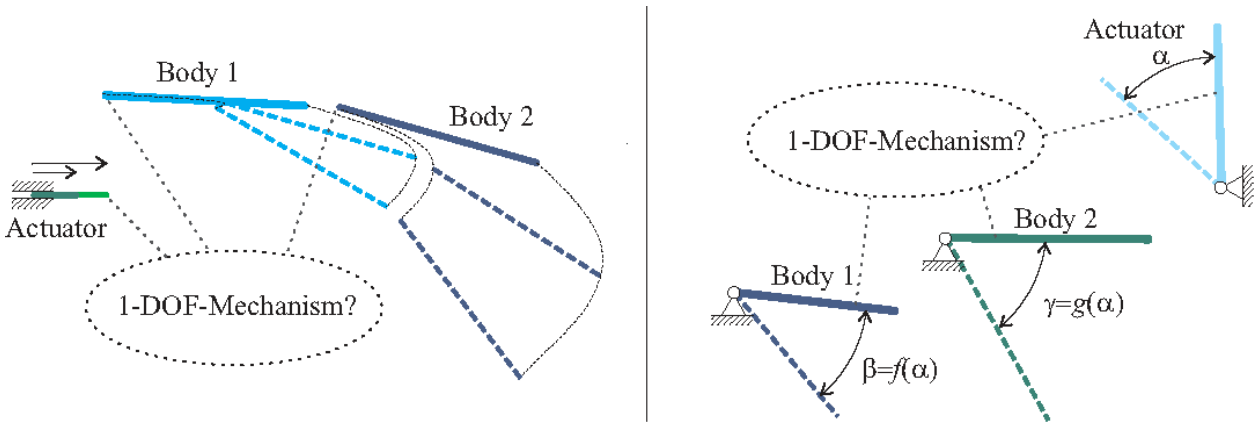

Figure 1: Multiple Rigid-Body Guidance (left) and Multiple Function Generation (right).

© 2005 SYNCOMECS Consortium Members

Graph Theory proves to be a useful mathematical tool for modelling and computer implementation of discrete problems, thus it has been extensively used for solving the type synthesis of mechanisms in the last four decades (Mruthyunjaya, 2003). In a recent work of the authors, a method to find type synthesis solutions from the Finite Element Method (FEM) description of a prescribed task was proposed. The problem of finding and codifying all-non isomorphic solutions for a given kinematic problem was solved using Graph Theory and combinatorial algorithms (Pucheta and Cardona, 2007a). An important characteristic of the method is that both the FEM description of the parts entered by the user in the initial problem and its automatically made Graph conversion are retained and completed with new members -links and joints- present in the final solution. Then, the mechanism can be dimensionally sized by many techniques.

The dimensional synthesis of mechanisms is a highly non-linear problem. In most cases, for any given mechanism topology, it is difficult to find a good initial guess for starting a gradient-based optimization. The geometrical methods based on Precise Positions, also called Precision-Point Methods, are of great help to find initial dimensions. There exist well known procedures to synthesize single open-chains (SOCs) like dyads and triads passing through three, four and more positions (Erdman and Sandor, 1997; Sandor and Erdman, 1984). We have programmed dyads and triads passing through three and four positions, whose solutions are exact and fast to compute (consequently, do not need the use of iterative methods). Depending on the initial data of these SOCs, we may need to propose some free parameters. To apply this analytical method for solving a given type synthesized solution, i.e. a mechanism topology, it is necessary to decompose the closed chain into several SOCs. This decomposition is not unique and different decompositions might lead to a different number of free parameters. In a previous work we compute many decompositions using the minimal set of independent loops of the topology, and then we retain those decompositions which present a set of SOCs with a minimal number of free parameters (Pucheta and Cardona, 2006). We also take the convention of preferring those

© 2005 SYNCOMECS Consortium Members

sets which solve the largest number of imposed motion constrains in a specified order, from the first to the last SOC.

Then, after retaining a decomposition we run a multi-objective optimization where we propose values for the free parameters to solve the set of SOCs which minimizes the size of the mechanism, and also we check some constraints useful for linkage design: minimal length of links, allowed space constraint, and a singularity constraint to avoid locking situations.

This sequence of procedures for type and initial dimensioning was successfully used to solve linkages with four-, six- and eight-bars rigid mechanisms. Although the present work deals with the design of rigid mechanisms, the solution of multiple tasks finds special application for the guidance of compliant members. This idea and the study of the Rigid-Body Replacement of binary links (Howell, 2001) are promising areas to obtain flexible mechanisms (Pucheta and Cardona, 2007a).

In Section 2 we review the available method for type synthesis of mechanisms and incorporate the proper changes in order to take into account multiple tasks. In Section 3 the decomposition method for multiple tasks is explained. In Section 5 we show the results for an example used throughout this paper.

2 TYPE SYNTHESIS REVIEW

Given structural requirements, the aim of Type Synthesis is to find the number of parts, number of links and joints, types of links and joints, and their connectivity. The work can be simplified if the potential mechanisms solutions are previously enumerated and stored in a data base. Then, it only remains to select those mechanisms for which some parts match with those given in the task. Since the order of the enumerated mechanisms could be of hundreds, even thousands, the visual inspection may easily lead us to neglect some feasible alternatives, for this reason we resorted to the aid of the computer.

The enumeration of mechanisms is actually a challenging area (Mruthyunjaya, 2003). The enumeration process is usually divided into: (i) the enumeration of basic kinematic chains (BKC) for a given number of degree-of-freedoms (Tsai, 2001), and (ii) the assignment of types of links and joints for each BKC, a process which is also called “Specialization of Mechanisms” (Yan and Hwang, 1991). We have followed this procedure to form different atlases of mechanisms, represented by graphs codified in an unequivocally way. Each kinematic chain is represented by the adjacency matrix of its graph G(E, V), where each link is represented by a vertex and each joint is the connection between vertices. The specialization of the links and joint types is formulated as an assignment problem and a colored graph representation is used. The adjacency matrix of the colored graph has integer entries representing link types on the diagonal entries and joint types on the outer diagonal ones. We call it Type Adjacency matrix T.

Using this matricial representation and an isomorphism identifier based on the Degree Code

© 2005 SYNCOMECS Consortium Members

we codified atlases with one and two degree-of-freedoms, rigid and flexible links, and revolute, prismatic, flexible, and clamped joints (Pucheta and Cardona, 2007b).
We also propose to represent the kinematic problem in hand by a graph that we called "Initial Graph". Since the kinematic problem and the atlases are represented by graphs, the type synthesis process consists in detecting and codifying all non-isomorphic subgraph occurrences of the Initial Graph inside a selected atlas.

The number of inputs desired for actuating the mechanism solution is managed by only selecting the atlas already available with the proper number of degree-of-freedoms. The number
of outputs of the mechanism is described by the "Initial Graph" construction. This graph is
built from the interpretation of the Finite Element description of the kinematics problem. Using
the Samcef Field graphic interface (SAMTECH Group, 2007), the geometric description of the
known mechanism's parts is entered in terms of nodes which are then used for defining bodies
(Wire, Face, and Lumped Mass elements) and the allowed space. Next, the user defines elements for assembling bodies (Hinge, GroundHinge, GroundPrismatic, and Fixed connections), and finally defines the motion constraints prescribed at the synthesis problem, either by setting the motorization of joints or by defining constraints (Clamp, Prescribed Displacement, Prescribed Rotation) over nodes and bodies. This initial situation is analyzed and automatically converted into a graph following these rules:

Vertices: Free bodies with imposed movements will be isolated vertices of the initial graph.
The remaining bodies, connected through joints, will be connected vertices of the graph.
Conventionally, the ground link will be the vertex zero. Depending on the number of
grounded bodies, this vertex may be binary, ternary, etc. The number of isolated fixations (represented by fixed nodes) is used to prescribe the degree of vertex zero (ground). For each isolated node with prescribed movements, we assign an isolated vertex in the graph, although this node is not attached to any element.

Edges: Joints will be edges of the initial graph connecting two of the previously defined ver-
tices; all edges are assumed to be binary (isolated joints are not allowed).

The application of these rules for multiple tasks like (PF) and (RBG) produces isolated-disconnected- vertices on the Initial Graph. For instance, in Figure 2-a we show the requirements for a mixed problem where the trajectories for two isolated nodes are imposed (the node in the right also has imposed rotations), thus we obtained two vertices in the initial graph in correspondence with the floating links developing the tasks (Figure 2-b).

© 2005 SYNCOMECS Consortium Members

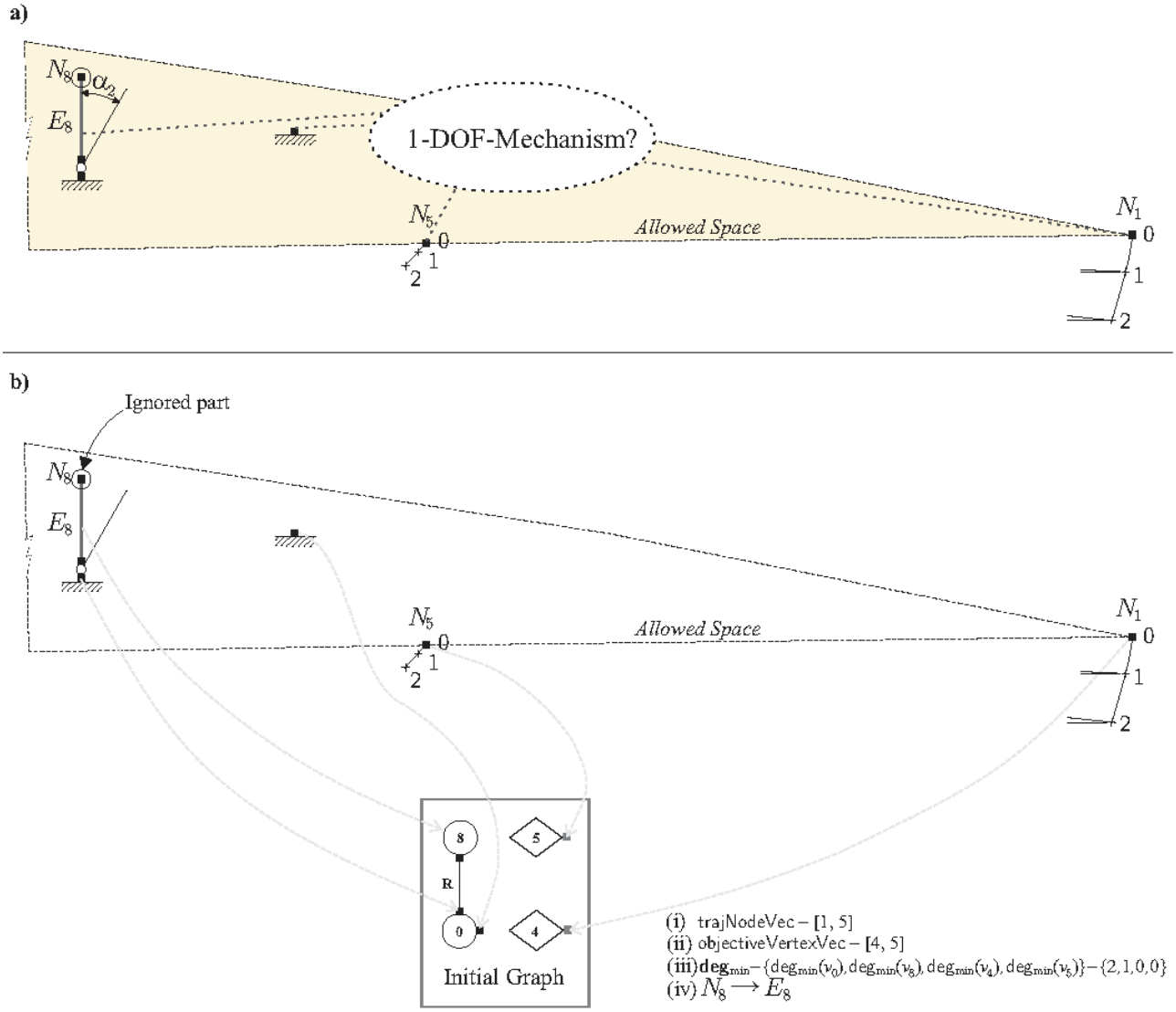

Figure 2: Translation from FEM (a) to graph (b) representation for a double task.

We allow defining adjacency matrices with both null rows and null columns corresponding with a disconnected body.

For tasks of PF and RBG it is undesirable to have floating links connected to the ground, thus we add a distance constraint limiting the distance between the ground v_0 to the floating links to a minimum value of 2.

Some results of the subgraph search for this example will be shown in Section 5, but we must remark that the subgraph search admits initial graphs with disconnected components. See for example, the first subgraph occurrence in Figure 3 of the following section. Since, the fulfillment of the distance constraint rejects the possibility of getting four-bars solutions, this first solution is a six-bars topology.

3 TOPOLOGY DECOMPOSITION

The decomposition of the topology into SOCs is achieved using some background of

© 2005 SYNCOMECS Consortium Members

Graph Theory. The number of independent closed loops, v , is a property of the graph. Since all mechanisms have closed topology it is always implicit in their number of vertices v and edges e, then v = v – e + 1. The set of independent loops of minimal length allows to find the significant dimensions of links (Erdman and Sandor, 1997).

The decomposition method consists in the following steps (Pucheta and Cardona, 2006):

S1) Topology decomposition: The kinematic chain (closed-loops chain mechanism) is decomposed into a set of separated closed-loops (known as cycles in Graph Theory, Harary, 1969 or circuits, Tsai, 2001) of minimal length.

S2) SOCs decomposition: For each set of closed-loops, each closed-loop is selected in a given order to be decomposed into SOCs, i.e. dyads, triads, quadriads, etc., using the node displacement constraints.

S3) SOCs evaluation: After analyzing data (geometry and synthesis data definitions), the SOCs solvability is evaluated in the resultant order.

S4) Retained ordered SOCs: The best valuated combination/s of open-chains is/are stored for dimensional synthesis.

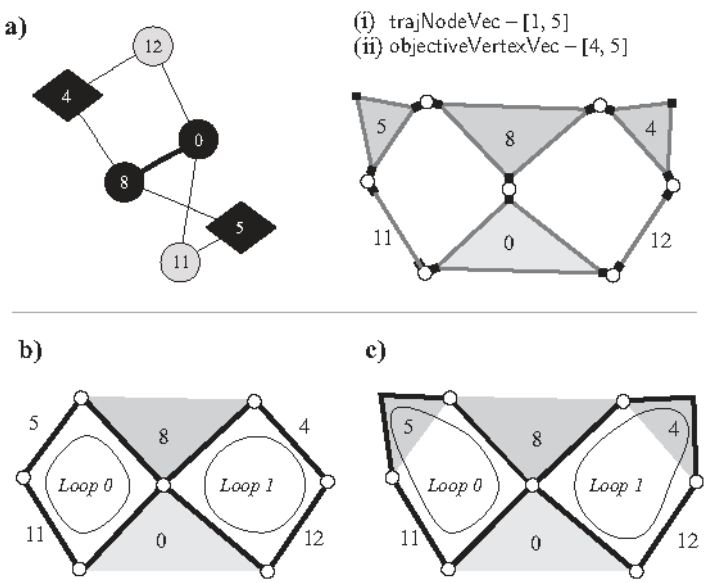

Figure 3: Minimal independent loops of the graphs and the additional vectors with information referred to nodes (i) and their associated vertices (ii).

This method is also suitable for multiple tasks, the main improvement is that we

© 2005 SYNCOMECS Consortium Members

form a vector of trajectory nodes called trajNodeVec, and a vector objectiveVertexVec with their corresponding vertices in the graph (Figure 3-a). These data are used for the determination of the significant dimensions in the linkage. The computation of the basis of minimum independent loops is made using the graph, see Figure 3-b.

As it is shown in Figure 3-c, the significant dimensions are found by means of the extension of the loop which visits a given vertex in objectiveVertexVec[i] passing through the corresponding node in the trajNodeVec[i] with equal index of position i. These loops are marked in order to do a decomposition in both orientations.

4 INITIAL SIZING

The type synthesis stage finished with the decomposition into single-open chains. Then, a second stage of initial sizing for synthesis is launched for each feasible alternative. The design space is defined by the set of free parameters, if any. The user can change the values of their bounds, and a genetic algorithm is used to sweep the design space. The fitness function consists in the minimization of the size of the mechanisms together with three weighted constraints: minimal length of link dimensions, non-inversion of transmission angle, and allowed space violation (Pucheta and Cardona, 2005). Eventually, instead of considering non-inversion of transmission angle as a constraint, a full kinematics analysis is made for each individual to compute the fitness function.

A posteriori of the synthesis task, the user can verify the validity of the proposed solution by means of analysis, and he can even optimize the solution staying within the same topology.

5 TEST: TWO BEAMS DEFLECTION

The proposed test problem consists in finding a mechanism able to produce the deflection of two curved beams. The boundary conditions are shown in Figure 4. The topology can be considered as a compliant mechanism itself. If this mechanism is actuated by the prismatic joint, its full kinematics description at any point of the beams can be obtained.

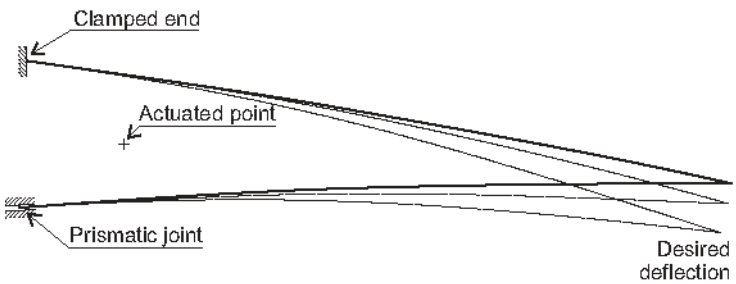

© 2005 SYNCOMECS Consortium Members

Figure 4: Boundary conditions for the deflection of two beams.

In a previous work, (Pucheta and Cardona, 2007a), we presented solutions for this problem where we guided the tip of the beams (Rigid-Body guidance) considering the prismatic joint (shown on the left of Fig. 4) as passive. We propose to solve this compliant synthesis problem using synthesis of rigid mechanisms with multiple tasks. In the following subsections the synthesis stages are illustrated.

2.3. A mixed path following and rigid-body guidance example

In this paper, we desire to guide the tip but also another point, for example, we can choose the
intermediate point, P_H , of the lower beam (Figure 5). The point is guided by a set of positions, without prescription of orientations. This means that we must add a hinged connection between the mechanism and the lower beam. Therefore, we reformulate the problem as a multiple task: a path following task is required for node P_H and a rigid-body guidance for the tip P_{tip} .

This problem also corresponds with Figure 2-a and the explanations given in the previous sections. Both movements must be coordinated with the rotation of a motorized crank. The mechanism solution must fit inside an allowed space.

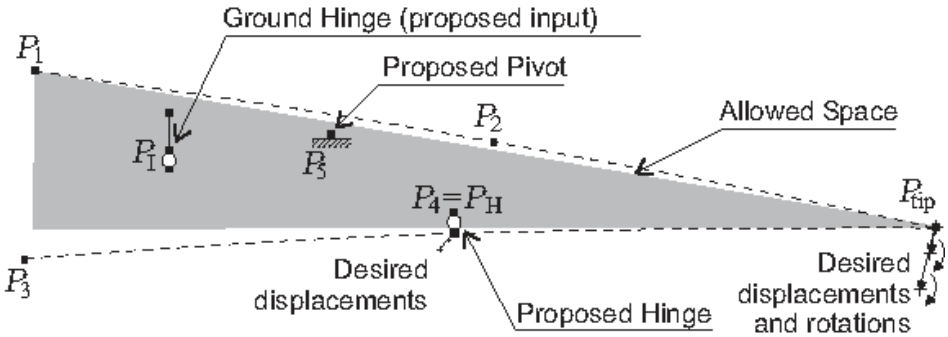

Figure 5: Deflection of two beams reformulated as a multiple tasks synthesis problem.

Data for this problem are coordinates and motion at the tip of the system, and at the lower beam intermediate point. The boundary conditions are one node clamped and the other one with known axial displacement (grounded prismatic joint).

5.2 Type synthesis outputs

The graphs for the first ten solutions are displayed in Figure 6. The algorithm for SOCs

© 2005 SYNCOMECS Consortium Members

decomposition gives us the Alternatives 0, 3, 4, 7, 8 and 9 as compatible to be solved analytically. Their sketches are shown in Figure 7.

5.3 Initial sizing using optimization

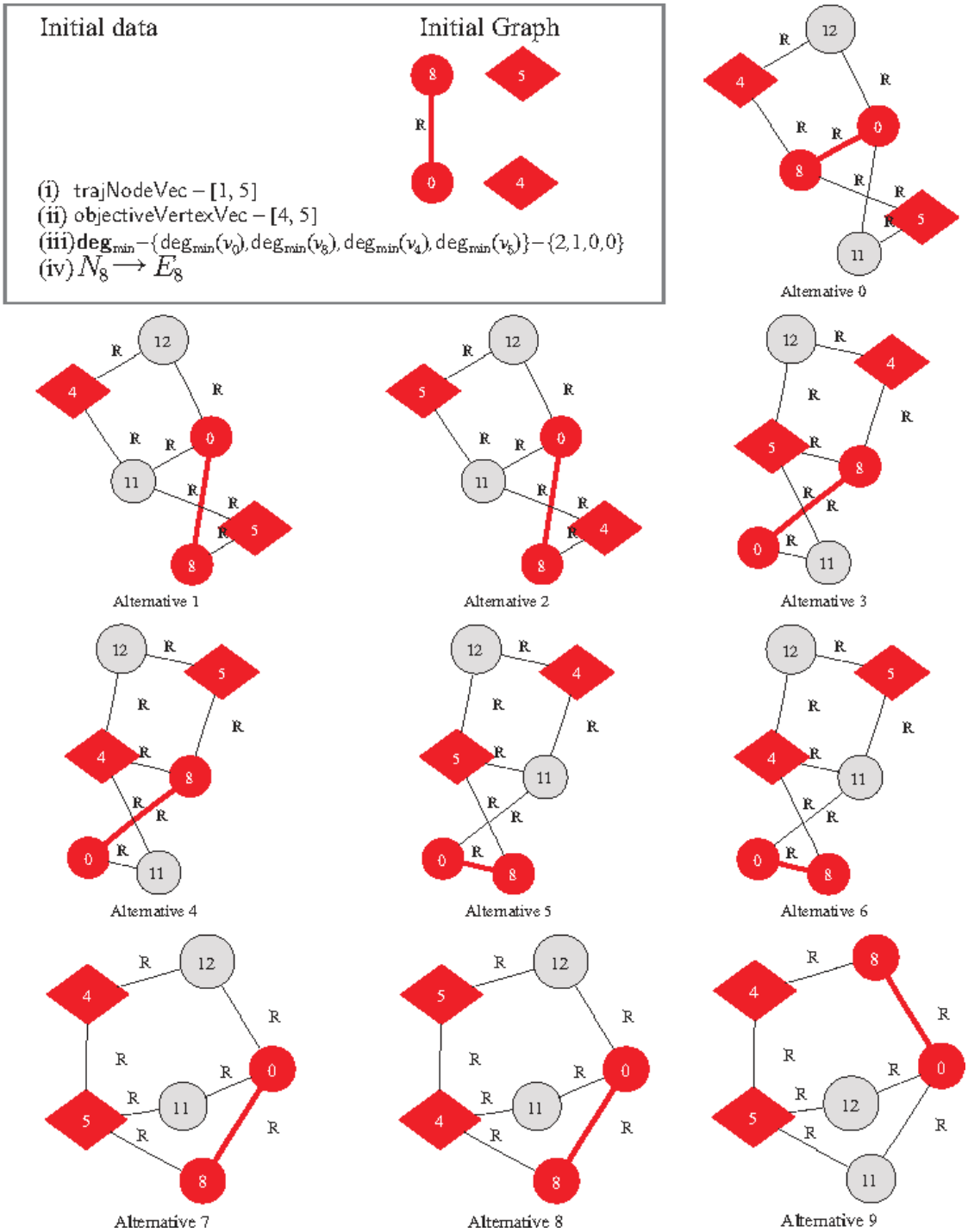

Figure 6: Data for the subgraph search and the first ten solutions of the type synthesis run.

A multi-loop solution corresponding to Alternative 7 is shown in Figure 8 where the beams were attached to the tip. Among the ten analyzed alternatives, this was the first one with a full satisfaction of constraints.

© 2005 SYNCOMECS Consortium Members

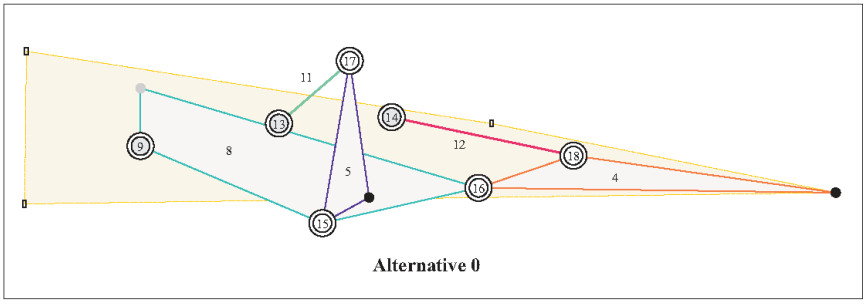

Alternative 0

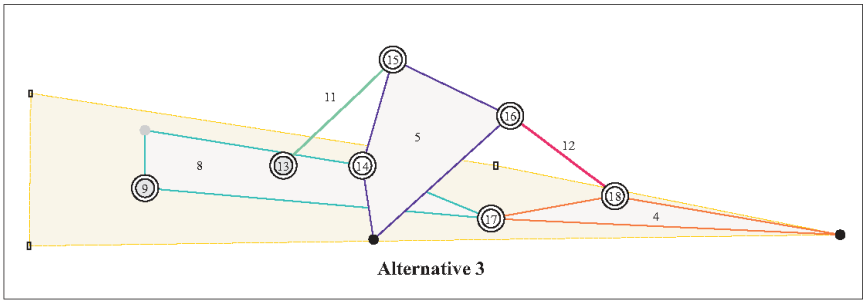

Alternative 3

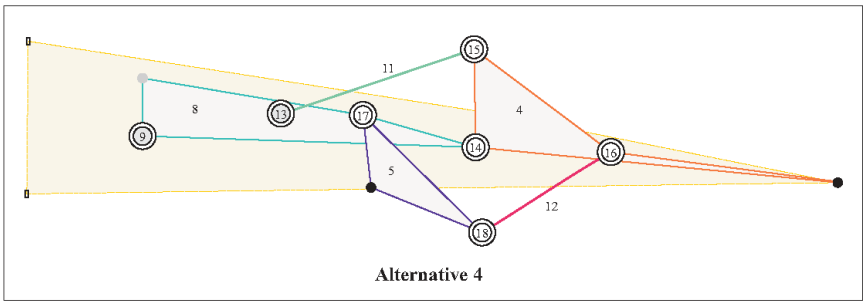

Alternative 4

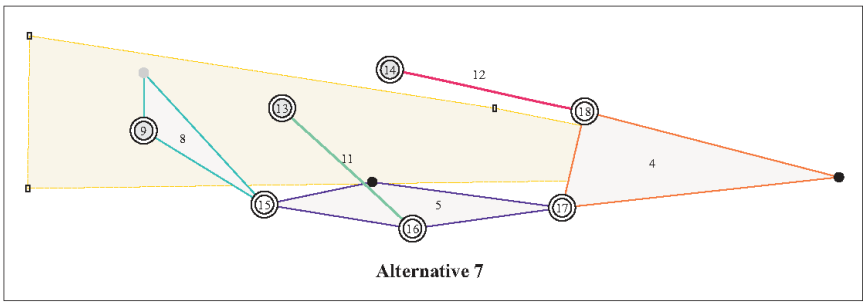

Alternative 7

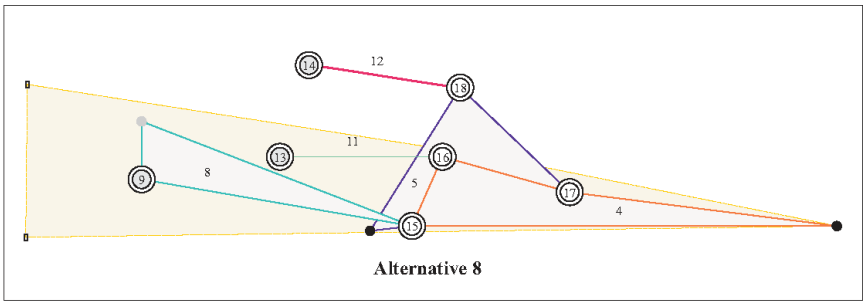

Alternative 8

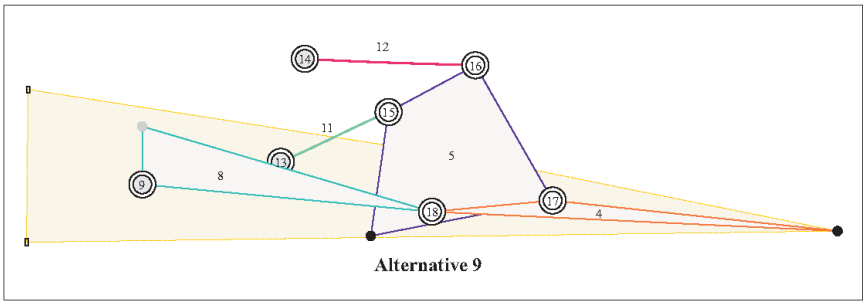

Alternative 9

© 2005 SYNCOMECS Consortium Members

Figure 7: Sketches of the feasible decompositions.

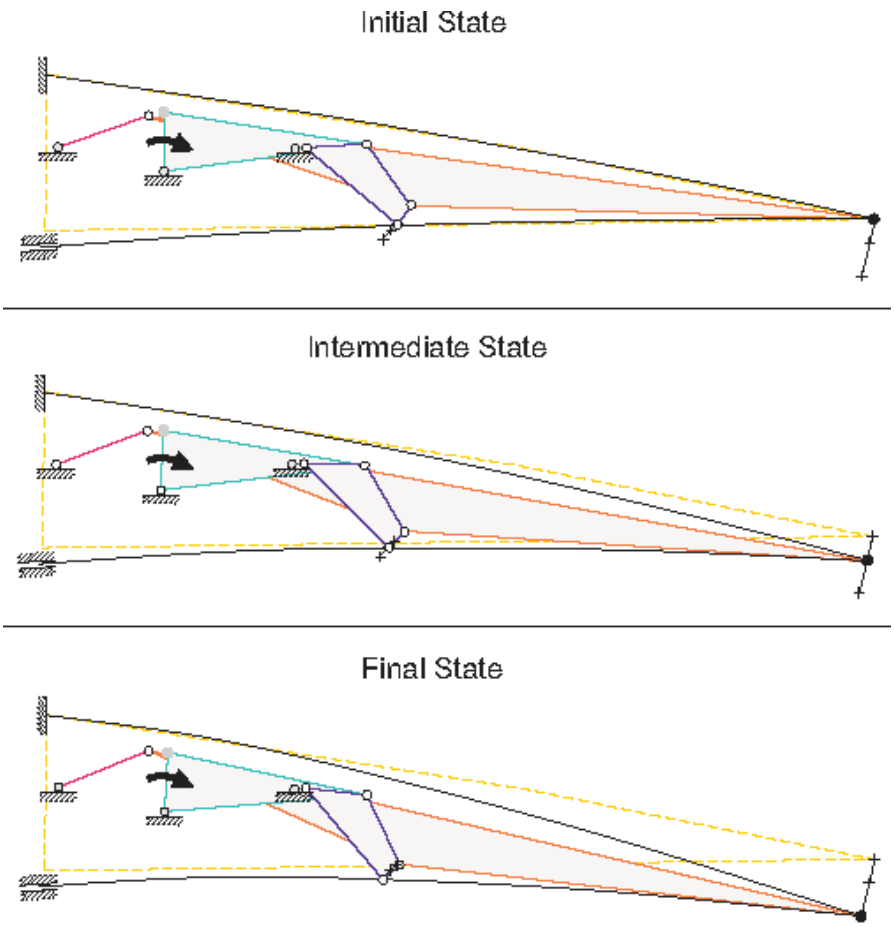

Figure 8: Alternative 7 multi-loop linkage passing exactly through three positions prescribed for a combined task.

6 TEST: THREE POSITIONS COORDINATION

In this case the prescribed parts leads to an initial graph of tree type. In Figure 9, the depicted initial graph is acyclic and has the form of a tree where the ground can be taken as the root.

© 2005 SYNCOMECS Consortium Members

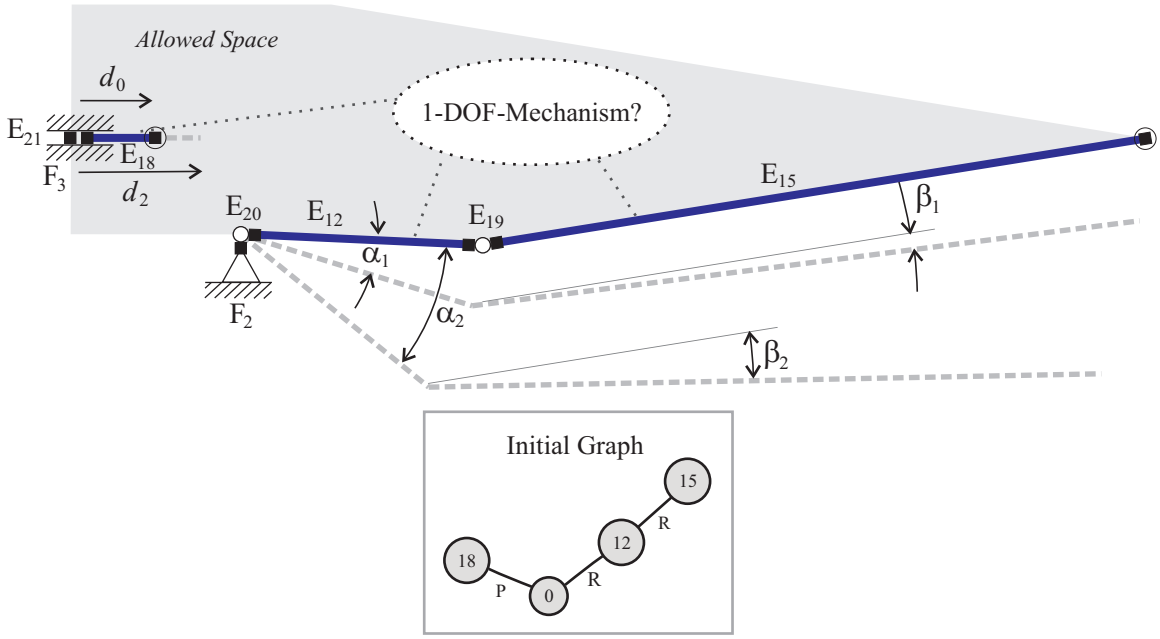

Figure 9. A three positions coordination problem between the rotations of two articulated bodies and the displacement of a prismatic actuator.

For the prismatic actuator only the final position is prescribed. The area where the new bodies and new pivots must hold is also prescribed by a Face defined by a closed-polygon.

6.1 The proposed analysis for known parts

The procedure to identify those already known dimensions and consequently those parts with already known kinematics behavior involves some manipulation on the initial graph in conjunction with the well-known Grüebler equation for the planar case:

$$f = 3(n-1) - 2j\,,$$

where *f* is the number of degrees of freedom, *n* is the number of bodies, *j* is the number of lower-pair joints (revolute or prismatic).

We need to make use of some basic Graph Theory definitions. A graph is connected if there exist a path for every two pairs of vertices. A component of a graph is a maximal connected subgraph. An isolated vertex forms a trivial component, consisting of one vertex and no edge. Then, the procedure is

© 2005 SYNCOMECS Consortium Members

the following:

I. The initial graph, G_{ini}, of the prescribed parts is built.

II. Sub-mechanisms are identified by pre-processing data in the following this steps:

a. Disconnect and delete the ground of the initial graph.

b. Compute the resultant connected *components,* H_i's.

c. For each component H_i, *consider all motion constraints as inputs*.

i. Connect the ground again, so that a sub-mechanism M_i is obtained.

ii. Compute the number of links and joints, n^i and j^i , respectively.

iii. Set a counter, $I^i = 0$, which identifies the number of inputs of the sub-mechanism. For every joint, detect the number of motion constraints, if this number is equal to the number of passing points defined for the problem, n_{pp}, increase in one the counter I^i.

iv. Compute the Grüebler equation: $f^i = 3(n^i - 1) - 2j^i$.

v. If $I^i = f^i$, mark and save the links, joints and nodes of the sub-mechanism for the initial kinematics analysis.

III. Run the kinematics analysis and save the components of displacements and rotations of those nodes marked in steps **II-c-v**.

In Figure 10, we can see very simple illustrations of the sub-mechanism formation for the problem presented in the introductory section. Note that the sub-mechanism M0 has incomplete motion constraints definition, because the user only specified the inital and final positions. Therefore, the nodes of the primatic joint must participate in the dimensional synthesis process for calculating the intermediate displacement d1.

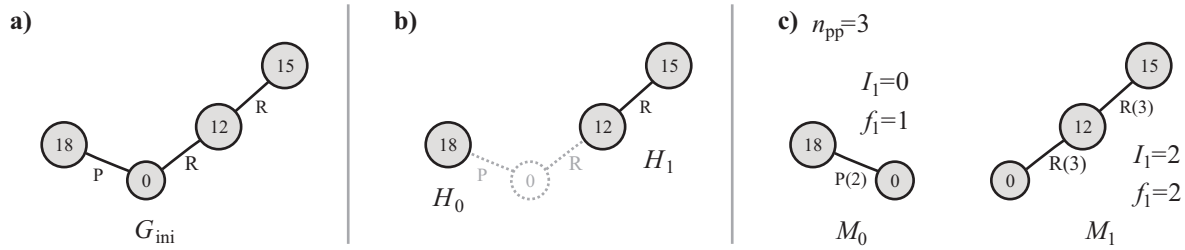

Figure 10. Algorithm for sub-mechanism identification: a) given graph; b) ground disconnection and components computing; c) sub-mechanisms formation.

We also should remark that the condition $I^i = f^i$ may result false for many well-posed problems for which dimensions are given but motion constraints are incomplete. Therefore, steps iii to v in II-c, requires a complex iterative algorithm for navigate through the vertices and edges of a given submechanism, in an increasing way, retaining the last set of vertices and edges for which the DOFs equals the number of inputs. The example developed for this work does not have this inconvenience.

6.2 Results

© 2005 SYNCOMECS Consortium Members

In this section we present some images representing results for the subgraph search, and initial sizing of this example. The initial graph for this problem, was shown in Figure 9. The subgraph search for the first ten occurrences is as shown in figure 11.

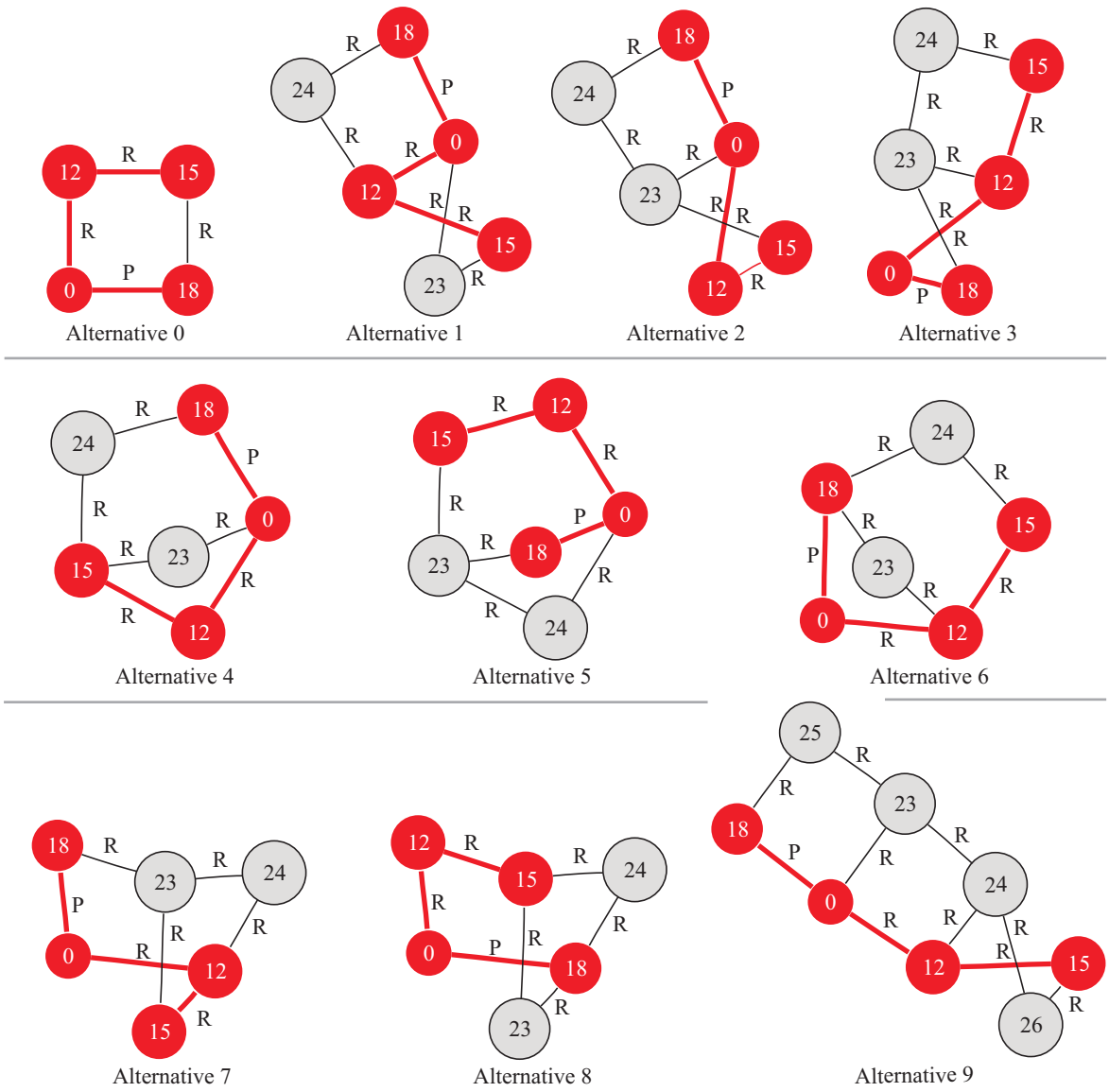

Figure 11. Non isomorphic graphs occurrences of the initial graph inside mechanisms of the atlas, obtained in the number synthesis stage. For clarity, edges are only labelled with their joint types (R: revolute, P: prismatic).

These 10 topologies are then analyzed and decomposed into single open-chains (dyads and triads passing through three positions) using the decomposition method proposed already described. In this case, our decomposition algorithm rejects the Alternative 0. The remaining alternatives are sketched in Figures 12 and 13.

© 2005 SYNCOMECS Consortium Members

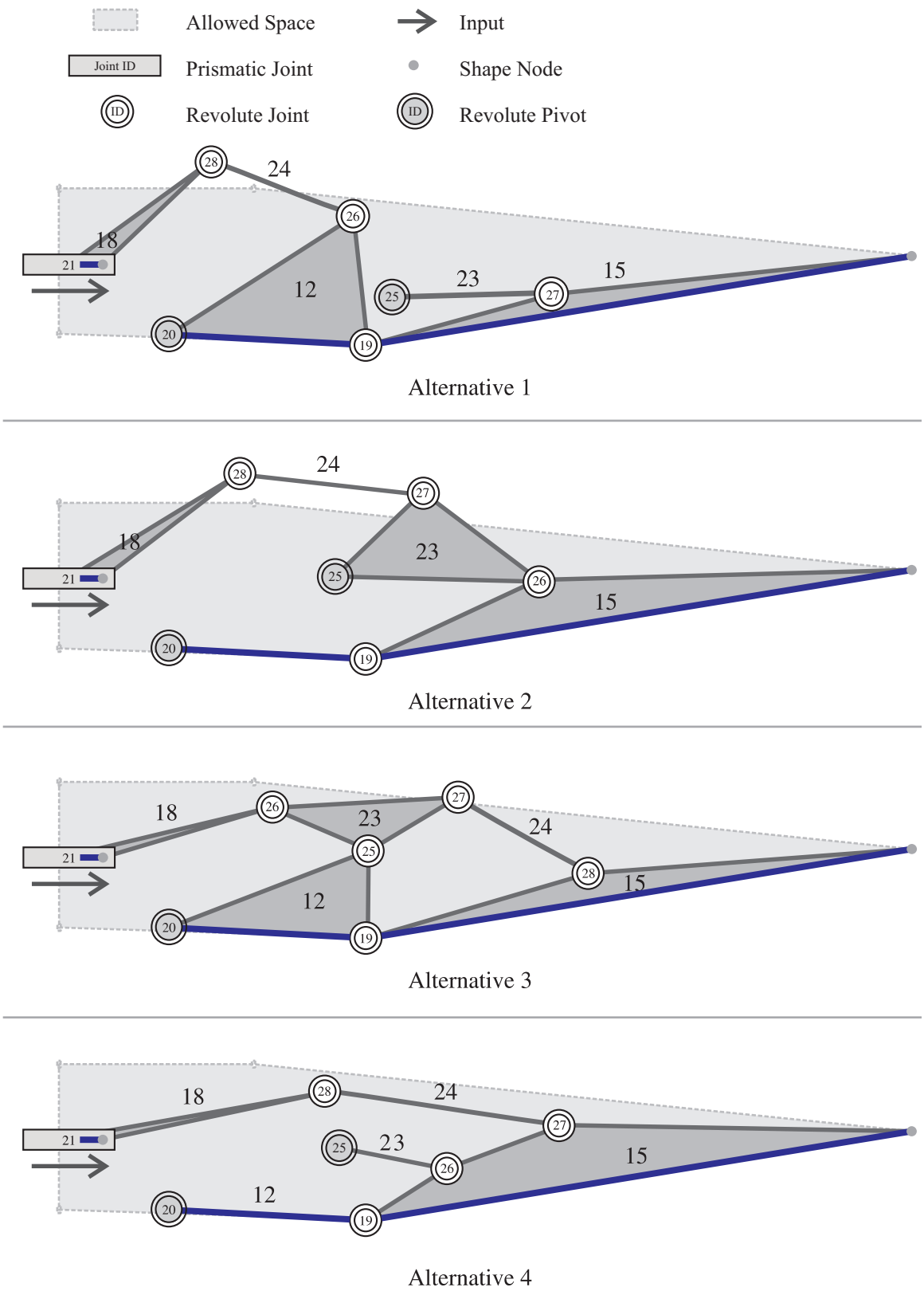

Figure 12. Sketches of the first eight alternatives found (continued).

Either from the graphs or, more easily, from the skecthes, we can realize that Alternatives 3, 6, 7, and 8, have a binary ground so that they use the imposed boundary conditions. The other feasible alternatives have a ternary ground, so that a new pivot location must be computed. When a pivot location is un-

© 2005 SYNCOMECS Consortium Members

known, the user must specify a box for the fixed node location, otherwise a box is taken by default by assigning the bounding box which contains all nodes.

© 2005 SYNCOMECS Consortium Members

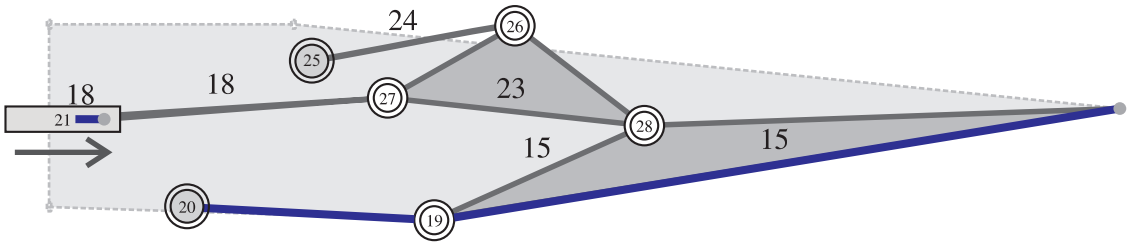

Alternative 5

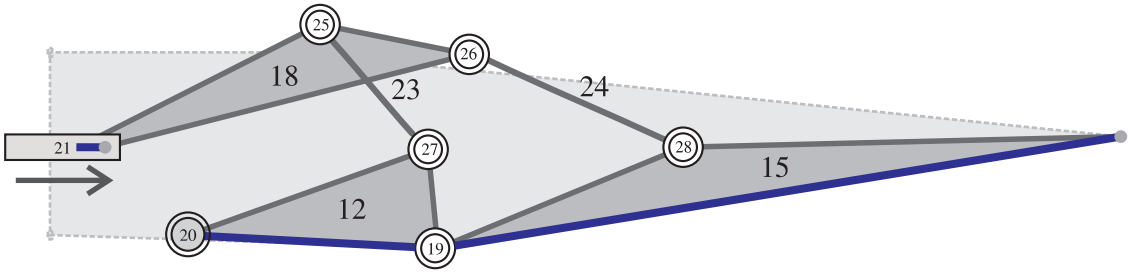

Alternative 6

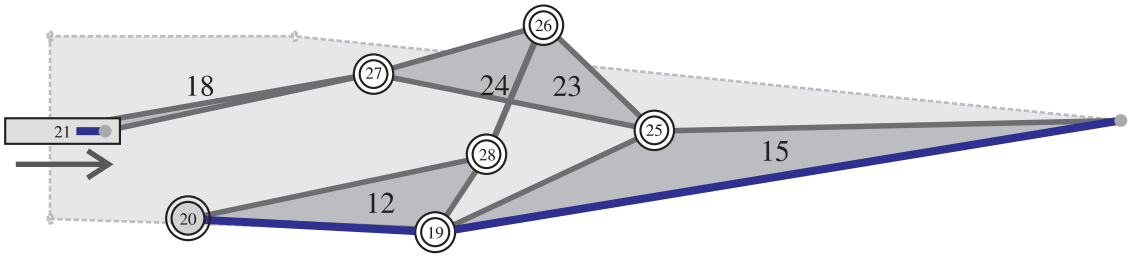

Alternative 7

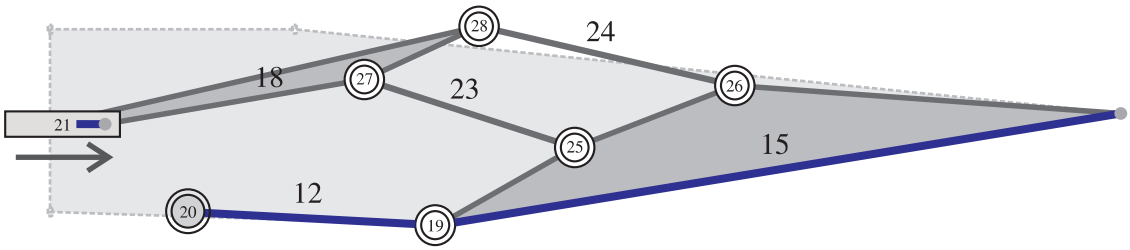

Alternative 8

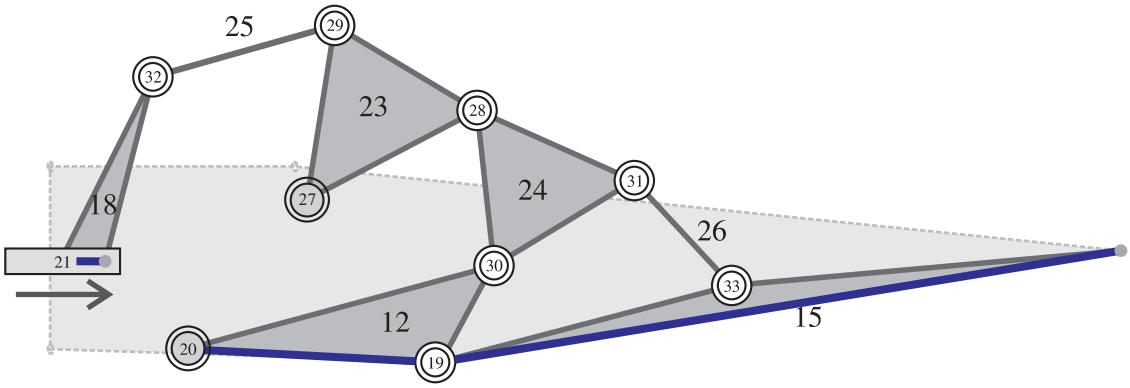

Alternative 9

Figure 13. Sketches of the first eight alternatives found.

© 2005 SYNCOMECS Consortium Members

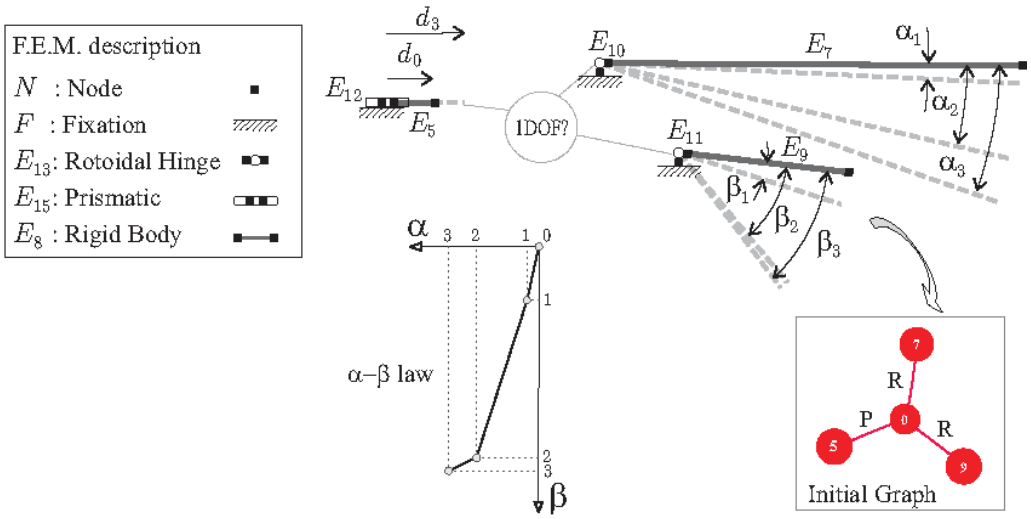

Figure 14. Double function generation problem.

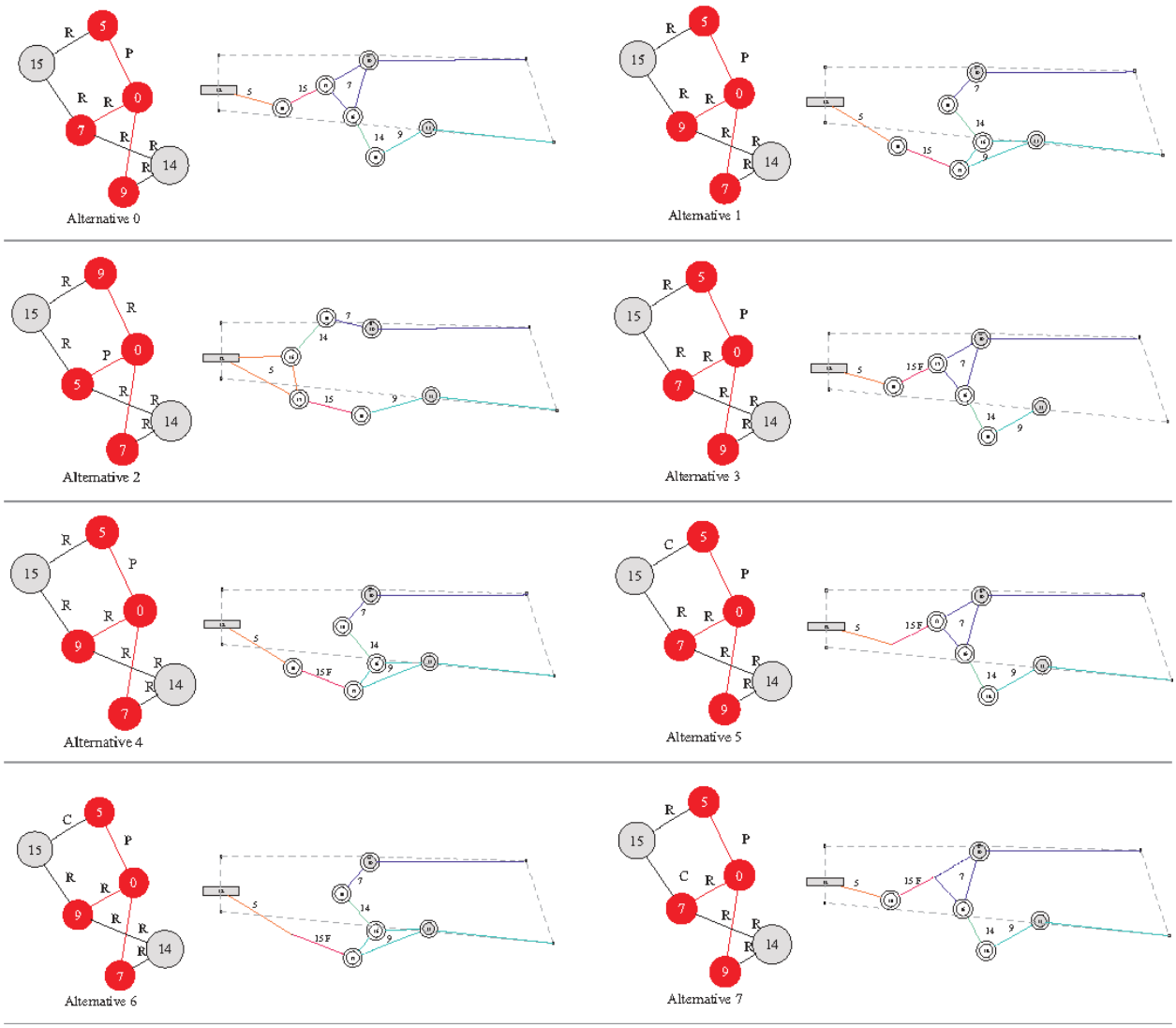

© 2005 SYNCOMECS Consortium Members

Figure 15. Outputs of the type synthesis solver and their corresponding physical sketches (Rigid alternatives are included)

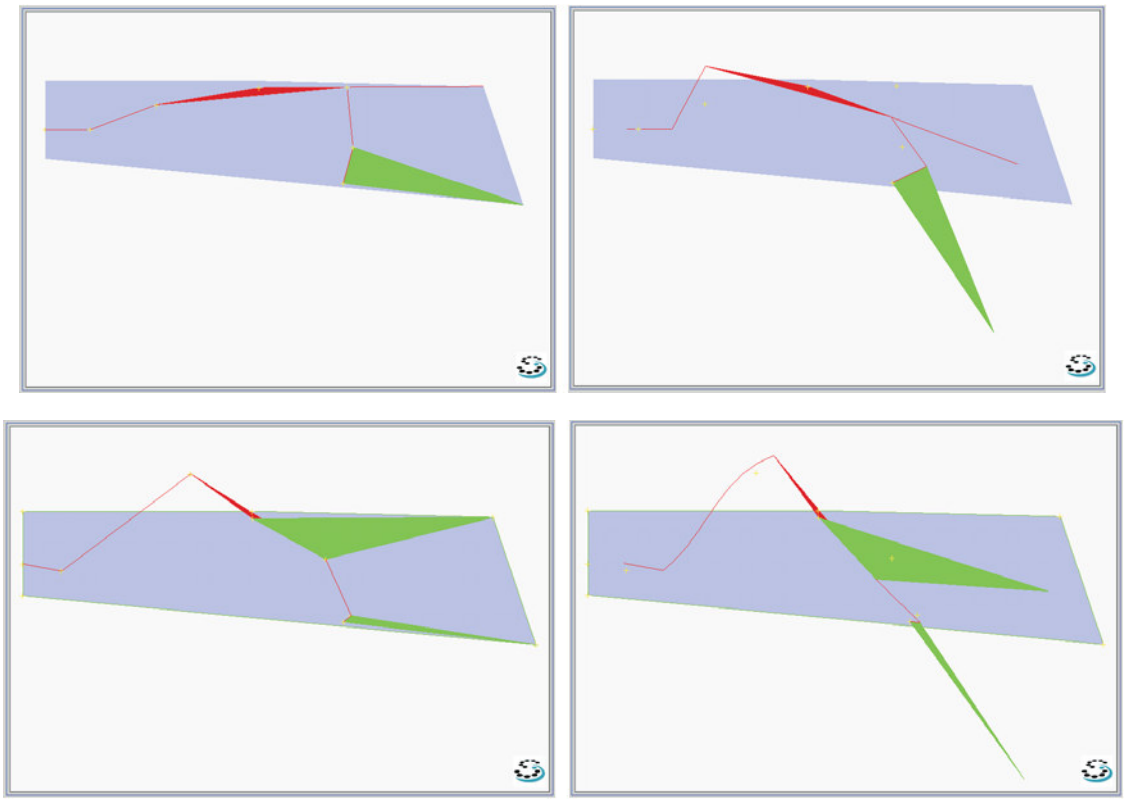

Figure 16. Solutions for alternatives 0 and 9

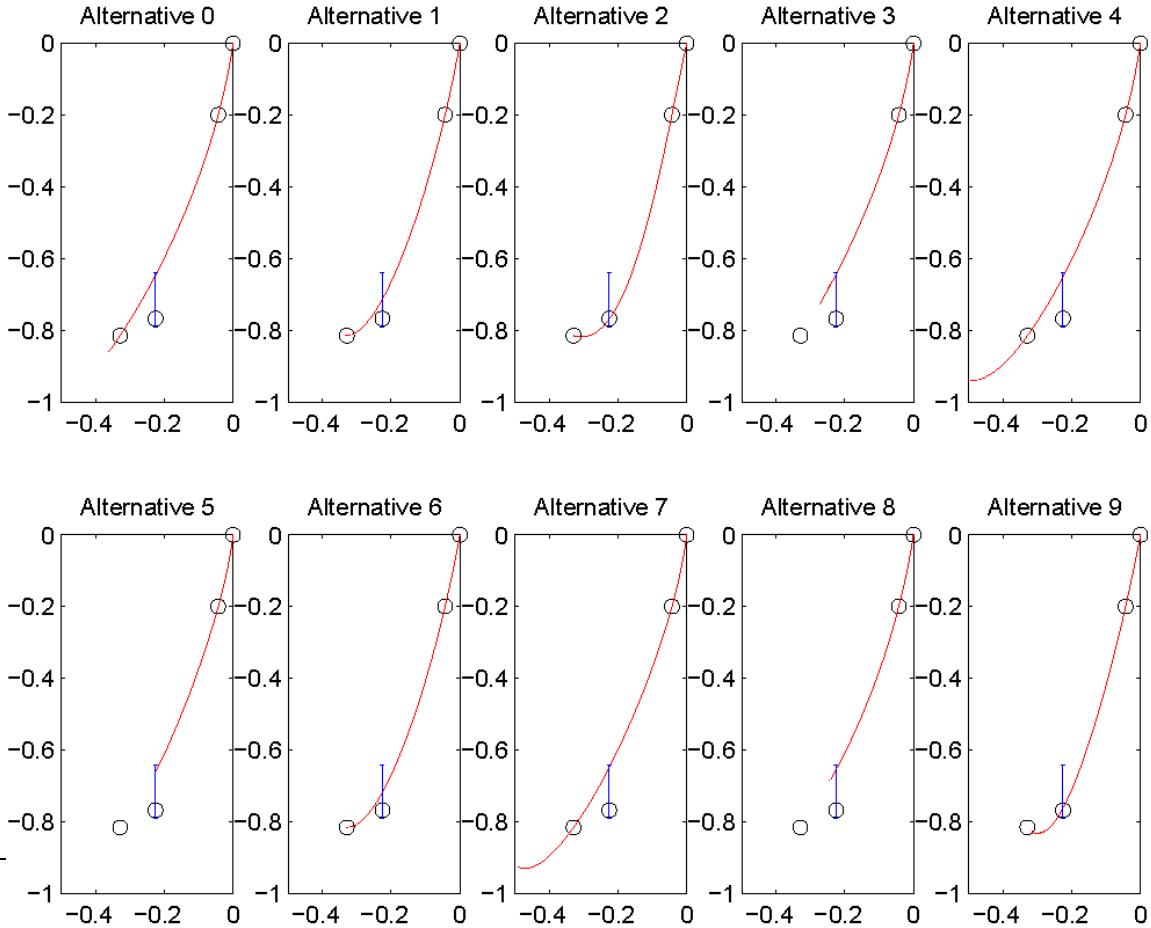

Figure 17. Kinematic response for the superior vs. inferior crank (objective in blue)

7 FLEXIBLE DOUBLE FUNCTION GENERATION EXAMPLE

The description of this example is illustrated in Fig. 14. The movement of the linear actuator must be coordinated with the rotations of two cranks. A nonlinear law is also prescribed for the relative rotations of cranks. The initial graph for such problem is also shown in the figure.

The second position of the inferior crank, was left free to take values inside a given interval. Fig. 15 shows the first eight alternatives computed for type synthesis, using an atlas of compliant mechanisms. Solutions 0, 1 and 2 are fully rigid, while the remaining ones have some flexible links with one or two clamped ends. We show two sized solutions in Figure 16 rigid and partially compliant. Finally, in Fig. 17 the behavior for all alternatives after the initial sizing is shown.

Although precision points synthesis does not assure a good behavior between passing points, in most cases an optimization stage can be made afterwards to decrease or eliminate kinematics errors. Some advantages of the presented method, like the low number of variables and the proximity to optimal solutions of the computed initial guess – mechanism topology with initial dimensions- are of great help for convergence.

2.5. CENAERO

Introduction

The cold stretch forming process is widely used by the aeronautical industry for forming aircraft parts such as the leading edges. In this technique, the plate is fixed in a hydraulic machine and its movement enables to stretch the plate on a block in order to give it the final shape.
However, this process faces several difficulties. Most important problem is the springback effect encountered after sheet cutting. Other unacceptable phenomena include sheet failures and visible surface defects. Industrial partners have expressed their difficulty in manufacturing parameters in order to avoid such problems.
In order to better control the process and avoid wastage of expensive sheets, use of numerical approach is a good approach. In this case, the whole process has to be simulated within software and various models (constitutive material, failure criterion, surface defects criterion) enable the measure of required quantities.
The final objective of this benchmark is to improve and optimize the whole process and reduce the defects. In order to reach this ambitious goal, the model has to be inserted into an optimization loop so that best parameters can be obtained.
All these steps are studied within this project, from the model construction to the final optimization. Most steps were validated against experimental validation. Furthermore, for all three limitations explained above, an optimal solution is proposed.

© 2005 SYNCOMECS Consortium Members

The stretch forming benchmark

In this section, the various stages of the stretch forming benchmark are presented as well as the Samcef model used to simulate it. In conclusion, objectives of this project have been summarized.

Process description

The stretch forming process enables to give a given shape to a planar aluminum plate by stretching it on a rigid block. The primary application of this process is the forming of the leading edges of aircraft wings. A typical illustration of such hydraulic machine can be seen in Figure 1. By controlling numerical commands of the actuators and hinges, numerous movements are possible.

Figure 1: The stretch forming hydraulic machine

The stretch forming process can be broken down into five stages as illustrated in Figure 2:
(a) The sheet is initially setup by consecutive clamping in the two jaws of the forming machine;
(b) The jaws approach each other to give an initial deformed shape to the sheet by buckling;
(c) The sheet is bent and stretched on the forming block;
(d) It is then released and springback can be observed due to the release of elastic strains;
(e) The sheet is cut sometimes causing a second springback.
.

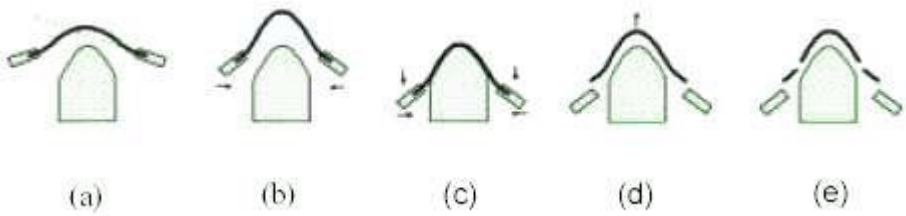

Figure 2: Process stage: (a) installation (b) bulking (c) stretching (d) release (e) cutting

Samcef model

Model presentation

In order to predict the quality of the final leading edge, the kinematics of the machine must be correctly taken into account. For this, using Samcef as finite element software is probably the

© 2005 SYNCOMECS Consortium Members

best solution given its powerful kinematics capabilities. It is imperative that the five stages described above must be accurately simulated by the model in order to predict the correct sheet response.

Major model characteristics can be summarized as follows:

- Three-dimensional model with all the machine kinematics
- Non-linear material constitutive laws
- Shell/3D finite elements for the sheet
- Rigid contact with/without friction
- All process stages are modeled, from the sheet fixation up to the cutting

The whole model is split into 9 sections in order to easily create variants by modifying a single parameter as presented hereafter.

Stretch forming machine model

Global description

The Loire FET2500 machine is made of eight independent actuators but linked to each other by means of hinges and a rigid structure. The two jaws lines are rigid and controlled by two actuators. The real machine and its CAD model can be seen in Figure 3

This machine has been entirely modeled within Samcef. The model incorporates a skelettic machine kinematics which can reproduce in a very precise way all the movements of the real machine by the numerical command file.

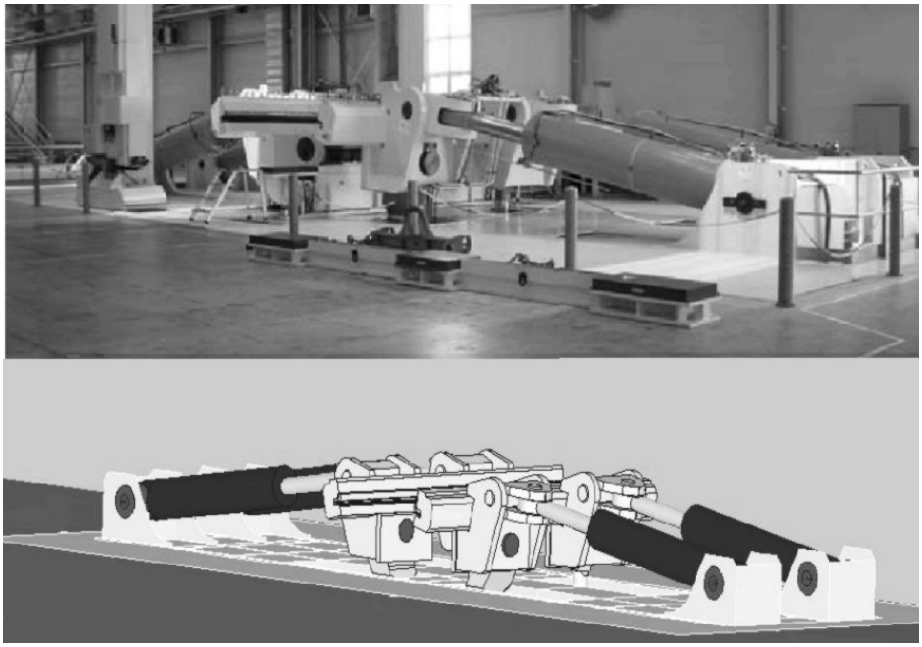

Figure 3: Loire FET2500 machine and its model

Global axes:

Global axes are defined as follow:

- X axis is in the stretching direction
- Y axis is along the ascending vertical
- Z axis is normal to the two others, from the desk to the machine

The origin is the central point with respect to the four lower points of the vertical actuators. The machine orientation is illustrated in Figure 4. In Figure 4, the right-hand side of the machine denotes the positive X axis (i.e.: the left-hand side for the operator).

© 2005 SYNCOMECS Consortium Members

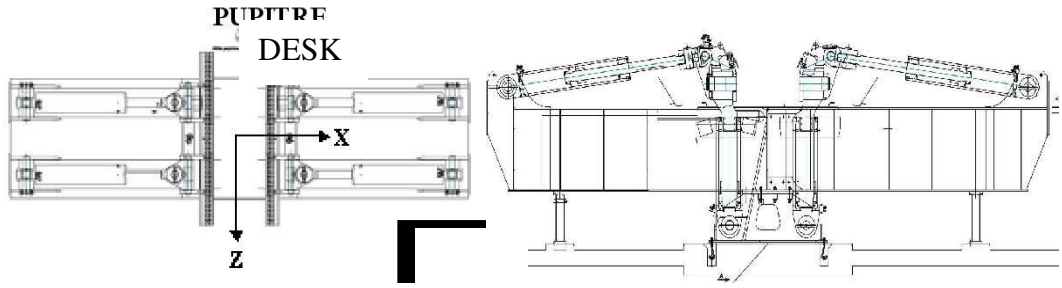

Figure 4: Machine orientation

Actuators nomenclature:
Machine actuators are designated by X, Y, Z and A for the right-hand side and X1, Y1, Z1 and A1 for the left-hand side. They can be broken down into the following categories:

- Horizontal actuator on the desk side: X/X1
- Vertical actuators on the desk side: Y/Y1
- Horizontal actuator on the side opposite to the desk: Z/Z1
- Vertical actuator on the side opposite to the desk: A/A1

Model details
The machine model has been constructed in four parts: each one being made of both horizontal and vertical actuators linked with kinematics joints as illustrated in Figure 5.

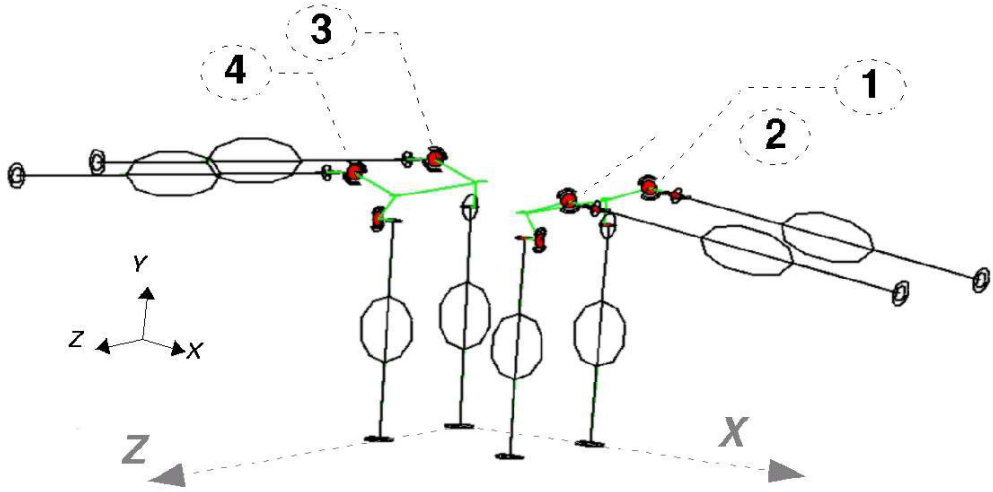

Figure 5: Kinematics machine skelet

The stroke variation of the actuators is imposed by varying the distance between two nodes of the model. The machine model has been generated using both machine plans and measurements of the real machine.
Major articulations have also been modeled for each couple of actuators. They slightly vary from one couple to another one.

Material constitutive laws

The whole sheet is modeled with an elasto-plastic constitutive law, with the exception of the in-jaw region which is modeled as elastic. Elasto-plastic parameters have been determined for the following materials:

- Al2024 T42
- Al2024 T3 1.6mm

© 2005 SYNCOMECS Consortium Members

- Al2024xW Clad 2.8 mm

The most widely used material for leading edges is **Al2024T3.** Isotropic elastic properties are considered. Plastic ones are obtained from experimental results. For applications where the material cannot be considered as isotropic, attention has been paid to the lamination direction which has an influence on the material parameters.

Clamping system

In the real machine, steel cylinders may be fixed to the machine jaws. In the model, these have been fixed to the jaws nodes so that they follow the movements of the jaws. This has been illustrated in Figure 6.

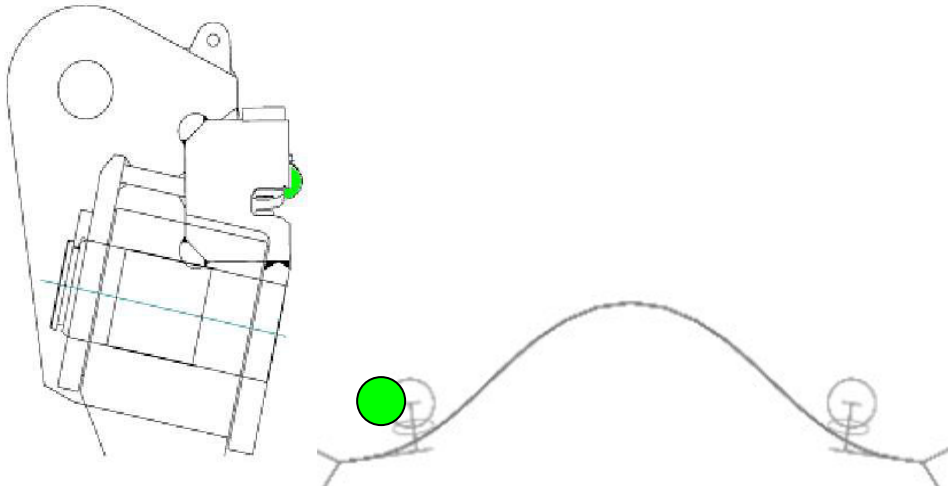

Figure 6: Clamping system model

Diameters and relative positions are user input variable parameters in order to have the flexibility to model any clamping system.
The contact algorithm applied between the clamping system and the sheet has been restricted to the zones where such contact might occur. This is activated once the jaws are closed.

Block model

The block is fixed between the machine jaws on a table which can be moved in the vertical direction (green part in Figure 11). The block is modeled using a rigid surface. Typically, the block profile is provided in a CATIA format and imported into Samcef in an .iges format (see Figure 7). Several industrial blocks have been modeled. Two of them are reported within this report (named block 1 and 2 hereafter).

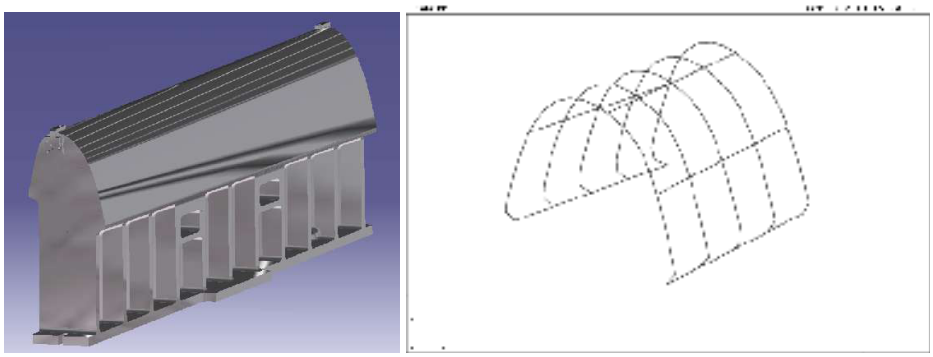

Figure 7: Block geometry in CATIA V5 (left) imported within Samcef (right)

© 2005 SYNCOMECS Consortium Members

Block/sheet contact zones have been modeled for zones which can enter into contact only and is activated only just prior to the contact.

Numerical commands

Numerical commands of the machine consist of a list of command lines. Each line gives the instantaneous length of each actuator (machine is displacement driven). The number of lines (i.e. passage points) might vary from 10 lines (as defined by the operator) up to more than 200 (typical S3F file) – see Figure 8. S3F files are written in text form which resulted in the requirement of a program to be written in order to convert it to a format readable by Samcef.

Figure 8: Numerical commands: machine display (left) and S3F text file (right)

Sheet model

The sheet is rectangular with its dimensions defined by user input variables. Several variants of the model have been explored based on their application. The most significant ones are as follows:

- Shell elements which can be cut
- Shell elements which cannot be cut
- Volumetric elements which can be cut
- Volumetric elements which cannot be cut
- Mix of shell and volumetric elements according to the region

The most suitable model is the shell one which can be cut. The plate model has the option of being split into several sub domains. The breakdown of sheet sub regions incorporated in the model is as follows:

- In jaws left/right
- Lower parts left/right
- Rejected region along cut line left/right
- Cutting lines
- Interior sides along cut line left/right
- Sheet top

This has been illustrated in Figure 9.

© 2005 SYNCOMECS Consortium Members

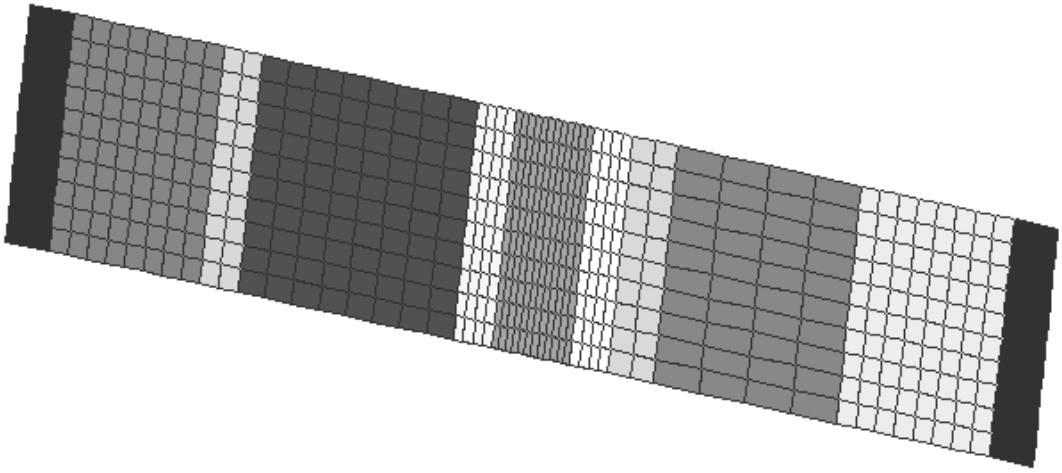

Figure 9: Su regions and corresponding meshes

Fixations

Initial fixation

The initial positioning of the sheet in the clamping system is done in three steps (see Figure 10). The sheet is initially fixed on one side to the right-hand side jaw of the clamping system. The jaws are then positioned such that the left side of the plate is in a position to be fixed to the clamping system. This is modeled by means of link elements between the end nodes row of the sheet and the jaws. A second row of nodes is then fixed to model the closing of the second jaw. This process has been illustrated in Figure 10.

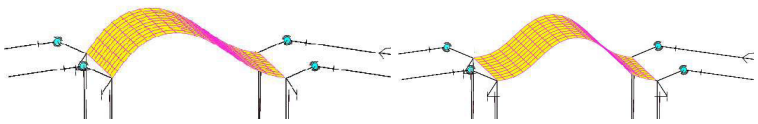

Figure 10: Fixation procedure: first side in-jaw, insertion in the second jaw, closing the second jaw

Sheet cutting

During the final stage of the simulation, the sheet has to be cut along two lines to test for springback effects. In order to incorporate this into the model, links have been defined on either side of the cutting line and are 'deactivated' at the time specified for cutting. To prevent large rigid body displacement and rotation, a specific set of nodes are fixed in space for the remainder of the simulation.

Parameterization

Numerous parameters come into account in order to perform the numerical simulation, which are as follows:

- Processing time
- Simulation steps (sheet fixation, stretching, stretching and cutting,…)
- Contact activation/deactivation times
- Cutting activation/deactivation times
- Jaw closing times
- Output variables and when
- Time stepping management
- Solver parameters, tolerances, …

Between most of these stages, a relaxation period is inserted in order to obtain a stable state.

© 2005 SYNCOMECS Consortium Members

Simulations

The complete model is illustrated in Figure 11.

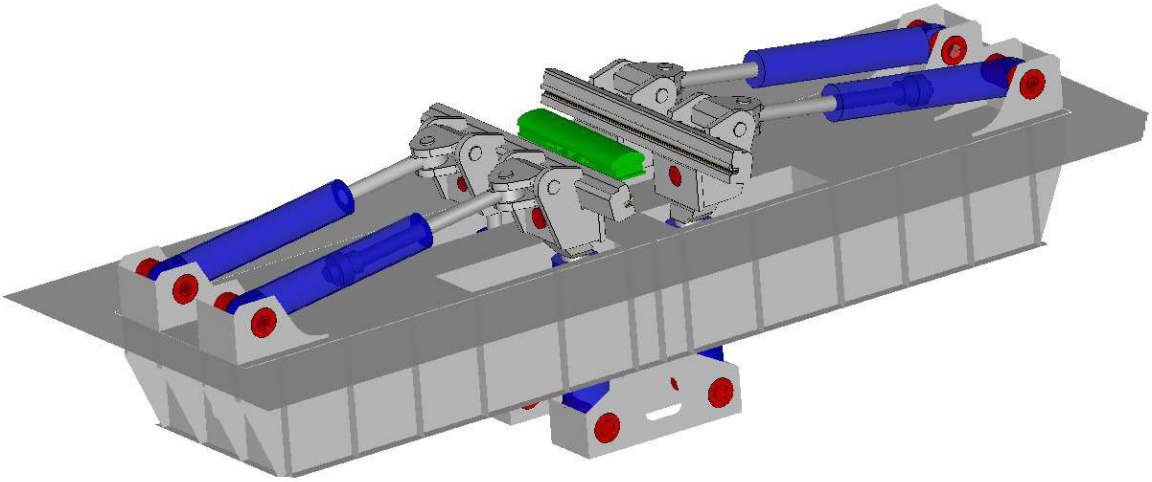

Figure 11: SamcefField model of the Loire FER2500 T stretching machine

The model being defined, a global simulation of the stretch forming process can be performed. Depending on the model parameters, this can take from 1 to 3 hours on an ordinary computer. The strain and stress state is available at the end of each step. This information is used to define various criterions for the failure and surface defects.

Model validation

In order to validate the kinematical model of the machine, several in-situ tests have been done.
As a first step, some static validations were done. After the construction of the model from engineering drawings some measurements on the real machine were made. This resulted in some corrections, especially in the area of the clamping system.
Next, kinematics validations were carried out. Numerical commands were applied so that extreme positions were reached. The real extension of each actuator was measured and compared to the numerical ones (see Figure 12: First trajectory of the kinematical validation). This led to some corrections of the initial positions of the actuators.

© 2005 SYNCOMECS Consortium Members

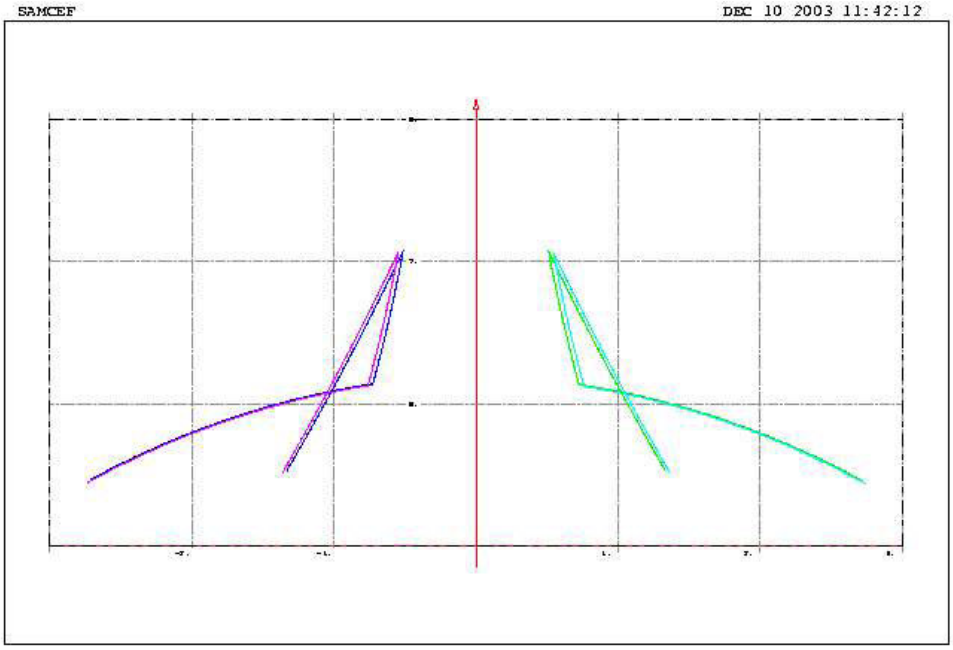

Figure 12: First trajectory of the kinematical validation

The final validation consisted of the insertion of a sensor within the clamping system with known dimensions. With the other extremity of this sensor, various positions were reached in the space. The comparison could be made with either a numerical command controlled machine or a displacement controlled machine. Maximum difference was lower than a millimeter which is lower than experimental tolerance and could have been due to the sensor sensitivity.

Benchmark objectives

During the stretching process, some undesired effects may occur. The three important undesired effects are examined in this study: shape defects due to the springback, failure risk and surface defects. The shape defect might, in the best case, can be corrected by subsequent operations (such as modification of the sheet shape) but at very high costs.
Due to the material complexity and the numerous parameters involved in the simulations, it is rather difficult for the operator to control all these effects, especially the springback and surface defects. Currently, a trial and error approach is adopted.
The main objective of this benchmark is to better control the process and predict springback, failure as well as surface defects. An additional benefit of this model is the understanding of the influence of the process parameters resulting in the reduction of costly experimental testing.
Model validation is required in order to know the reliability of the predictions. For this, experimental results are needed.
Finally, the major objective is to propose for each defect optimal simulation parameters in order to reduce or avoid it.

Springback: predictions and optimization

Springback measurements

Springback measurements are done before and after the cutting operation during real production since these tests are non destructive. As discussed earlier, two block profiles were used as test cases. Al2024W was chosen as the material for the sheet.
Three different profiles were obtained for the springback as illustrated in Figure 13:

- Two maximum at points A and B

© 2005 SYNCOMECS Consortium Members

- Two maximum at points A and D or B and C
- Three maximum at points A, B and C or A, B and D

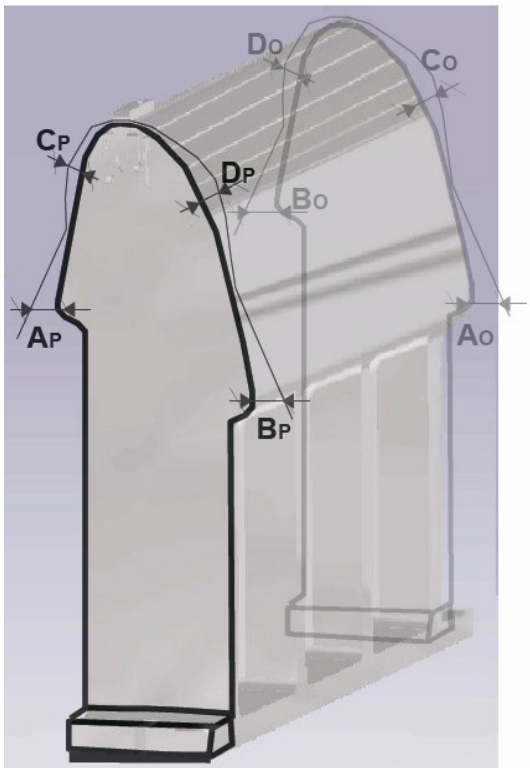

Figure 13: Springback measurements

The tests provided numerous experimental results which were suitable for the numerical validation.

Experimental validation

In order to reproduce correctly the springback, it is important to take gravity into account. Furthermore, some friction must be considered at the interface between the sheet and the block. For this, a classical friction law is used which relates the normal to the friction forces through a scalar friction coefficient (typically 0.1)

Block 1

Comparison of springback measured at different points with the simulation is shown in Figure 14.

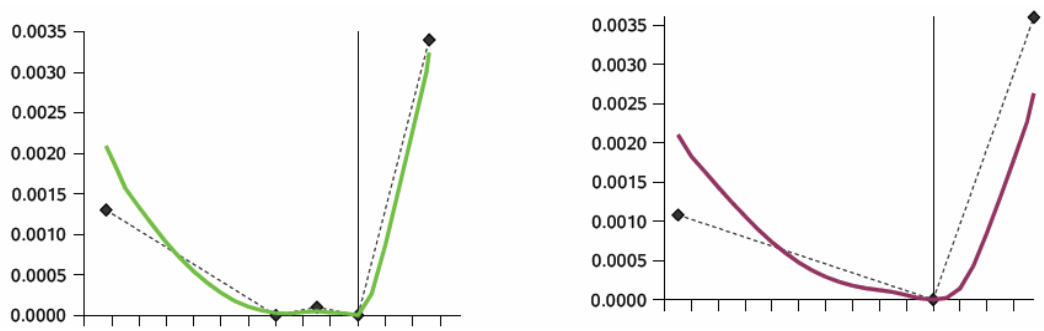

Figure 14: Springback validation on desk side (left) and the opposite side (right). Dots are experimental measures and continuous lines are numerical predictions.

Qualitatively, these results are very good, even if some differences exist at both extremities. These discrepancies may be due to the initial position of the sheet within the clamping system.

© 2005 SYNCOMECS Consortium Members

Block 2

For the second block shape, similar results were obtained which can be seen in Figure 15.

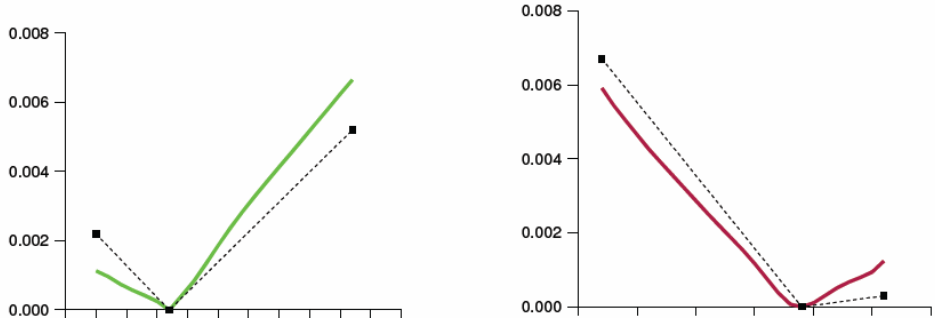

Figure 15: Springback validation on desk side (left) and the opposite side (right). Dots are experimental measures and continuous lines are numerical predictions.

Again, both results are very similar even if some differences exist at both extremities.

Final shape optimization

Now that we are able to correctly simulate the process and compute the associated spring-back, an optimization is possible. The main goal in this section is to minimize the sum of the absolute values of the springback computed at several points (5 on each side, as showed above).

Basically, two approaches are possible: block shape optimization and numerical commands optimization.

Block shape optimization

A first solution consists of reducing block width to obtain an accurate final shape after springback.

Parameters:

For this, the optimization parameter is the block thickness. Other possibilities would be a global scale factor or ruling splines modifications.

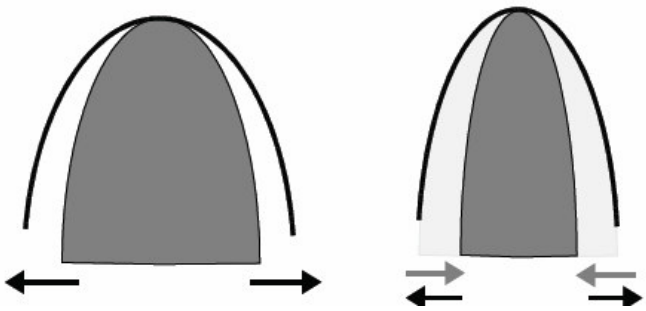

Figure 16: Variation of the block thickness in order to take into account the springback

For the first optimization, a single parameter is the factor controlling the block thickness, i.e.:

$$X_{corr} = k * X_{nom},$$

where *corr* refers to the corrected thickness, *nom* refers to the nominal value and *k* is the factor to optimize.7

Objective

The objective is defined as the sum of 8 computed springback absolute values (4 on each block extremity – see Figure 13).

Optimization

© 2005 SYNCOMECS Consortium Members

By modifying the *k* value, it is possible to find a final shape very close to the nominal one, at least for the 170-35202-001 block. The optimum value found with Samcef was 0.992 for *k*. Even if this value might seem very close to the initial one (1.), springback at all points is always lower than 1.5mm while it was sometimes close to 5mm with the nominal block!
The major drawback of this first method is that a block has to be designed for the particular conditions of one simulation while when considering other parameters, an additional block might be required. Another disadvantage of such approach is that the actual block is used as nominal one in order to check the final shape. Making use of a second block would be much more expensive. However, given the very good results obtained with this procedure, such an operation should be considered when springback is very critical.

Numerical commands optimization

A second approach is the optimization of the numerical commands of the machine such as the trajectories and the forming speeds. However, this is a very difficult task given the numerous parameters involved in the simulation.
A parametric study showed the following results:

- The greater the stretching the smaller the springback is. However, increasing stretching leads to a higher risk of failure or surface defects.
- The trajectory has almost no effect on the springback
- A modification of the friction coefficient at the block/sheet interface has a significant influence on the objective
- Friction coefficient in the clamping system has almost no influence on final results

Let us present here the parametric study over the stretching level. Stretching level can be modified by increasing the final length of actuators Y and Y1 during the stretching phase. Typical value for the 170-35202-001 block is 1.650m. Increasing it of only 1cm, a very good solution is obtained, even better than with the block shape optimization. Unfortunately, as we will see later, such additional stretching strongly increases failure and surface defect risks. For industrial purposes, this approach should thus be avoided.

Failure detection

Failure criterion

One of the most widely used failure criterion is based on the Forming Limit Curve (FLC). It consists of a critical curve in the principal strains plane which defines two zones: a safe one and one where failure might appear (see Figure 17). These curves can be obtained experimentally, in an analytical way or by a combination of both approaches. For stretch forming applications, only one half of the diagram is useful given the fact that the two principal strains are of opposite signs due to the stretching in a single direction.

© 2005 SYNCOMECS Consortium Members

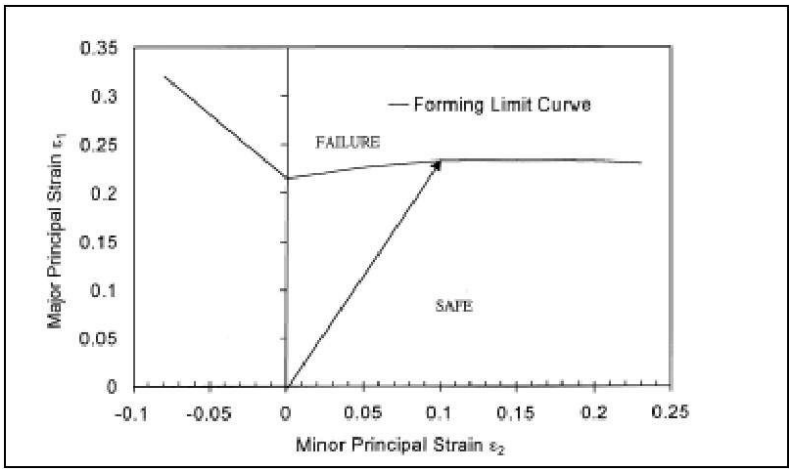

Figure 17: Typical forming limit curve

Such criterion is particularly suitable for our application since it is developed for thin sheets. The use of this criterion is done as a post-process of the main simulation as:

- Principal strains are extracted at all FE nodes at each time from the Samcef result file.
- For each node, at each time, the distance with respect to the forming limit curve is computed.
- Distance maps with respect to the forming limit curves are plotted within Samcef as an isovalue field.

Experimental tests

Two horizontal stretching tests have been carried out on 2.8*1080*1500 mm sheets. A first test reached failure (which occurred at about 6% of elongation) and a second one at 2% of elongation. Local strains were measured on the sheet surfaces.
Numerical results showed a good coherence between numerical results and experimental data (see Figure 18). Critical zones were located exactly at the same points while the error on the strains measures was lower than 5%.

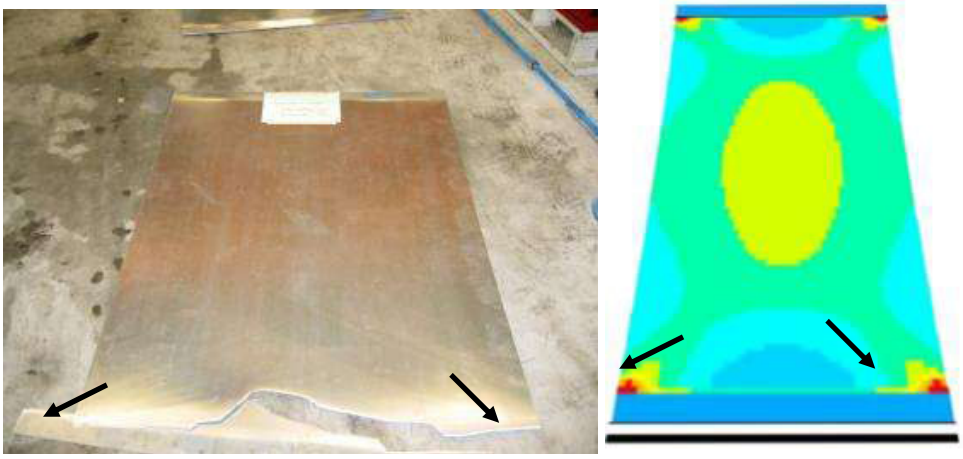

Figure 18: Failure experimental results (left) and critical zones obtained numerically (right)

Aluminum Al2024 cl sheets were used for these tests. However, less stretchable sheets were used for this test in order to easily reach failure (T3 heat treatment instead of W).
Two different industrial blocks were used. The block influences the sheet size and three tests were carried out on each block.
For all tests, strains were measured at several points on the sheet. A typical failure initiation is illustrated in Figure 19 and appears on the block top.

© 2005 SYNCOMECS Consortium Members

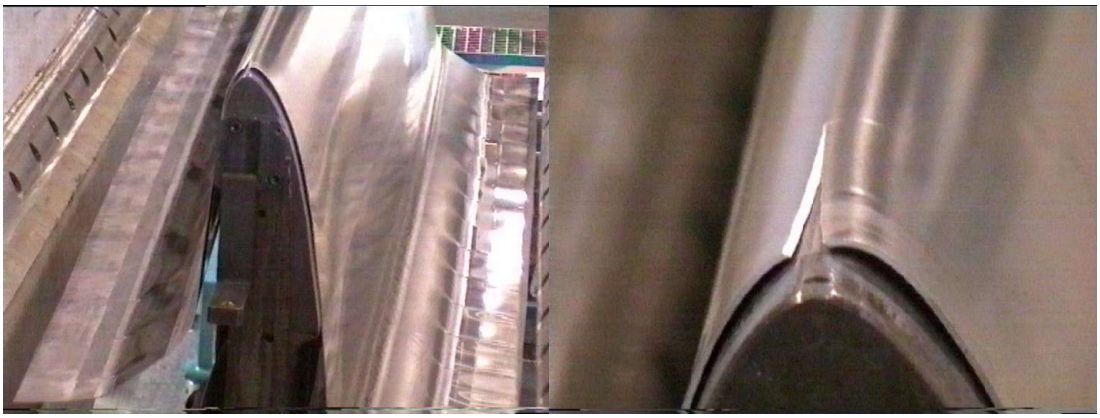

Figure 19: Failure initiation on the block top (left) and detail (right)

Model validation

Block 1

Experimental failure happened after a time of 7’03’’. At the corresponding time in the model (numerical commands are the same in both cases), we note a critical zone where failure criterion has just been reached (see Figure 20). On this figure, blue color means that the element is far from the failure limit curve while once red, the element is very close to it.

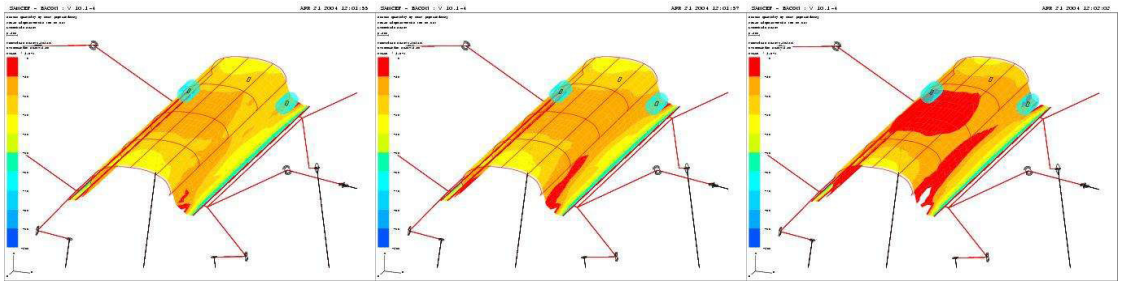

Figure 20: Failure apparition. Distance to critical curve at time t=6' 50'' (left), t=7'03'' (middle) and t=7'15'' (right)

Failure criterion might thus be considered as correct since critical numerical zone corresponds perfectly to the numerical one. Furthermore, failure times are also coherent and crack start in the same region.

Block 2

This second block is much thinner than the first one so that failure prevention is more critical. However, as for the first block, excellent agreement between simulation and experimental data were observed (see Figure 21).

© 2005 SYNCOMECS Consortium Members

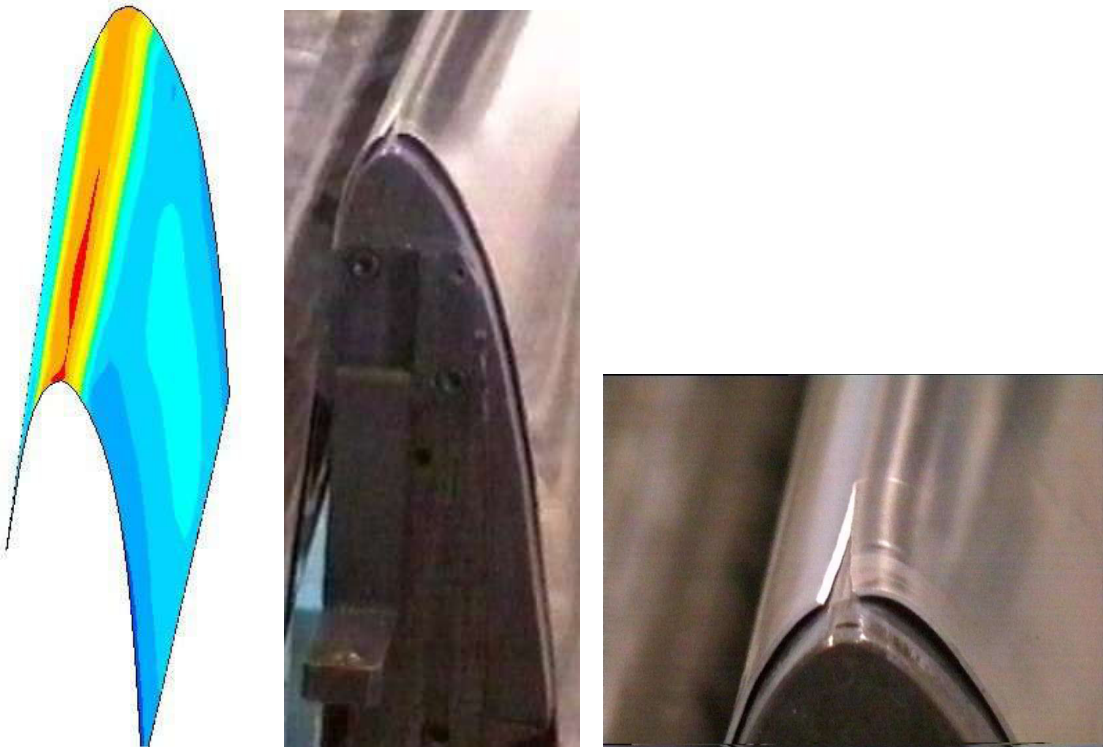

Figure 21: Failure simulation on the 170-35402-001 block

At the end of this experimental campaign, we can conclude that our criterion based on the failure limit curve is perfectly suitable for prediction failure during the stretch forming process.

Surface defects: predictions and optimization

Two major kinds of surface defects exist: Portevin-Le Châtelier (PLC) one and Lüders one. These induce a succession of dark and bright lines on the final workpiece (see Figure 22).

Figure 22: Surface defects at the macroscopic level

Such phenomena are unacceptable for the production of leading edges especially if they are not painted. For this study, our efforts are concentrated on the PLC effect. In order to predict an eventual apparition, our approach is based on a criterion similar to the one used for failure prediction. For this, the critical curve will be provided by an analytical model.

<u>Surface defects criterion</u>

PLC effect is a phenomenon due to dynamic interactions between dislocations and solute atoms which lead to local instabilities and strain softening in the stress/strain plot (see Figure 23).

© 2005 SYNCOMECS Consortium Members

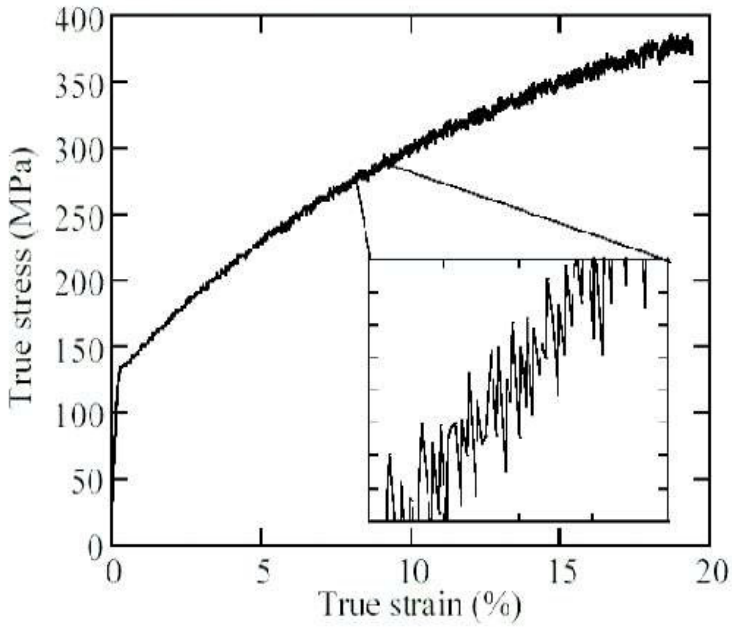

Figure 23: PLC effect on a stress/strain plot

With such phenomena, there might be two different strain rates for a given stress so that a succession of various strain rates appears (see Figure 24).

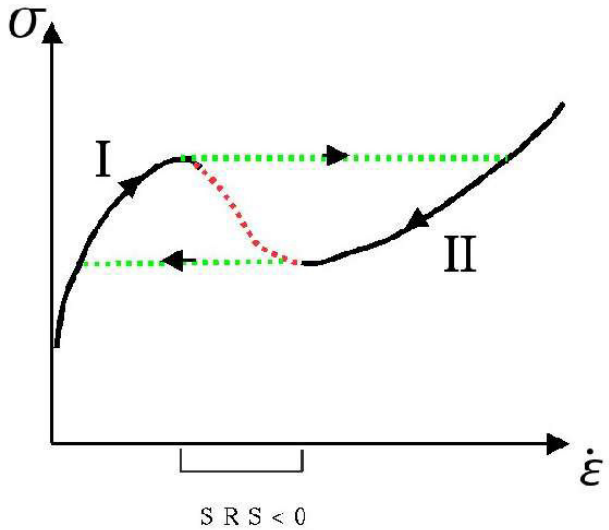

Figure 24: Cycles induces by the PLC effect

This phenomenon is highly dependent on the strain state, strain rates, temperature, material properties and alloy microstructure (especially the ratio of solute atoms/dislocations).For a given configuration, we can consider constant material properties and temperature so that two variables remain: the strain and the strain rate. A stop/restart or any shock during the process might thus lead to an apparition of such defect.

The first approach is to develop a criterion similar to the one used for failure prediction (failure limit curve). But in this case, the critical curve will be defined by strain and strain rate states. Different approaches exist in order to define this curve. The one used here is obtained from an analytical model developed by Prof. Estrin from TU Clausthal university and is presented in the next section.

The use of this criterion is done as a post-process of the main simulation for each finite element and at each time step as:

© 2005 SYNCOMECS Consortium Members

- Extraction of principal strains at the beginning and end of the time step
- The principal strain rate is computed as the ratio between principal strains and the time step.
- Distance (strain) with respect to the PLC curve is computed

Finally, a signed distance map is plotted within Samcef at each time step in order to determine whether or not surface defects might appear. Typically, a negative sign means that the element at the given time is on the safe side while with a positive sign, surface defects might start to propagate.

PLC constitutive model

From a physical viewpoint, PLC effect occurs only for alloys, not for pure metals. Even if for the latter several kinds of obstacles exist (e.g.: intersection, immobility, impurities…), macroscopic response remains stable. On the contrary, when dealing with some types of alloys, concentration of fast diffusing solute atoms increase with the waiting time of a dislocation facing an obstacle. These interactions lead to unsteady, collective motion of dislocations within grains and across grain boundaries (see Figure 25). This leads to strain localization increases and the presence of macroscopic shear bands.

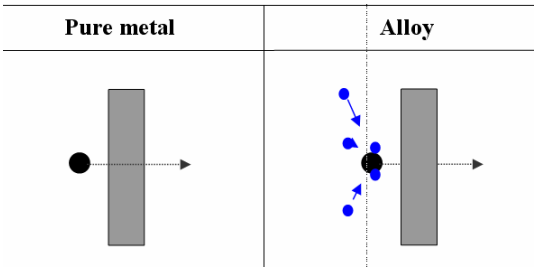

Figure 25: Concentration of diffusing solute atoms increase with the waiting time of dislocations facing an obstacle

The model presented in this section was developed by Prof. Estrin from TU Clausthal University.

Constitutive model starts from the classical additive strain decomposition over a time step:

$$\Delta\varepsilon = \Delta\varepsilon^{el} + \Delta\varepsilon^{pl}, \quad \Delta\sigma = C : \Delta\varepsilon^{el},$$

where the total strain increment is split into the elastic strain increment and the plastic strain increment. Also, the usual flow rule is used:

$$\dot{\varepsilon}^{pl} = \dot{p}\frac{3}{2}\frac{s}{\sigma_{eq}}$$

where p is the accumulated plastic strain, s is the deviatoric stress and σ_{eq} is the equivalent von Mises stress.

PLC dynamic is inserted in the strain hardening expression and is a function of the stress due to dislocation density evolution (σ_d), the instantaneous strain rate sensitivity (S) and the solute concentration rate $\dot{C}_s$ as:

$$\dot{p} = \dot{p}_0 \exp\left(\frac{\sigma_{eq} - \sigma_d(p)}{S(p)} - P_1\dot{C}_s\right).$$

The solute concentration evolution is a function of the ageing time t_a and the solute concentration at saturation C_m:

© 2005 SYNCOMECS Consortium Members

$$C_s = [1 - \exp(f(p, t_a))]C_m$$

Ageing time differential equation for a given waiting time is given by:

$$\frac{dt_a}{dt} = 1 - \frac{t_a}{t_w}$$

The full model has been implemented in an Abaqus UMAT. This model could have been inserted within the stretch forming model. However, this would have led to numerous problems. The first one would be the coupling between the Abaqus UMAT and Samcef which would require rewriting the whole model (25 pages for the UMAT !). Also, making use in a direct way of this model would require a much finer mesh in order to correctly capture the local instabilities. In addition to this, computational time would also increase considerably due to the complexity of the resolution of this constitutive model. Finally, as we are not interested in the dynamics of the PLC effect but only by its apparition or not, we proposed an alternative solution.

Boundary of instability can be easily determined by varnishing the strain rate sensitivity:

$$S(p, \dot{p}) = \frac{\partial \sigma}{\partial (\log \dot{p})} = 0 .$$

This defines a critical curve and is illustrated in Figure 26 for Aluminum 2024. Parameters of the Estrin model have first been determined experimentally within its research group.

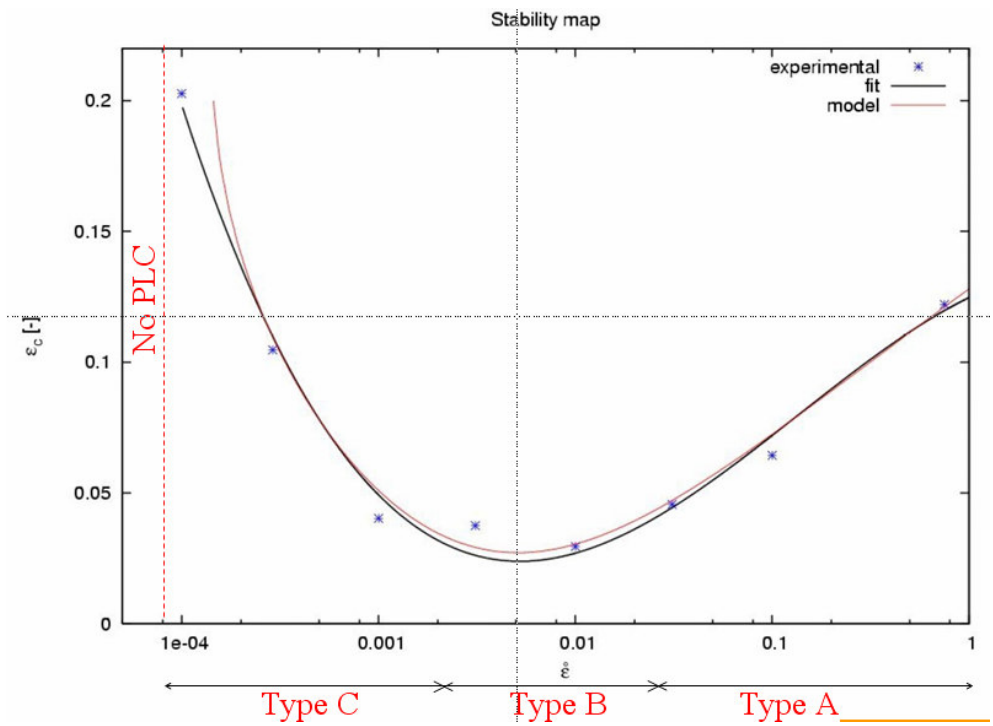

Figure 26: Critical curve for PLC apparition in strain / strain rate space

Some interesting observations can be made. First of all, this model is suitable for reproducing all three types of PLC effects commonly called Types A, B and C according to the strain rate ranges. Also, we notice that under a given strain rate, no PLC effect occurs.

The critical curve being constructed, the remaining work is to check all elements at each time during the stretching period whether or not it lies in the safe region. This has to be done automatically within Samcef. For this a least-square fit of the critical curve obtained by the model was done as:

$$f(\dot{\varepsilon}^{pl}) = a_1(\log \dot{\varepsilon}^{pl})^3 + a_2(\log \dot{\varepsilon}^{pl})^2 + a_3 \log \dot{\varepsilon}^{pl} + a_4 = \varepsilon_c$$

© 2005 SYNCOMECS Consortium Members

This fitting curve is also shown in Figure 26. By making use of a post-process bacon script, strain rates can be computed as well as distance with respect to the critical curve as illustrated in Figure 27.

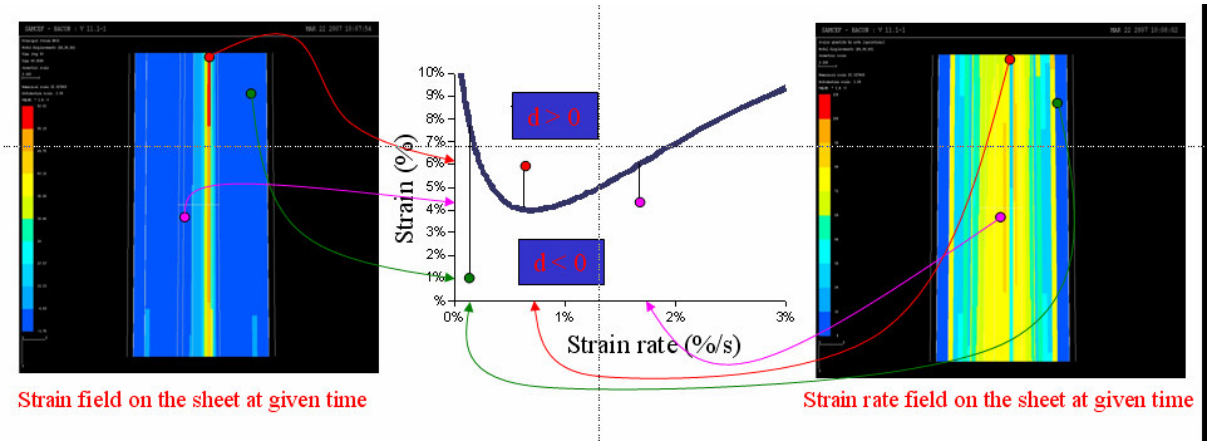

Figure 27: Construction of the distance map w.r.t. critical curve

Finally a distance map can be constructed as illustrated in Figure 28.

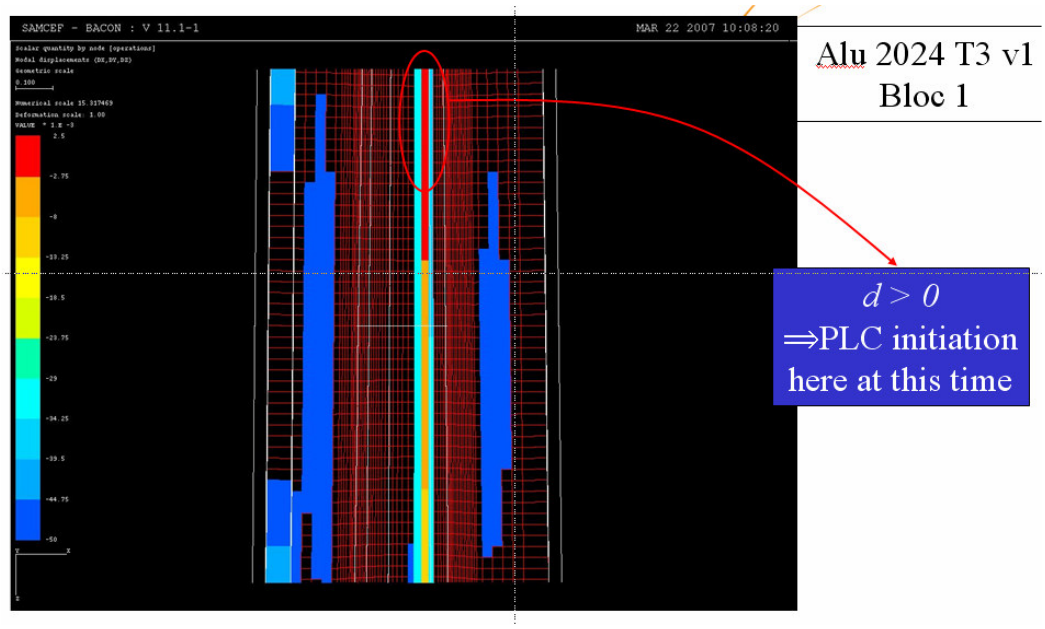

Figure 28: Distance map with respect to critical curve

For one value of critical strain, we can thus obtain zero, one or two corresponding strain rates. Red zones indicate that surface defects might appear. When this is violated by the application, a process optimization has to be achieved as explained in the next section.

Surface defects optimization

Since surface defects are rate dependent, a good way to solve this problem is to modify the numerical commands of the machine. All sheets material used hereafter are Al2024 as the one used to develop the PLC criterion. The most critical block (number 2) with respect to PLC has been used for the optimization. No PLC is predicted by the model with block 1.

© 2005 SYNCOMECS Consortium Members

Parameters
PLC effect occurs during the stretching period. It is thus logical to play on the machine kinematics in order to solve this problem. For this, the stretching time (usually 5 s for a stretching of about 4 %) is considered as optimization parameter. However, one should notice the narrow range of acceptable values for this parameter. Typically, due to technical limitations of the machine, the stretching period cannot be much shorter (by no way less than 3 s). On the other hand, long stretching times are difficult to reproduce with the machine, at least in a smooth manner. Such long stretching times are very critical for the Portevin-Le Châtelier effect. This is a major machine limitation since very long stretching times would maybe give a maximum strain rate over the sheet lower than the minimal critical strain rate (see Figure 26), so that it guarantees no surface defects. Anyway, in order to guarantee such regime, the stretching time might be several orders of magnitudes higher than the current one, which would be unacceptable for industrial purpose.

Objective
The objective is the distance with respect to the PLC critical curve. This scalar is constructed as follows:

- For each time step during the stretching period
  - For gauss point of each sheet element
    - Compute strain rate (unavailable within Samcef) by finite differences
    - Compute the distance with respect to the critical curve as:
      - Principal strain predicted minus principal strain of the critical curve for the same strain rate
      - Such computation means that for a negative distance, the element lies on the safe side while a positive value is critical for surface defects
  - Consider the maximum distance over all gauss points
- Consider the maximum distance over all time-steps: this is the objective

This has been done in a post-processing Samcef routine. Given the fact that the safe side corresponds to a negative objective, the distance has to be minimized.

Optimization
In order to solve this problem, a Boss4o / Mecano / BaconPostC model has been developed. The parametric study is illustrated on Figure 29 (including manual simulations and results from optimization).

© 2005 SYNCOMECS Consortium Members

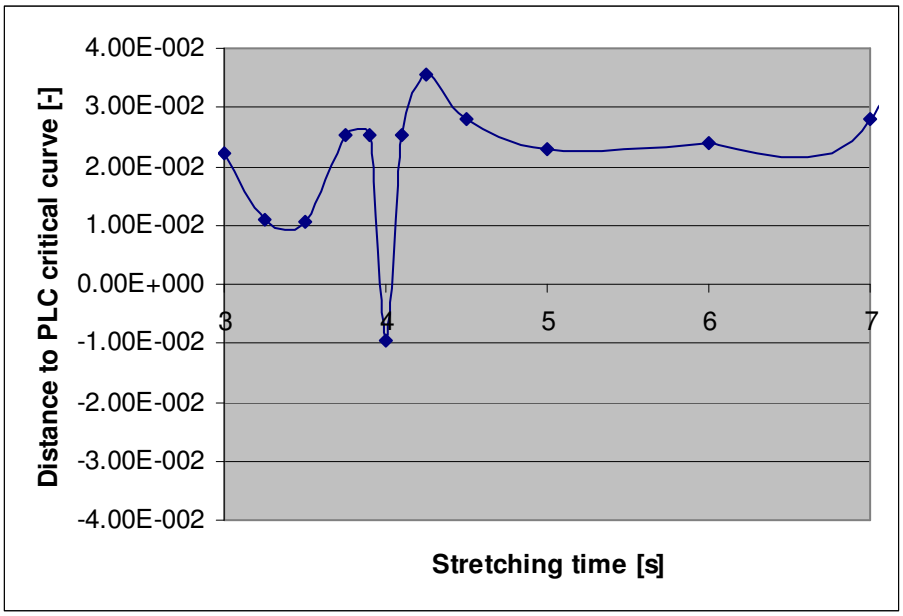

Figure 29: Variation of the distance to the PLC critical curve with the stretching time. Negative values means that the whole process is surface defects free while a positive value means that surface defects might develop.

It might be surprising that only stretching time close to 4.05 s guarantees no surface defects. Unfortunately, this optimum is rather unstable and difficult to reproduce on the real machine. However, positive values do no mean that surface defects will necessary propagate but the higher this value is, the higher a slight shock might cause surface defects propagation. Smoothing the process is thus very crucial. That's why recommended stretching times for Al2024 are included within the range 3 to 4 seconds.
It is also important to note that this process is very sensible to the block shape. As stated before, no PLC is predicted for the other block used in the experiments. Finally, heat treatment for the aluminum sheet has also a strong influence on surface defects propagation. Typically, under the same conditions, a stretch forming test on the same material but undergoing one or another heat treatment might give completely different results. This is for sure a better alternative if surface defects if very critical.

© 2005 SYNCOMECS Consortium Members

2.6. CT INGENERIOS

2.6.1 Project Background

The test cases of the project will be based on pre-existing know-how includes actual design of A380 main landing gear door, three years of work from CT Ingenieros stress group as subcontractor of airbus Spain. Principal problem of this design are very clear for stress team, which will guarantee a highly quality of the analysis an criteria to value the results.

2.6.2 Project Objectives

The objective of this collaboration in the subject project is to build an integrated software, based in old method to develop a new method applicable for the design of aeronautical compliant mechanical systems and contribute with the CT Ingenieros Experience to solve aeronautical problems.

2.6.3 Description of the work

The activities in subject project are executed in four steps.

First step, complete development of the specification and elements used.

Second Step, development of the test cases with old method. This step was subdivide in the two different at the same time.

1. Selection of main landing gear door as benchmark case. Analyse Main landing gear door with actual FEM tools give a SAMCEF FIELD models. These models include hydraulic opening mechanism, closing mechanism and gravitational opening mechanism. Three mechanisms are replaced with compliance mechanism

2. Selection of main landing gear door in close position as benchmark case. Main landing gear door are analysed, to reduce weight, as distributed compliance mechanism. Main landing gear door have to assurance low tolerance with theoretical contour in cruise load. These requirements can be fulfilled with more weight rigid structure or with distributed compliant mechanisms. Two models have been made to validate these benchmarks. First model is similar to models used in Airbus Spain and it is necessary to validate final tools results. Second model is made in SAMCEF Bacon and give similar results to first models.

Third Step, validation the new software development in subject project, made a new analysis based in previous step and compare the result and improvement of the integrate software.

Fourth step, dissemination and exploitation of the result of the results.

© 2005 SYNCOMECS Consortium Members

2.6.4 Expected results

CT Ingenieros expected that the result obtained was a similar o result obtained in with the old validated methods. Finally the results are in order that these results, this demonstration validate the new method.

But the new development methods improve significantly the time of work and automatic of the process of analysis. Improvement with the subject project the competition between companies.

2.6.5 Two representative pictures or graphics

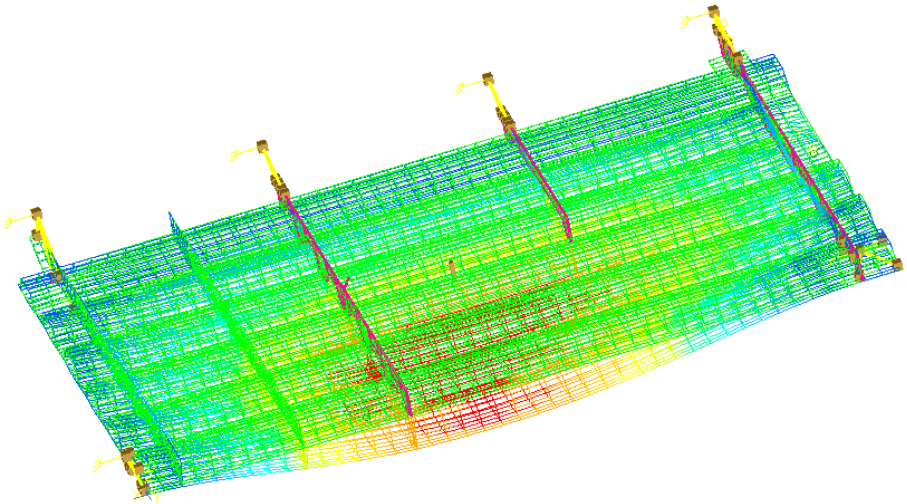

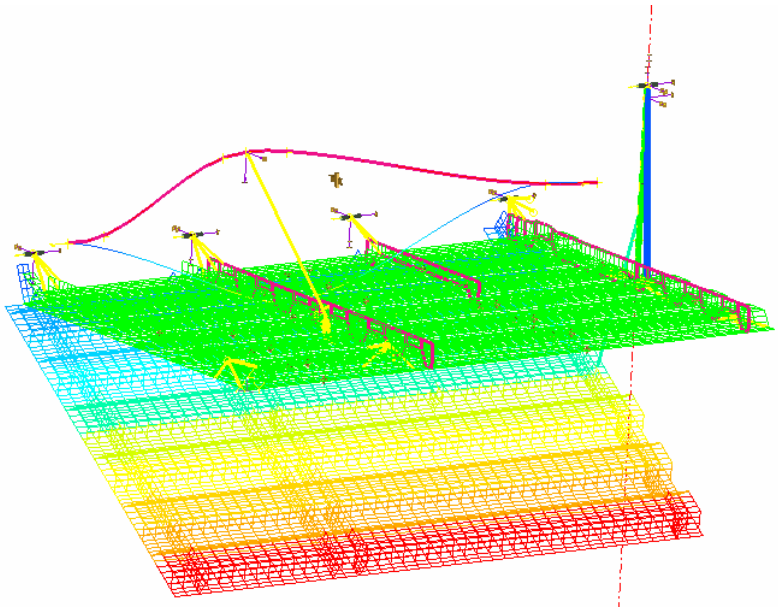

© 2005 SYNCOMECS Consortium Members

2.7.ABB Sace

2.7.1 Project Objectives

This report summarises the work carried out by ABB during the whole SYNCOMECS project; ABB's objective was to introduce a new methodology into design departments able to predict the behaviour of distributed flexible systems (both single components and complete mechanisms) in order to reduce costs and increase reliability.

2.7.2 Developments

R&D activities carried out during first 6M

- (WP2) Design of a compliant solution for RCBO tripping mechanism using existing tools. Instead of the synthesis tool under development, a "trial and error" approach will be followed. Starting from the mechanical model of the rigid mechanism, already available, targeted pieces will be replaced by a tentative flexible solution. The idea will be virtually checked with static and dynamical simulations
- (WP3) Design of a compliant solution for the Shunt trip device lever. The use of existing tools will lead to several direct structural analyses maybe driven by BOSSQuattro software as task manager. The initial shape of the lever will be defined with a "trial and error" approach in this case too.

R&D activities carried out from 6M to 12M

- (WP2) Numerical optimization of the compliant solution for RCBO tripping mechanism using existing software tools. The same "trial and error" approach will be followed. No BOSSQuattro optimizations are planned yet due to the complexity and high instability of the mechanical models.
- (WP2) Manufacturing of the first compliant solution with fast prototyping techniques and assembly of the first RCBO mechanism.
- (WP3) Numerical optimisation of the compliant solution for the shunt trip device lever.

R&D activities carried out from 12M to 18M

- (WP2) Use of BLDB tool to check possible alternatives to the developed compliant solutions
- (WP3) Test of IFEM tool on simple non linear cases close to ABB typical applications
- (WP3) Test of IFEM tool on ABB WP3 benchmark case
- (WP7) Collection of detected bugs & wish lists coming from end users during fists tests on developed software tools

Summary of activities carried out from 18M to 24M

- (WP7) Tests on SYNTOOL to check possible alternatives to the developed compliant solutions for the RCBO mechanism.
- (WP7) Collection of detected bugs & wish lists coming from end users during task 7.1, 7.2 and 7.3 related activities
- (WP7) Release of the D10 deliverable (M26)

Summary of activities carried out from 24M to 30M

© 2005 SYNCOMECS Consortium Members

- (WP7) Tests on Integrated Software System to optimize compliant solutions for the RCBO mechanism.
- (WP7) Release of the D15 deliverable (M30)

© 2005 SYNCOMECS Consortium Members

2.8.ALENIA Aeronautica

2.8.1. Task 1.1: Definition of the design scope

The objective of Task 1.1 is to investigate and to answer the following questions:

What type of mechanical systems will be designed: Compliant Mechanisms and Complex Non-linear Structures ?

A full non-linear formulation will allow us to consider both compliant mechanisms and structures in an unified approach:

- **Complex non-linear structures** are essential to many aircraft subparts. Critical components are submitted to complex loading patterns which include requirements from forces of different nature and, in some cases, together with strict dimensional and shape requirements under loading. These systems need careful optimisation analysis to match all these impositions.
- **Compliant Mechanisms** are mechanical devices in which motion is allowed from parts that flex, bend or have different forms of flexibility. This is in sharp contrast to rigid-link mechanisms that only move as their moveable joints allow. Compliant mechanisms, with built-in flexible segments, are simpler, replace multiple rigid parts, can often save weight, noise, friction, space, and reduce costs of parts, materials and assembly labour.

How can these systems be described and represented for both conceptual and detailed design?

The Compliant Mechanisms Design Process can be divided into two phases:

- Synthesis (Conceptual Design). Depending on the system purposes, the mechanisms may be composed by different combinations of components and topologies. Modelling can be based on a library of basic components (*BLDB Tool*) that, once linked to each other, could lead to the kinematical chain definition. Specialised elements should also be available, allowing wide parameters setting and user customisation.
- Detailed Mechanism Design (Detailed Design). The detailed structural model is generated and precisely analysed and optimised.

The Complex Non-linear Structures Design Process is always an inverse problem that will be solved by direct inverse deformation analysis when possible or by classical optimisation process otherwise.

What are the design requirements of these mechanical systems ?

The **SYNCOMECS** partners have concentrated their main interest and experience on mechanisms and complex non-linear structures that have been selected to be a basis for the description of Design Scope. These mechanical systems are :

- Variable Stator Vane Mechanism.
- Blade/ Vane Cooling Process.
- Adaptive Wing. Flap and Slat Trailing Edge Mechanisms.

© 2005 SYNCOMECS Consortium Members

- Landing Gear Retraction Mechanism.
- Bi-Stable All-Plastic Actuator Mechanism.
- Residual Current Device (RCD) Tripping Mechanism.
- Shunt Trip Device.
- Leading Edge. Stretch forming using an hydraulic press.
- AGU NACA, Air Generator Unit System Air Inlet.
- Main Body Landing Gear Doors Mechanism.
- Wing Let Morphing.

Other mechanisms have also been described for the extended application of the "**SYNCOMECS** prototype".

Main design requirements are:

- To obtain the kinematics law specified and to respect the space of allocation and the shape requirements.
- Minimize the loads acting on the system, the actuator forces and the mass of system.
- To respect the robustness of the design and the maintainability of the mechanical system.
- To avoid Fracture and Surface defects.
- Minimize Cost and reliability of mechanical system.

2.8.2. Task 1.2: Survey and analysis of the state-of-the-art

The objective of Task 1.2 is to examine what the currently available design methodologies are and what kind of new design methods will be developed or improved by the **SYNCOMECS** partners.

The know-how of the academic partners and the in-house/commercial software or process already used by partners have been presented and reported in the specifications document, with some bibliographic references, in order to explain and teach all the other partners, the techniques and methodologies that will be used in the project for the Synthesis of Compliant Mechanisms, Optimisation/algorithmic and Analysis processes for Compliant Mechanisms and Complex non-linear Structures.
The design of all mechanical systems is carried out in several phases, which cover a pre-evaluation phase (choice of the baseline concept), a definition phase (detailed study of the configuration chosen in terms of dimensioning, feasibility and cost) and a design / industrialisation and certification phase.
The dimensioning and verification process carried out during testing is supported by a number of software applications which are the result of end-users experience.

From a calculation standpoint, the current design methodology is an iterative process:

- Non-linear Mechanical Systems with compliance have been studied using methods derived from rigid body counterpart and adapted to the inclusion of some flexible parts in the system. The design of the flexible parts has been fully attained by the designer and no automatic procedures have been used to support conceiving phase.
- Techniques of inverse deformation analysis can be seen as methods for dimensional synthesis of complex non-linear structures for particular applications. Complex non-linear Structures deformations have been studied by partners by using experimental data and it-

© 2005 SYNCOMECS Consortium Members

erative processes to minimise deviation of target displacements (results from the dimensioning exercise are fed into the mechanical data input and the process is repeated).

Therefore **SYNCOMECS** partners need to have a modern computation tool able to successfully replace the classical 'trial and error' method. There is scope for a more interactive optimisation process, as the current process requires a lot of manual intervention. There is also room for improvements to GUIs.

2.8.3. Task 1.3: Specification of the design system

The objective of Task 1.3 is to work out the complete specifications for the design system. Specifications reported in the specifications document cover:

- Specifications of the design methodologies to be used and developed.
- Specifications of IT technologies to be used, in terms of *development platform* and *commercial software tools.*
- Specifications of Software Modules to be developed, in terms of software tools, interface definitions and criteria for assessing the performance of developed software tools.

- **Specification of the Design Methodologies**

Design process can be divided into two main process:

- Compliant Mechanisms Design Process
- Complex Non-linear Structures Design Process

The Compliant Mechanisms Design Process can be divided into two phases:

- Synthesis (Conceptual Design). Starting from Design Specifications, the space of possible design alternatives are explored to find a topology of mechanism suitable to describe the intended motion requirements (Type Synthesis) and a preliminary analysis and optimisation are performed to find optimal values for "dimensions" to satisfy criteria and kinematical/ structural requirements (Dimensional Synthesis).
- Detailed Mechanism Design (Detailed Design). The detailed structural model is generated and precisely analysed and optimised. The required physical effects (flexibility, damping, etc) are introduced in the numerical model, as well as new related parameters.

The dimensioning of a mechanism consists mainly of obtaining the kinematical laws specified by the aerodynamics, or other motion requirements. It is also required to minimise the loads in the mechanism, respect space allocation, expected life time, weight, cost, etc.

The Complex Non-linear Structures Design Process is always an inverse problem that will be solved by direct inverse deformation analysis when possible or by a more classical optimisation process otherwise. This last approach requires the knowledge of the sensitivities of each design variable involved (parameters on BOSS quattro module). The optimisation processes allow to reduce development costs, trial and error design loops and time to market. Several optimisation algorithms are available, each one with their specificities.

- **Specification of the IT Technologies**

The new developments will add functionality to existing software tools of current industrial use.

© 2005 SYNCOMECS Consortium Members

The Development Platform on which the software will be coded is Windows Operating System.
The Commercial Software Tools that will be applied are:
- CATIA V5 (CAD Tool to import already existing CAD models)
- SAMCEF SW (Pre-Post-FEM Tools).

- **Specification of software modules**

Basic software tools planned to be used as inputs (Pre-Existing Know How) of the project are :

Software tools	From	Objective
BLDB/ Type Synthesis	INTEC	Basic Rigid Mechanism synthesis
SAMCEF Field	SAMTECH	GUI for FEM and MBS computation. Parametric pre/post processor for SAMCEF Mecano.
SAMCEF Mecano	SAMTECH	Multi-body flexible mechanisms solver, integrating FEM and MBS Tools.
BOSS quattro	SAMTECH	Task Manager and Multi-Disciplinary Optimisation Platform.

New developments will be performed during the project:

Software tools	From	Objective
IFEM Tool – SAMCEF Mecano	SAMTECH / INTEC	**I**nverse deformation **F**inite **E**lement Tool.
SYN Tool	INTEC	**SYN**thesis Tool for Compliant mechanisms, integrated to OOFELIE.
FEM Tool - SAMCEF Mecano	SAMTECH	Novel algorithms to compute quantities needed for the MDO Tool.
GUI Tool - SAMCEF Field	SAMTECH	It will be extended to the synthesis of compliant mechanical systems.
MDO Tool - Boss quattro	SAMTECH	Novel algorithms will be developed and integrated to this tool.

2.8.4. Task 1.4 : System Specification Revision

This task deal with improvement needs relevant to existing software as well as additional and/or more detailed specifications for the software tools on development within the SYNCOMECS Project.
The issued **D1 deliverable "*System Specification*"** collects the software specifications for the SYNCOMECS system tool defined from industrial specifications of functional requirements by all the project's partners. Since new problems can appear during the whole project respectively for developers and end-users, it is essential to perform subsequent revisions for the system specifications. These revisions will be taken continuously but two major revisions with a new software specifications document to be issued have been foreseen within the project.

© 2005 SYNCOMECS Consortium Members

WP1's Deliverable	Deliverable Title	Deliverable Date	Nature	Dissemination Level
D1	System specifications for the SYNCOMECS software	3rd m	R	RE
D7	System specifications subsequent revision for Milestone 2	18th m	R	RE
D12	System specifications subsequent revision for Milestone 3	25th m	R	RE

where

RE *= Restricted to a group specified by the consortium (including the Commission Services).*

R = Report

- ***First Revision***

The first revision design system specifications with additional requirements or specifications as well changes of the previous ones collected in the D1 deliverable, came from WPs 2 and 3 where partners gained experience and knowledge on their compliant system test cases and in particular on compliant system design.

Information obtained from the first WP2&3 tests have been used to steer the development of new software tools and give a clear statement of what the industrial needs are as well as using the existing software and methodologies to study and design compliant systems have given ideas for improvements needs relevant to the existing software.

Goals of this task was collect all this experience from the WP2 (lead by SNECMA) and WP3 (lead by CENAERO), where partners have studied the compliant test cases by means of the existing tools and methodologies, and lead to a better understanding of the problems relevant to the target applications and to the requirements and specifications for the SYNCOMECS system tool.

All the partners, end-users and developers, were involved: (1) the developers have prepared a summary of the development status of the tools, (2) the end-users have collected their WP2&3 experience filling a specific questionnaires prepared by Alenia Aeronautica, (3) the WP2&3 leaders have summarised the problems from the end-user monthly reports where each end-users, once a month, report any problems relevant to WP2&3 the activities. Therefore the task1.4 revision has been the result of common efforts and requests from all the end-user partners.

The main request from the end-user partners is relevant to the *D1 Design System Specification* : **all the specifications/requirements requested collected in D1 documents are still valid and have to be satisfied** since no one has been relapsed or deleted. Therefore the D7 document and the system specification revisions reported **do not** supersede the D1 document but, thanks to the experience gained during WP2 and 3, complete the D1 document and its system specifications.

The revised specifications reported within D7 deals with (1) the improvement requests to the existing software in order to be more suitable for design of compliant system and with (2) additional requirements and specifications to the new software tools under development in the SYNCOMECS Project; (3) go into details of D1's specifications

In conclusion the main results from the Task 1.4 have been:

- the D1's design system specifications have not been modified or relapsed.
- D7 deliverable with additiional specifications, improvements needs, and requirements details
- a call for a dedicated meeting on the synthesis tool.

© 2005 SYNCOMECS Consortium Members

Due to the importance of the compliant mechanisms synthesis tool within the project, SYN-Tool have been and will be the subject of a dedicated meeting where INTEC, the developer, will present to the end-user partners the developing status of this tool as well as the potential and capability of this tool to satisfy the D1's specifications and requirements to solve the benchmark test cases proposed by each partners.
The capability to deal and solve the proposed end-users test cases is essential therefore additional and/or more detailed design software specifications relevant to the compliant mechanism synthesis tool could be proposed during this meeting since each partner will try to solve his test case with the support and help of the developers. . Details and explanations of the requirements and design system specifications relevant to SYNTool have been given by the end-users partners as well as by Samtech to INTEC, the SYNTool developer.

- ***Second Revision***

The task 1.4 Second system specification revision follows tasks 7.1 and 7.2 (lead by ABB) and starts from the first revision's D7 conclusions with the goals to collect the WP7's experiences relevant to the design system specifications.

WP7's tasks deal with the evaluation and validation of the developed versions of SYNCOMECS tools. First, each single module has been tested as a standalone software in order to verify its own functionality. After that, the first attempts of integrated design environment and methodologies have been tested concurrently in order to evaluate the actual co-operation and compatibility of the software modules

Basically all the WP7's tests have provided information about the actual capability, limitations, and reliability of the software modules or of the first attempts of integrated SYNCOMECS system therefore the tests carried out on the specified case studies have given new ideas with reference to the design system specifications and their revision of the integrated software system performances concerning the whole design support.

The second revisions have been taken continuously during the WP7 with several specific meeting where the main subject have been the development of the design system tools with reference to their capability, limitations, etc. in short with reference to the system specifications and the level of satisfaction (WP7) as well as needs of their revision (WP1 task1.4).

The conclusions of the first revision called a meeting dedicated to the survey of the tools development with reference to the satisfaction of the requirements in order to highlight need for specification revision, modification, details and so forth. This meeting held in Cambridge, first of a series of jointly WP7 – WP1's task1.4 meetings/workshops, was the begin of the second revision continuous process.

The second revision process has been a dynamic continuous process within WP7 where the design system specifications revision has been discussed and accepted during a series of dedicated workshop meetings between end-user partners, who calls for system specifications, and software developer partners, who has accepted the revision and implemented them within the under development tools.

The second revision process has been carried on during each of the following meetings :

- Workshop Meeting - All Softwares - (CAMBRIDGE 20-22-November 2006)
- Phone Meeting - Software Status - (1-December 2006)
- Workshop Meeting - SYNTool ABB/ALENIA - (ABB 6/7-March 2007)
- Workshop Meeting - SYNTool SNECMA - (SAMTECH 15-March 2007)
- Workshop Meeting - SYNTool 2 - (SAMTECH 03/04 - April 2007)

© 2005 SYNCOMECS Consortium Members

- Workshop Meeting - SYNTool CTING - (CTING 09/10 - May 2007)

The design system specification revision was discussed during the 24th Month Meeting - (CTING 27/28 - March 2007) where a summary of the previous workshops has been presented by Samtech.

All of these workshops had the common goals to keep in touch developers and end-users in order to avoid misunderstanding and problems relevant to the design system specifications and to explain the end-users tools capabilities wishes and needs. During these workshops the developers have presented the status of their tools under development and have trained the end-user explaining how to satisfy their design system requirements meanwhile the end-users have explained and detailed the system specifications required by their benchmark test cases.

The second revision in collaboration with WP7 as well as the tools developing WPs (4,5 and 6) has been deeply discussed within a dynamic process and step by step the system specifications have been revised during each workshop meetings, nevertheless specific questionnaires has been prepared by Alenia as task1.4 leader to collect possible partners revision needs in addition to the specifications revision from the dedicated workshops.

The main result/request from this second specification revision process concerns the design system specifications collected within D1 and revised within D7 since all the D1 and D7 's specifications has been not relapsed and therefore they have to be satisfied by the final integrated SYNCOMECS tool.

The revision process as well as the revision requests and the relevant report have evolved through workshops since developers updated the software by means of the end user specifications requests meanwhile end users found out bugs, problems and specification revision needs within the evaluation/validation within WP7. Revision and requests relevant to specification have been collected and summarised in a report updated after each workshop meeting in order to keep informed end users about the software problems and the specifications requests solved by the developers as well as the developers about the specifications revision requests coming from the validation of the latest tools version.

Specification revision requests as well as previous specification requests confirmation can be found in the minutes of all the workshop meetings with the common subject of tools capabilities, level of specification satisfaction and specification revision. (D12 as reference)

The D12 does not report a fully list or a summary of all the specification revision requests since the second revision has been a continuous dynamic process where step by step the specification revision needs have been discussed between the end-users and the developers. Revision requests have been proposed by the end-users and some of them satisfied by the tools developers through the WP7 since the specification meeting called by the conclusion of the first revision process.

2.8.5. WP2,WP3 and WP7

Unfortunately, we can't describe in detail what has been done for confidentiality reasons. Each of the test cases used with SYNTool, IFEM and SYNCOMECS integrated tools are relevant to original research and may not be published yet

© 2005 SYNCOMECS Consortium Members

2.9.SNECMA Moteurs

2.9.1. Project objectives and main achievements

Snecma had 2 major objectives in the SYNCOMECS project:

- ✓ Improvement of the blade cooling process using an inverse method
- ✓ Improvement of the VSV design process using optimisation tool and improved simulation tool

Application of Inverse method to the blade cooling process

The optimization of blades is a cross-functional process based on aerodynamic, thermal, mechanical or acoustic simulation. In an initial phase, a major step in the design process is the "cold blade approximation". This step consists in determining the geometry of the blade to be manufactured ("cold blade"). The inputs are the geometry of the aerodynamic blade during operation ("hot blade") and the loads at this operating point. The loads sustained by the blades are centrifugal forces due to the rotation speed, as well as aerodynamic pressures, and possibly thermal gradients. The geometry of the cold blade must be determined in such a way that its deformed body is equal to the aerodynamic profile of the hot blade.

In the past, this problem was handled according to simple methods. The first method only consists in making a linear or non-linear static analysis of the hot blade and removing the displacements in order to obtain the cold blade.

In order to further refine the calculations, iterative and semi-empirical methods have been developed. These methods require substantial calculation times and are penalized by the introduction of new composite materials and by the strongly 3D shapes.

The inverse method, as formed in equation and developed on MECANO (IFEM), is thus a very interesting progress in terms of both the implementation of the method and the computation performance. As with all the methods that have been used up to now, it is important to recall that we are making a simplifying assumption. In the initial phase, we do not make any coupling between the mechanics and the aerodynamics, in other words we consider that the pressure load data is independent from the initial shape and the load history.

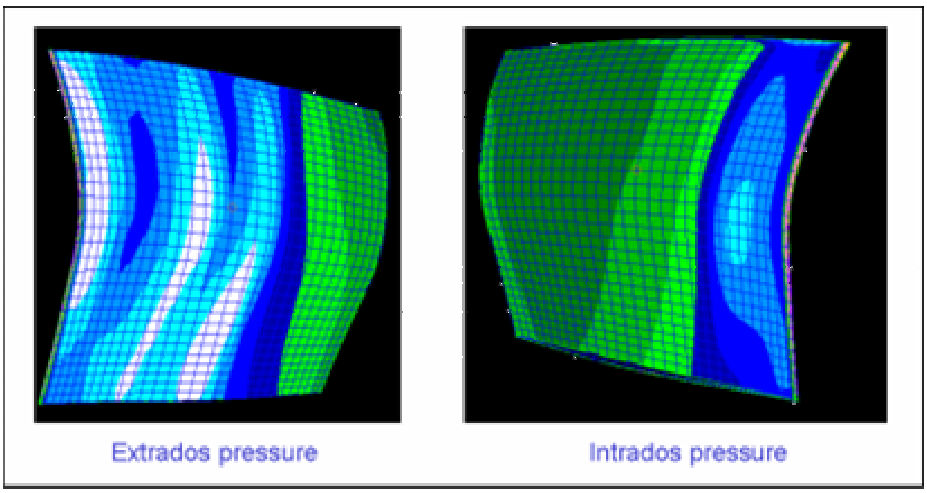

Fig. 1 – Meshing and loading of the test blade

© 2005 SYNCOMECS Consortium Members

Various degrees of tests have been achieved and this paper presents a metallic blade that has been processed in order to substantiate the new inverse method. As mentioned before, the blade used as test case is subjected to a pressure field and is in rotation (which induces internal centrifugal loads). The following picture shows the result obtained by the inverse method ("cold blade"):

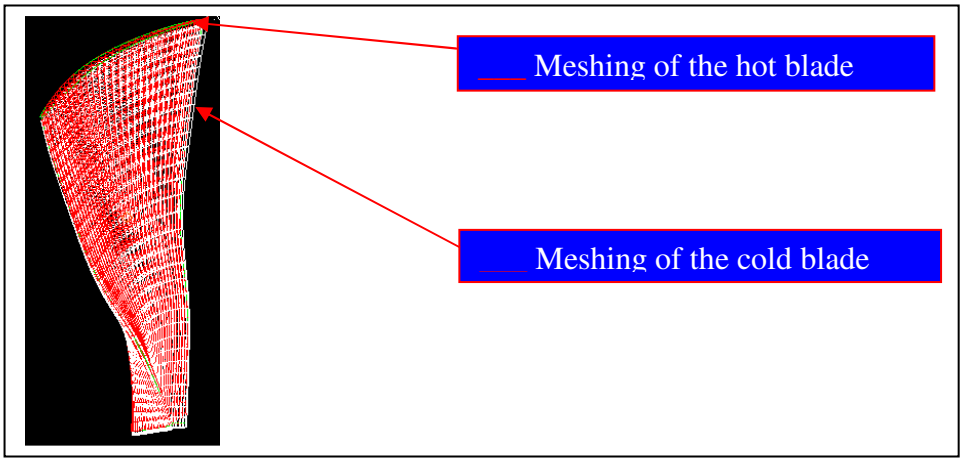

Fig. 2 – Meshing of the hot blade and the cold blade

In order to validate the results of the inverse MECANO method, we just have to use the standard MECANO method (direct method), using the meshing of the cold blade, as subjected to the same pressure loads and centrifugal forces. The next figure shows the superimposition between the hot blade (aerodynamic objective) and the cold blade subjected to these loads. The superimposition of these two meshings demonstrate that the result, as found according to the inverse method, gives a result that is totally coherent and fairly accurate.

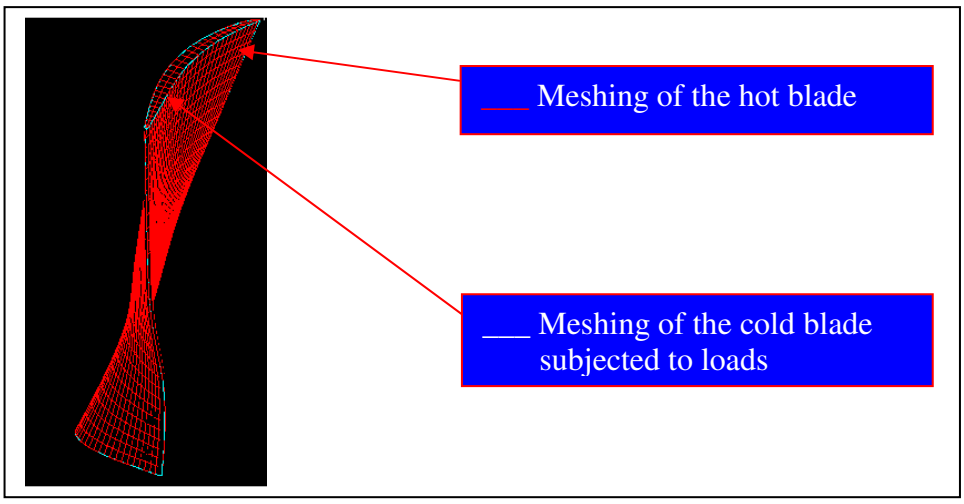

Fig. 3 – Superimposition of the hot blade and the cold blade subjected to loads

Using several test cases, we can give the following conclusion on the inverse method:
– Accuracy: The results, as found according to the inverse method, give results that are totally coherent and fairly accurate (theoretical cases and industrial cases).
– Performance: The examples of a turbojet engine blades subjected to centrifugal and pressure loads has shown that the method is accurate and delivers high performance levels in terms of time and calculation (1 single MECANO analysis instead of 5 - 10 analyses).

© 2005 SYNCOMECS Consortium Members

Mechanism: Variable Stator Vane (VSV)

The design of an aeronautical mechanism is a process where the designer is confronted to the difficult task of managing a wide range of variables and mechanism configurations, subjected to severe aerodynamic and manufacturing constraints. The purpose of the proposed integrated tool is to reduce the trials and errors work usually done during the conceptual design phase of mechanical systems.

Also, as all operations, starting from type synthesis to detailed stress analysis, are all performed with the same tool, problems related to data transfer are avoided. Compared to classical methods based on rigid multibody solvers, the use of Finite Element software for mechanism simulation allows easily introducing flexibility at very early stage of the design process. This prevents from missing some possibly unexpected dynamical effects, which can require strong design modifications later in the design process

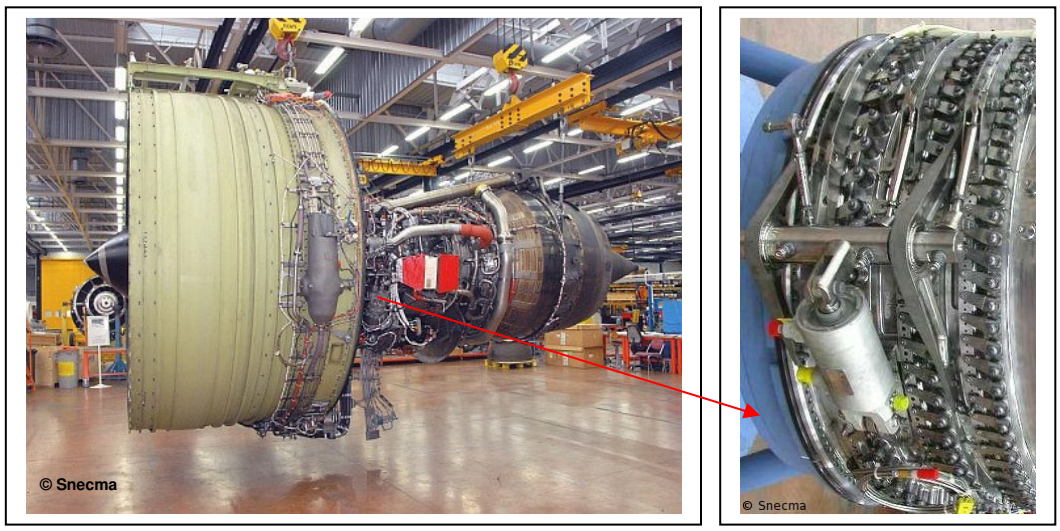

Fig. 4 – Example of engine and VSV system

Different levels of tests were performed using the SYNCOMECS process:

☑ 2D single stage model (architecture of the mechanism): The main goal of design is to obtain good orientations of the blades during a mission, using a minimum number of components (or minimising mass)

☑ 2D multistage model (geometrical optimization of the ground hinges, hinges and so)

☑ 3D detailed multistage model (mechanical validation): Once the general architecture is chosen, it is important to validate the detailed design using 3D modelling. Indeed, it is important to be able to provide 3D models which take into account all physical aspects (contacts, friction, aerodynamic loads, and so)

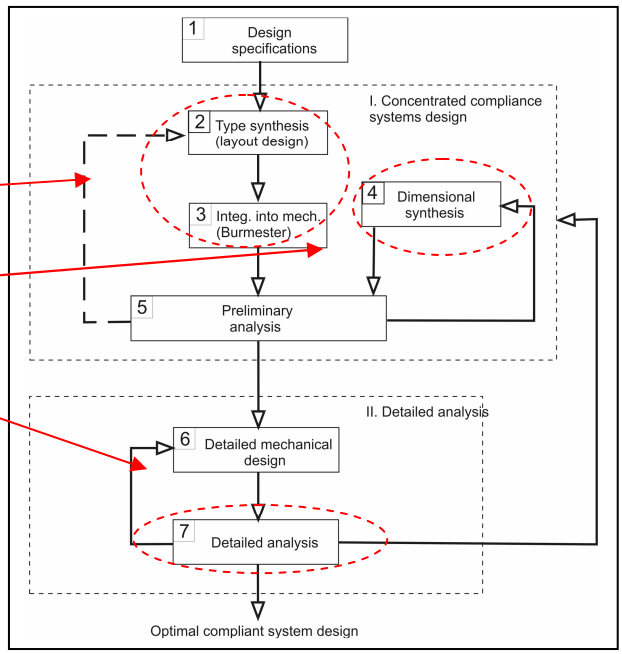

© 2005 SYNCOMECS Consortium Members

Several models were evaluated: different geometrical positions, rigid and flexible Atlases, orientation of the actuator (horizontal and vertical positions) and aerodynamic laws.

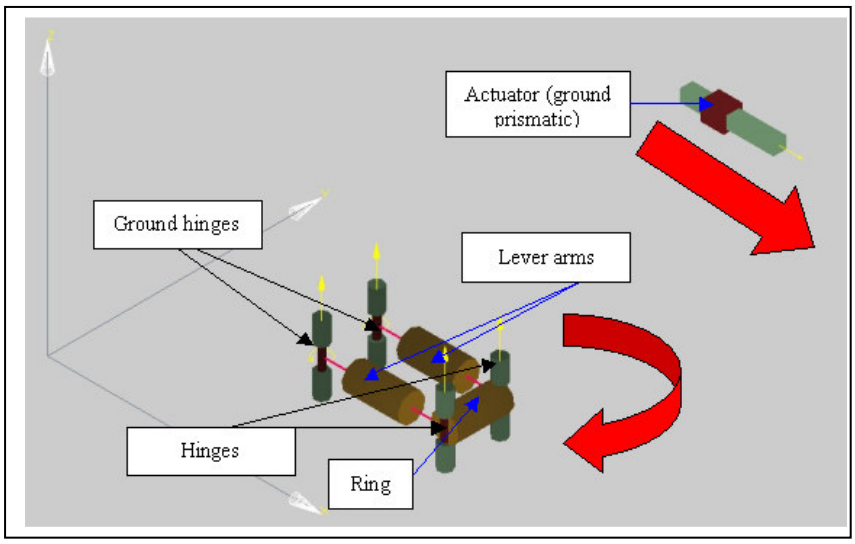

Fig. 5 – Example of simple model (initial data)

Using the SYNTOOL software with various options, we could find a large range of possible mechanisms in the case of a single stage problem. The following pictures present some examples of "alternatives" (from the simplest to the more complex solutions) and examples with flexible beams.

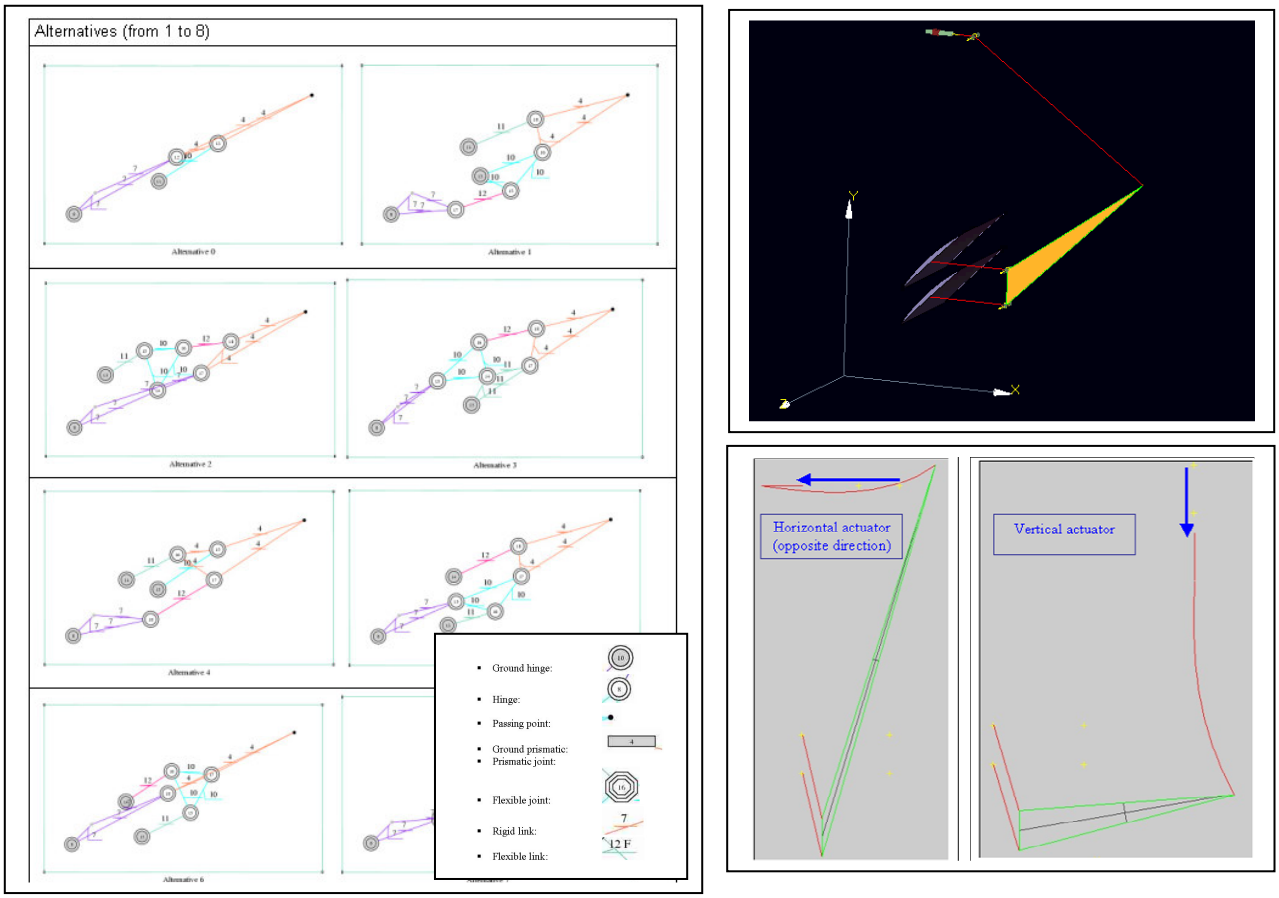

Fig. 6 – Examples of alternatives in a simple stage model(rigid and flexible atlases)

© 2005 SYNCOMECS Consortium Members

The next steps were dedicated to the optimisation and simulation phase: we have chosen a multistage VSV system to evaluate the performance of the different steps (modelling tool, solver, calculation of sensitivities, optimisation task). In our case, parameters of the optimisation problem are the positions of the hinges and ground hinges and objective functions are the aerodynamic angles for the 3 stages.

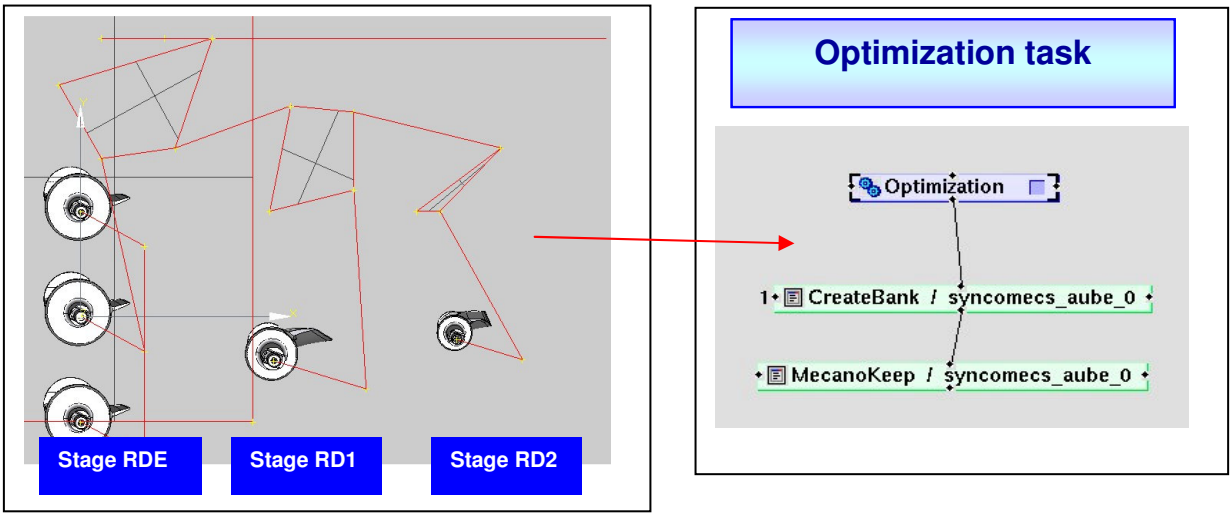

Fig. 7 – Examples of a multistage model & optimization task

Different strategies were used to solve the optimization problem: due to the large range of parameters, we have chosen to progressively solve the problem (from RDE to RD2). This strategy minimizes the risk to reach local optima. As we can see it in the following graph, the optimised VSV model fulfils most of the requirements, the optimisation for the 3 stages is very accurate.

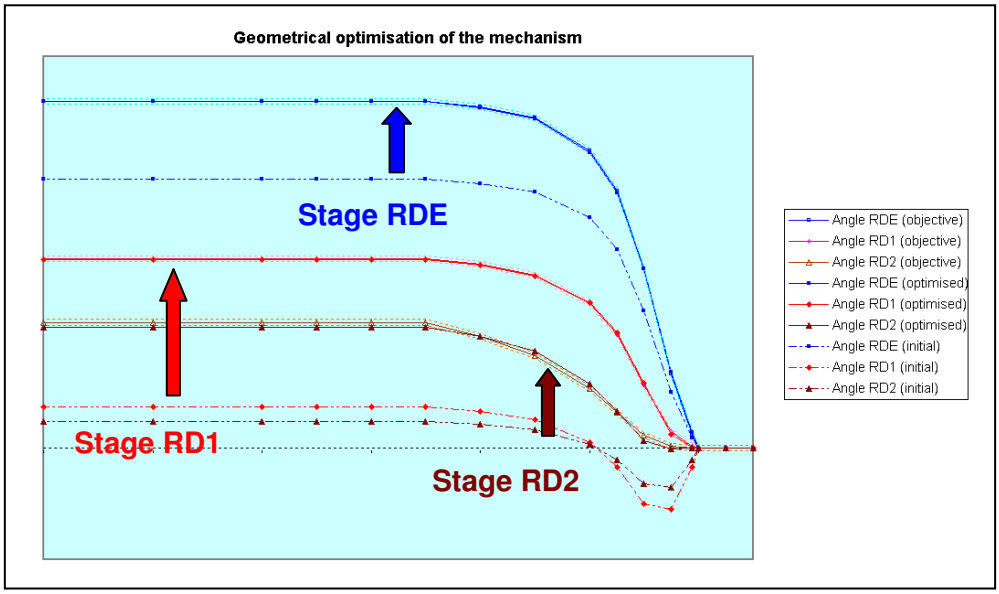

Fig. 8 – Verification of the aerodynamic laws (angles vs rating of engine)

© 2005 SYNCOMECS Consortium Members

Finally, once the concept and preliminary design is defined, 3D simulation using CAD data can be achieved to validate the design. Studied structure is submitted to thermal and aerodynamic loading and one the critical points of this system is to guarantee that the position of the blades will be correct and that the components will meet all mechanical requirements.

This particular context requires the definition of complex articulated flexible models. Using the latest versions of the SYNCOMECS project we have achieved an impressive flexible model: critical components were meshed with volume elements in order to take into account the deformation, flexibility was introduced in bodies in some components in order to reduce the size of the model by using super element techniques, while other components are assumed rigid to maintain calculation cost at a reasonable level. The final model contains about 500 components and the size of model is at the upper limit of our know-how. This Impressive model has been successfully performed. Such model will be useful for the future systems, but it is important to improve the performance of the pre-post processor if we want to generalize such model in the future.

© 2005 SYNCOMECS Consortium Members